

Systematic analysis of single heavy baryons Λ_Q , Σ_Q and Ω_Q

Guo-Liang Yu^{1,*}, Zhen-Yu Li², Zhi-Gang Wang^{1,†}, Lu Jie¹, and Yan Meng¹

¹ *Department of Mathematics and Physics, North China Electric Power University,
Baoding 071003, People's Republic of China*

² *School of Physics and Electronic Science, Guizhou Education University,
Guiyang 550018, People's Republic of China*

(Dated: June 20, 2022)

Motivated by great progresses in experiments in searching for the heavy baryons, we systematically analyze the mass spectra and the strong decay behaviors of single heavy baryons Λ_Q , Σ_Q and Ω_Q . The calculations of the mass spectra are carried out in the frame work of Godfrey-Isgur (GI) relativized quark model, where the baryon is regarded as a three-body system of quarks. Our results show that the mass of single heavy baryon with λ -mode is lower than those of the ρ -mode and λ - ρ mixing mode, which indicates that the lowest state is dominated by the λ -mode. Basing on this research, we systematically calculate the mass spectra of the baryons with λ excited mode. With these predicated mass spectra, the Regge trajectories in the (J, M^2) plane are constructed, and the slopes, intercepts of the Regge trajectories are obtained by linear fitting. It is found that all available experimental data are well reproduced by model predictions and fit nicely to the constructed Regge trajectories. In order to make a further confirmation about the assignments of the observed baryons, and to provide more valuable infirmations for searching for the model predicted states, we perform a systematic study on the strong decay behaviors of S -wave, P -wave and some D -wave baryons in the 3P_0 model.

PACS numbers: 13.25.Ft; 14.40.Lb

1 Introduction

In the field of heavy baryon physics, scientists have made great progresses in experiments as well as in theories, which makes the mass spectra of heavy baryon families become more and more abundance. In the past few decades, almost all of the $1S$ single heavy baryons have been well established and some of the $1P$ states $\Lambda_c(2595)$ [1], $\Lambda_c(2625)$ [2], $\Lambda_b(5912)$ and $\Lambda_b(5920)$ [3, 4] have also been well observed in experiments and been confirmed in theory[5, 6]. Besides of these states, many other single heavy baryons have also been discovered by Belle, BABAR, CLEO and LHCb, such as $\Lambda_c(2765)$ [7], $\Lambda_c(2940)$ [8–10], $\Lambda_b(6072)$ [11], $\Lambda_b(6146)$ [12], $\Lambda_b(6152)$ [12], $\Sigma_c(2800)$ [13], $\Sigma_b(6097)$ [14], $\Omega_c(3000)$, $\Omega_c(3050)$, $\Omega_c(3065)$, $\Omega_c(3090)$, $\Omega_c(3119)$ [16], $\Omega_b(6330)$, $\Omega_b(6316)$, $\Omega_b(6350)$ and $\Omega_b(6340)$ [15]. Some of these baryons may

*Electronic address: yuguoliang2011@163.com

†Electronic address: zgwang@aliyun.com

belong to the low-lying S - or P -wave states, while some of them can be assigned to D -wave baryons, all of these assignments needs further confirmation in more ways. In order to identify their quantum numbers and assign each baryon a suitable position in the mass spectra, it is necessary to systematically investigate single heavy baryon spectroscopy and study their strong decay behaviors.

In the past decades, the single heavy baryons have been extensively investigated by many theoretical methods/models, including various quark model[17–44], the heavy hadron chiral perturbation theory[45–50], lattice QCD[51–54], light cone QCD sum rules[55–62], QCD sum rules[63–82] and relativistic flux tube model[83]. To our knowledge, only Ref.[19] focused on the mass spectra of the heavy baryons from ground states to the high excited states systematically in the quark-diquark picture. In this literature, heavy baryons are considered in the heavy-quark-light-diquark approximation, which can simplify the complicated relativistic three-body problem. Under this quark-diquark picture, the single heavy baryon is considered as the bound system of a heavy quark and a light diquark. Thus, the initial three-body problem is reduced to two-step two-body calculations. Another important work was carried out by Roberts and Pervin[20]. With the non-relativized quark model, they studied various excited states of single heavy baryons by solving three quark systems explicitly. On the other hand, a Gaussian expansion method(GEM) was introduced in the non-relativized quark model to solve the three-quark system in Ref.[21]. In the calculations of the matrix elements of the Hamiltonian of three-body system, particularly when complicated interactions are employed, integrations over all of the radial and angular coordinates become laborious even with GEM. In Ref.[21], they developed an infinitesimally-shifted Gaussian basis function to simplify this process.

In this work, we extend the method of infinitesimally-shifted Gaussian basis function to the Godfrey-Isgur (GI) relativized quark model to study the mass spectra of the single heavy baryons. The GI relativized quark model was first developed by Godfrey and Isgur to study the mass spectra of mesons and baryons[17, 18]. Recently, this quark model has also been used to investigate the mass of tetraquark states[84–86]. When solving for the eigenfunctions and eigenenergies of the Hamiltonian with variational methods in GI model, they took as trial wave functions an expansion of the true wave functions in a large harmonic oscillator basis[17, 18]. Actually, the spatial wave function of a three-body system can also be expanded in terms of a set of Gaussian basis functions, which forms an approximate complete set in a finite coordinate space. It was found that GEM is one of the best method for three and four body bound states[21], which can help us to obtain precise energy eigenvalues of excited states. Especially, taking infinitesimally-shifted Gaussian function as the basis function has the advantage of simplifying the calculation of matrix elements[21]. The first goal of our present work is to calculate the mass spectra of the excited heavy baryons up to rather high orbital and radial excitations. With these results, we will construct the heavy baryon Regge trajectories in the (J, M^2) planes and determine their Regge slopes and intercepts.

For a further understanding of these excited baryons, it is significant to perform a systematic study

of their strong decay behaviors. As a phenomenological method, the 3P_0 quark model was developed to study the OZI-allowed hadronic decay widths[87–90]. Now, this model has been extensively used to describe the strong decays of the heavy mesons in the charmonium and bottomonium systems[91–105], the baryons[106–112] and even the tetraquark states[113]. In this work, 3P_0 model will be employed to study the strong decay properties of the S -wave, P -wave and some D -wave single heavy baryons. The calculated strong decay widths in this work will be confronted with the experimental data in the future and will be helpful in searching for new states of single heavy baryons from the Belle, BABAR, CLEO and LHCb collaborations.

The paper is organized as follows. In Section II, we present the the GI relativized quark model of heavy baryons based on the method of infinitesimally-shifted Gaussian basis functions. With this method, we systematically investigate the mass spectra of single heavy baryons Λ_Q , Σ_Q and Ω_Q . In Sec III the heavy baryon Regge trajectories in the (J, M^2) plane are constructed with the predicted mass spectra, and slopes, intercepts of parent and daughter trajectories are also obtained by linear fitting. In Sec IV, the strong decay behaviors of the S -wave, P -wave and some D -wave heavy baryon states are studied by 3P_0 model. And Sec V is reserved for our conclusions.

2 Mass spectra of single heavy baryons Λ_Q , Σ_Q and Ω_Q

2.1 The Jacobi coordinate and GI relativized quark model

In this work, the single heavy baryon is regarded as a three-body system which has two light quarks(u , d or s quarks) and one heavy quark(c or b quark) inside. In order to express internal motions of the quarks in this three-body system, we commonly introduce three sets of Jacobi coordinates as in Fig.1. Each set of Jacobi coordinate is called a channel(c) which is defined as,

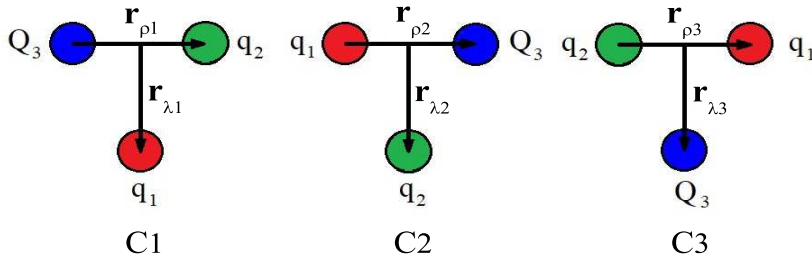


FIG. 1: Jacobi coordinates for the three body system.

$$\mathbf{r}_\lambda = \mathbf{r}_k - \frac{m_i \mathbf{r}_i + m_j \mathbf{r}_j}{m_i + m_j} \quad (1)$$

$$\mathbf{r}_\rho = \mathbf{r}_i - \mathbf{r}_j \quad (2)$$

where assignments of (i, j, k) are given in Table I. The Jacobi coordinate of $c = 3$ can be expressed in

Channel	i	j	k
$c = 1$	2	3	1
$c = 2$	3	1	2
$c = 3$	1	2	3

TABLE I: The quark assignments (i, j, k) for the Jacobi coordinates

terms of the coordinate $c = 1$ or $c = 2$,

$$\mathbf{r}_{\rho_3} = \alpha_{31(32)}^r \mathbf{r}_{\rho_{1(2)}} + \beta_{31(32)}^r \mathbf{r}_{\lambda_{1(2)}} \quad (3)$$

$$\mathbf{r}_{\lambda_3} = \gamma_{31(32)}^r \mathbf{r}_{\rho_{1(2)}} + \delta_{31(32)}^r \mathbf{r}_{\lambda_{1(2)}} \quad (4)$$

where the transforming coefficients for $c : 3 \rightarrow 1$ and $3 \rightarrow 2$ are,

$$\alpha_{31}^r = -\frac{m_3}{m_2+m_3}, \beta_{31}^r = 1, \gamma_{31}^r = -\frac{m_2(m_1+m_2+m_3)}{(m_1+m_2)(m_2+m_3)}, \delta_{31}^r = -\frac{m_1}{m_1+m_2},$$

$$\alpha_{32}^r = -\frac{m_3}{m_1+m_3}, \beta_{32}^r = -1, \gamma_{32}^r = \frac{m_1(m_1+m_2+m_3)}{(m_1+m_2)(m_1+m_3)}, \delta_{32}^r = -\frac{m_2}{m_1+m_2}.$$

Under the definitions of Jacobi coordinate in Eqs.(1) and (2), we can also define the relative momentums $\mathbf{p}_{\rho_i}, \mathbf{p}_{\lambda_i}$ ($i = 1, 2, 3$) in these three channels. In the baryon center-of-momentum frame, the relative momentums have similar transformations as the Jacobi coordinates in Eqs.(3) and (4),

$$\mathbf{p}_{\rho_3} = \alpha_{31(32)}^p \mathbf{p}_{\rho_{1(2)}} + \beta_{31(32)}^p \mathbf{p}_{\lambda_{1(2)}} \quad (5)$$

$$\mathbf{p}_{\lambda_3} = \gamma_{31(32)}^p \mathbf{p}_{\rho_{1(2)}} + \delta_{31(32)}^p \mathbf{p}_{\lambda_{1(2)}} \quad (6)$$

where

$$\alpha_{31}^p = -\frac{m_1}{m_1+m_2}, \beta_{31}^p = \frac{m_2(m_1+m_2+m_3)}{(m_1+m_2)(m_2+m_3)}, \gamma_{31}^p = -1, \delta_{31}^p = -\frac{m_3}{m_2+m_3},$$

$$\alpha_{32}^p = -\frac{m_2}{m_1+m_2}, \beta_{32}^p = -\frac{m_1(m_1+m_2+m_3)}{(m_1+m_2)(m_1+m_3)}, \gamma_{32}^p = 1, \delta_{32}^p = -\frac{m_3}{m_1+m_3}.$$

In the following, we give a brief introduction to the Hamiltonian of GI relativized quark model. The relativistic Hamiltonian for a three-body system can be written as[17, 18],

$$\hat{H} = \sum_{i=1}^3 (p_i^2 + m_i^2)^{1/2} + \sum_{i<j} \tilde{H}_{ij}^{conf} + \sum_{i<j} \tilde{H}_{ij}^{hyp} + \sum_{i<j} \tilde{H}_{ij}^{so} \quad (7)$$

where the first term is the relativistic kinetic energy term, \tilde{H}^{conf} is the spin-independent potential which contains a linear confining potential $\tilde{S}(r_{ij})$ and the one-gluon exchange potential $G'(r_{ij})$,

$$\tilde{H}_{ij}^{conf} = \tilde{S}(r_{ij}) + G'(r_{ij}) \quad (8)$$

with

$$\tilde{S}(r_{ij}) = -\frac{3}{4} \mathbf{F}_i \cdot \mathbf{F}_j \left[br_{ij} \left[\frac{e^{-\sigma_{ij}^2 r_{ij}^2}}{\sqrt{\pi} \sigma_{ij} r_{ij}} + \left(1 + \frac{1}{2\sigma_{ij}^2 r_{ij}^2}\right) \frac{2}{\sqrt{\pi}} \int_0^{\sigma_{ij} r_{ij}} e^{-x^2} dx \right] + c \right] \quad (9)$$

$$\sigma_{ij} = \sqrt{s^2 \left[\frac{2m_i m_j}{m_i + m_j} \right]^2 + \sigma_0^2 \left[\frac{1}{2} \left(\frac{4m_i m_j}{(m_i + m_j)^2} \right)^4 + \frac{1}{2} \right]} \quad (10)$$

The $\mathbf{F}_i \cdot \mathbf{F}_j$ stands for the color matrix and F_n reads

$$F_n = \begin{cases} \frac{\lambda_n}{2} & \text{for quarks,} \\ -\frac{\lambda_n^*}{2} & \text{for antiquarks} \end{cases} \quad (11)$$

with $n = 1, 2 \dots 8$. It should be noticed that the one-gluon exchange potential $G'(r_{ij})$ is achieved by introducing momentum-dependent factors,

$$G'(r_{ij}) = \left(1 + \frac{p_{ij}^2}{E_i E_j} \right)^{\frac{1}{2}} \tilde{G}(r_{ij}) \left(1 + \frac{p_{ij}^2}{E_i E_j} \right)^{\frac{1}{2}} \quad (12)$$

with

$$\tilde{G}(r_{ij}) = \mathbf{F}_i \cdot \mathbf{F}_j \sum_{k=1}^3 \frac{2\alpha_k}{3\sqrt{\pi}r_{ij}} \int_0^{\tau_k r_{ij}} e^{-x^2} dx \quad (13)$$

$$\text{and } \tau_k = \frac{1}{\sqrt{\frac{1}{\sigma_{ij}^2} + \frac{1}{\gamma_k^2}}}.$$

In, Eq.(7), \tilde{H}^{hyp} is the color-hyperfine interaction which includes tensor interaction and the contact interaction,

$$\tilde{H}_{ij}^{hyp} = \tilde{H}_{ij}^{tensor} + \tilde{H}_{ij}^c \quad (14)$$

with

$$\tilde{H}_{ij}^{tensor} = - \left(\frac{\mathbf{S}_i \cdot \mathbf{r}_{ij} \mathbf{S}_j \cdot \mathbf{r}_{ij} / r_{ij}^2 - \frac{1}{3} \mathbf{S}_i \cdot \mathbf{S}_j}{m_i m_j} \right) \times \left(\frac{\partial^2}{\partial r_{ij}^2} - \frac{1}{r_{ij}} \frac{\partial}{\partial r_{ij}} \right) \tilde{G}_{ij}^t, \quad (15)$$

$$\tilde{H}_{ij}^c = \frac{2\mathbf{S}_i \cdot \mathbf{S}_j}{3m_i m_j} \nabla^2 \tilde{G}_{ij}^c \quad (16)$$

For the spin-orbit interaction, it can be divided into two parts which can be written as,

$$\tilde{H}_{ij}^{so} = \tilde{H}_{ij}^{so(v)} + \tilde{H}_{ij}^{so(s)}, \quad (17)$$

with

$$\tilde{H}_{ij}^{so(v)} = \frac{\mathbf{S}_i \cdot \mathbf{L}_{ij}}{2m_i^2 r_{ij}} \frac{\partial \tilde{G}_{ii}^{so(v)}}{\partial r_{ij}} + \frac{\mathbf{S}_j \cdot \mathbf{L}_{ij}}{2m_j^2 r_{ij}} \frac{\partial \tilde{G}_{jj}^{so(v)}}{\partial r_{ij}} + \frac{(\mathbf{S}_i + \mathbf{S}_j) \cdot \mathbf{L}_{ij}}{m_i m_j r_{ij}} \frac{1}{r_{ij}} \frac{\partial \tilde{G}_{ij}^{so(v)}}{\partial r_{ij}} \quad (18)$$

and

$$\tilde{H}_{ij}^{so(s)} = - \frac{\mathbf{S}_i \cdot \mathbf{L}_{ij}}{2m_i^2 r_{ij}} \frac{\partial \tilde{S}_{ii}^{so(s)}}{\partial r_{ij}} - \frac{\mathbf{S}_j \cdot \mathbf{L}_{ij}}{2m_j^2 r_{ij}} \frac{\partial \tilde{S}_{jj}^{so(s)}}{\partial r_{ij}} \quad (19)$$

In Eqs.(15),(16),(18) and (19), \tilde{G}_{ij}^t , \tilde{G}_{ij}^c , $\tilde{G}_{ij}^{so(v)}$ and $\tilde{S}_{ii}^{so(s)}$ are achieved from $\tilde{G}(r_{ij})$ and $\tilde{S}(r_{ij})$ by introducing momentum-dependent factors,

$$G_{ij}^t = \left(\frac{m_i m_j}{E_i E_j} \right)^{\frac{1}{2} + \epsilon_t} \tilde{G}(r_{ij}) \left(\frac{m_i m_j}{E_i E_j} \right)^{\frac{1}{2} + \epsilon_t} \quad (20)$$

$$G_{ij}^c = \left(\frac{m_i m_j}{E_i E_j} \right)^{\frac{1}{2} + \epsilon_c} \tilde{G}(r_{ij}) \left(\frac{m_i m_j}{E_i E_j} \right)^{\frac{1}{2} + \epsilon_c} \quad (21)$$

$$G_{ij}^{so(v)} = \left(\frac{m_i m_j}{E_i E_j} \right)^{\frac{1}{2} + \epsilon_{so(v)}} \tilde{G}(r_{ij}) \left(\frac{m_i m_j}{E_i E_j} \right)^{\frac{1}{2} + \epsilon_{so(v)}} \quad (22)$$

$$\tilde{S}_{ii}^{so(s)} = \left(\frac{m_i^2}{E_i^2} \right)^{\frac{1}{2} + \epsilon_{so(s)}} \tilde{S}(r_{ij}) \left(\frac{m_i^2}{E_i^2} \right)^{\frac{1}{2} + \epsilon_{so(s)}} \quad (23)$$

with $E_i = \sqrt{m_i^2 + p_{ij}^2}$. The p_{ij} is the magnitude of the momentum of either of the quarks in the ij center-of-mass frame and these relative momentums p_{23} , p_{13} and p_{12} correspond to p_{ρ_1} , p_{ρ_2} and p_{ρ_3} in three channels.

2.2 Wave function of single heavy baryon

In quark model scheme, the full wave function for a definite baryon is built from a linear superposition of the channel wave function, which can be written as,

$$\Psi_{full}^{JM} = \sum_{c\alpha} C_{c,\alpha} \Psi_{JM}^c(\mathbf{r}_{\rho_c}, \mathbf{r}_{\lambda_c}) \quad (24)$$

where the index α denotes $n_\rho, n_\lambda, l_\rho, l_\lambda, L, s, j$, and c denotes the Jacobi coordinate channel with $c = 1, 2, 3$ as illustrated in Fig.1. $\Psi_{JM}^c(\mathbf{r}_{\rho_c}, \mathbf{r}_{\lambda_c})$ is the wave function for channel c and it is described in terms of antisymmetric color-singlet wave function ϕ_{color} , multiplying flavor ϕ_{flavor} , spin and space wave function ψ_{JM}^c

$$\Psi_{JM}^c(\mathbf{r}_{\rho_c}, \mathbf{r}_{\lambda_c}) = \phi_{\text{color}} \otimes \phi_{\text{flavor}} \otimes \psi_{JM}^c \quad (25)$$

with

$$\phi_{\text{color}} = \frac{1}{\sqrt{6}}(rgb - rbg + gbr - grb + brg - bgr), \quad (26)$$

$$\psi_{JM}^c = \left[\left[[\chi_{1/2}(q)\chi_{1/2}(q)]_{s,m_s} \Phi_{l_\rho, l_\lambda, L}^c \right]_{j,m_j} \chi_{1/2}(Q) \right]_{JM}, \quad (27)$$

where r, g, b are the color of the quark and $\chi_{1/2}$ is the spin wave function. Within the flavor SU(3) subgroups, the single heavy baryons belong either to a sextet(6_F) of flavor symmetric states, or an antitriplet($\bar{3}_F$) of flavor antisymmetric states. For the Σ_Q and Ω_Q baryons, they belong to flavor-symmetric sextet ϕ_{6_F} , while Λ_Q baryon is flavor-antisymmetric antitriplet $\phi_{\bar{3}_F}$. In Eq.(27), $\Phi_{l_\rho, l_\lambda, L}^c$ is the spatial wave function which is constructed from the wave functions of the two Jacobi coordinates ρ and λ , and takes the form

$$\Phi_{l_\rho, l_\lambda, L}^c = \left[\phi_{l_\rho m_{l_\rho}}(\mathbf{r}_{\rho_c}) \phi_{l_\lambda m_{l_\lambda}}(\mathbf{r}_{\lambda_c}) \right]_L \quad c = 1, 2, 3 \quad (28)$$

In this work, the spatial wave function of a three-body system is expanded in terms of a set of Gaussian basis functions. Thus, $\phi_{l_\rho m_{l_\rho}}(\mathbf{r}_{\rho c})$ and $\phi_{l_\lambda m_{l_\lambda}}(\mathbf{r}_{\lambda c})$ in Eq.(28) are written as,

$$\phi_{n_\rho l_\rho m_{l_\rho}}(\mathbf{r}_{\rho c}) = N_{n_\rho l_\rho} r_{\rho c}^{l_\rho} e^{-\nu_{n_\rho} r_{\rho c}^2} Y_{l_\rho m_{l_\rho}}(\hat{\mathbf{r}}_{\rho c}) \quad (29)$$

$$\phi_{n_\lambda l_\lambda m_{l_\lambda}}(\mathbf{r}_{\lambda c}) = N_{n_\lambda l_\lambda} r_{\lambda c}^{l_\lambda} e^{-\nu_{n_\lambda} r_{\lambda c}^2} Y_{l_\lambda m_{l_\lambda}}(\hat{\mathbf{r}}_{\lambda c}) \quad (30)$$

with

$$N_{n_\rho l_\rho} = \sqrt{\frac{2^{l_\rho+2} (2\nu_{n_\rho})^{l_\rho+3/2}}{\sqrt{\pi} (2l_\rho+1)!!}} \quad (31)$$

$$N_{n_\lambda l_\lambda} = \sqrt{\frac{2^{l_\lambda+2} (2\nu_{n_\lambda})^{l_\lambda+3/2}}{\sqrt{\pi} (2l_\lambda+1)!!}} \quad (32)$$

$$\nu_{n_\rho} = \frac{1}{r_{n_\rho}^2}, \quad r_{n_\rho} = r_{a1} \left[\frac{r_{n_{amax}}}{r_{a1}} \right]^{\frac{n-1}{n_{amax}-1}} \quad (n = 1, \dots, n_{amax}) \quad (33)$$

$$\nu_{n_\lambda} = \frac{1}{r_{n_\lambda}^2}, \quad r_{n_\lambda} = r_{b1} \left[\frac{r_{n_{bmax}}}{r_{b1}} \right]^{\frac{n-1}{n_{bmax}-1}} \quad (n = 1, \dots, n_{bmax}) \quad (34)$$

In momentum space, the Gaussian basis functions can be written as,

$$\phi_{n_\rho l_\rho m_{l_\rho}}(\mathbf{p}_{\rho c}) = N'_{n_\rho l_\rho} p_{\rho c}^{l_\rho} e^{-\frac{p_{\rho c}^2}{4\nu_{n_\rho}}} Y_{l_\rho m_{l_\rho}}(\hat{\mathbf{p}}_{\rho c}) \quad (35)$$

$$\phi_{n_\lambda l_\lambda m_{l_\lambda}}(\mathbf{p}_{\lambda c}) = N'_{n_\lambda l_\lambda} p_{\lambda c}^{l_\lambda} e^{-\frac{p_{\lambda c}^2}{4\nu_{n_\lambda}}} Y_{l_\lambda m_{l_\lambda}}(\hat{\mathbf{p}}_{\lambda c}) \quad (36)$$

with

$$N'_{n_\rho l_\rho} = (-i)^{l_\rho} \sqrt{\frac{2^{l_\rho+2}}{\sqrt{\pi} (2\nu_{n_\rho})^{l_\rho+3/2} (2l_\rho+1)!!}} \quad (37)$$

$$N'_{n_\lambda l_\lambda} = (-i)^{l_\lambda} \sqrt{\frac{2^{l_\lambda+2}}{\sqrt{\pi} (2\nu_{n_\lambda})^{l_\lambda+3/2} (2l_\lambda+1)!!}} \quad (38)$$

An important property in the dynamics of a single heavy baryon system is the heavy quark symmetry. In the heavy quark limit, one heavy quark within the heavy baryon system is decoupled from two light quarks. Under this picture, the interactions which depend on the spin of the heavy quark disappear. Thus, two states whose quantum number are $J = j + 1/2$ and $J = j - 1/2$ will be degenerate, where j denotes the light-spin-component. It can be seen from Fig.1 that the picture of Jacobi coordinate channel 3 properly reflects the characteristic of the heavy quark symmetry. As it is showed in Fig.1, the degree of freedom between two light quarks is commonly called the ρ -mode, while the

degree between the center of mass of two light quarks and the heavy quark is called the λ -mode. In the SU(3) limit in the light quark sector, the λ - and ρ -modes are mixed. While in the heavy quark limit, it was indicated by Ref.[21] that the excitation energy of the λ -mode is lower than that of the ρ -mode for the P -wave baryon. They drew the conclusion that the lowest state of a P -wave single heavy baryon is dominated by the λ -mode. The first motivation of our present work is to further study the mass spectra of different excitation modes, λ -mode, ρ -mode and λ - ρ mixing mode, with higher orbital excitation. Basing on these above considerations, we perform our calculations in the channel 3 and rewrite the full wave function of a single heavy baryon as,

$$\Psi_{full}^{JM} = \sum_{n_\rho, n_\lambda} C_{n_\rho, n_\lambda} \Psi_{JM}^3(\mathbf{r}_{\rho 3}, \mathbf{r}_{\lambda 3}) \quad (39)$$

2.3 Evaluation of matrix elements

In the calculations of the Hamiltonian matrix elements of three-body system, particularly when complicated interactions are employed, integrations over all of the radial and angular coordinates become laborious even with Gaussian basis functions. This process can be simplified by introducing the infinitesimally-shifted Gaussian basis functions. For Jacobi coordinates ρ and λ in channel 3, these new sets of basis functions can be written as[114],

$$\phi_{n_\rho l_\rho m_{l_\rho}}(\mathbf{r}_\rho) = N_{n_\rho l_\rho} \lim_{\varepsilon \rightarrow 0} \frac{1}{(\nu_{n_\rho} \varepsilon)^{l_\rho}} \sum_{k=1}^{k_{max}} C_{l_\rho m_{l_\rho}, k} e^{-\nu_{n_\rho} (\mathbf{r}_\rho - \varepsilon \mathbf{D}_{l_\rho m_{l_\rho}, k})^2} \quad (40)$$

$$\phi_{n_\lambda l_\lambda m_{l_\lambda}}(\mathbf{r}_\lambda) = N_{n_\lambda l_\lambda} \lim_{\varepsilon \rightarrow 0} \frac{1}{(\nu_{n_\lambda} \varepsilon)^{l_\lambda}} \sum_{K=1}^{K_{max}} C_{l_\lambda m_{l_\lambda}, K} e^{-\nu_{n_\lambda} (\mathbf{r}_\lambda - \varepsilon \mathbf{D}_{l_\lambda m_{l_\lambda}, K})^2} \quad (41)$$

where ε is the shifted distance of the Gaussian basis. Taking the limit $\varepsilon \rightarrow 0$ is to be carried out after the matrix elements have been calculated analytically. The coefficient $C_{lm,k}$ and the shift-direction vector $\mathbf{D}_{lm,k}$ are dimensionless numbers independent of ν_n and ε , and they can be described as,

$$C_{lm,k} \equiv \sum_{j=0}^{\lfloor \frac{l-m}{2} \rfloor} A_{lm,j} \sum_{s=0}^p \sum_{t=0}^q \sum_{u=0}^j (-1)^{l-u-t-s} \binom{p}{s} \binom{q}{t} \binom{j}{u} \quad (42)$$

where $p = l - m - 2j$, $q = j + m$ and

$$\mathbf{D}_{lm,k} \equiv \frac{1}{l} [(2s - p)\mathbf{a}_z + (2t - q)\mathbf{a}_{xy} + (2u - j)\mathbf{a}_{xy}^*] \quad (43)$$

with

$$A_{lm,j} = \left[\frac{(2l+1)(l-m)!}{4\pi(l+m)!} \right]^{\frac{1}{2}} \frac{(l+m)!(-1)^j}{(-2)^m 4^j j!(m+j)!(l-m-2j)!} \quad (44)$$

In Eq.(43) \mathbf{a}_z , \mathbf{a}_{xy} and \mathbf{a}_{xy}^* are called the shift vectors which are defined as $\mathbf{a}_z \equiv (0, 0, 1)$, $\mathbf{a}_{xy} \equiv (1, i, 0)$, $\mathbf{a}_{xy}^* \equiv (1, -i, 0)$. For relation(43) and Eq.(44), when $m < 0$, we should change $A_{lm,j} \rightarrow (-1)^m A_{l-m,j}$ and $\mathbf{D} \rightarrow \mathbf{D}^*$.

In the following, we show how to obtain matrix elements of the various pieces of the Hamiltonian in the Jacobi coordinate channel 3. For most of the terms in the Hamiltonian, they are the form of $\tilde{H}_{ij}(\mathbf{r}_{ij})$, and so we have to integrate functions of \mathbf{r}_{12} , \mathbf{r}_{13} and \mathbf{r}_{23} , where $\mathbf{r}_{12} = \mathbf{r}_{\rho_3}$, $\mathbf{r}_{13} = \mathbf{r}_{\rho_2}$ and $\mathbf{r}_{23} = \mathbf{r}_{\rho_1}$ in three Jacobi coordinate channels, respectively. The matrix element of $\tilde{G}(\mathbf{r}_{12})$ which is independent of spin and orbital,

$$\begin{aligned} & \langle [\phi_{n_{\rho_a} l_{\rho_a} m_{l_{\rho_a}}}(\mathbf{r}_{\rho_3}) \phi_{n_{\lambda_a} l_{\lambda_a} m_{l_{\lambda_a}}}(\mathbf{r}_{\lambda_3})]_L | \tilde{G}(\mathbf{r}_{12}) | [\phi_{n_{\rho_b} l_{\rho_b} m_{l_{\rho_b}}}(\mathbf{r}_{\rho_3}) \phi_{n_{\lambda_b} l_{\lambda_b} m_{l_{\lambda_b}}}(\mathbf{r}_{\lambda_3})]_L \rangle \\ &= \langle [\phi_{n_{\rho_a} l_{\rho_a} m_{l_{\rho_a}}}(\mathbf{r}_{\rho_3}) \phi_{n_{\lambda_a} l_{\lambda_a} m_{l_{\lambda_a}}}(\mathbf{r}_{\lambda_3})]_L | \tilde{G}(\mathbf{r}_{\rho_3}) | [\phi_{n_{\rho_b} l_{\rho_b} m_{l_{\rho_b}}}(\mathbf{r}_{\rho_3}) \phi_{n_{\lambda_b} l_{\lambda_b} m_{l_{\lambda_b}}}(\mathbf{r}_{\lambda_3})]_L \rangle \end{aligned} \quad (45)$$

can be calculated directly. The matrix elements of $\tilde{G}(\mathbf{r}_{13})$ and $\tilde{G}(\mathbf{r}_{23})$ can be expressed as,

$$\langle [\phi_{n_{\rho_a} l_{\rho_a} m_{l_{\rho_a}}}(\mathbf{r}_{\rho_3}) \phi_{n_{\lambda_a} l_{\lambda_a} m_{l_{\lambda_a}}}(\mathbf{r}_{\lambda_3})]_L | \tilde{G}(\mathbf{r}_{\rho_k}) | [\phi_{n_{\rho_b} l_{\rho_b} m_{l_{\rho_b}}}(\mathbf{r}_{\rho_3}) \phi_{n_{\lambda_b} l_{\lambda_b} m_{l_{\lambda_b}}}(\mathbf{r}_{\lambda_3})]_L \rangle_{k=1,2} \quad (46)$$

We have to perform the integration over \mathbf{r}_{ρ_1} or \mathbf{r}_{ρ_2} in channel 3, which requires the Jacobi coordinate transformations $(\mathbf{r}_{\rho_3}, \mathbf{r}_{\lambda_3}) \rightarrow (\mathbf{r}_{\rho_k}, \mathbf{r}_{\lambda_k})_{k=1,2}$. Then, the infinitesimally-shifted Gaussian basis functions in channels 3 are expressed in Jacobi coordinates $(\mathbf{r}_{\rho_k}, \mathbf{r}_{\lambda_k})_{k=1,2}$. The structure of the final expression of the matrix elements about Eqs.(45) and (46) are illustrated explicitly in **Appendix A.1**.

For the kinetic energy terms, they can easily be derived that the momentum of each quark can be expressed by relative momentum in baryon center-of-momentum frame, where $\mathbf{p}_1 = \mathbf{p}_{\lambda_1}$, $\mathbf{p}_2 = \mathbf{p}_{\lambda_2}$, $\mathbf{p}_3 = \mathbf{p}_{\lambda_3}$. Then the calculation of kinetic energy matrix element,

$$\begin{aligned} & \langle [\phi_{n_{\rho_a} l_{\rho_a} m_{l_{\rho_a}}}(\mathbf{p}_{\rho_3}) \phi_{n_{\lambda_a} l_{\lambda_a} m_{l_{\lambda_a}}}(\mathbf{p}_{\lambda_3})]_L | \sqrt{\mathbf{p}_3^2 + m_3^2} | [\phi_{n_{\rho_b} l_{\rho_b} m_{l_{\rho_b}}}(\mathbf{p}_{\rho_3}) \phi_{n_{\lambda_b} l_{\lambda_b} m_{l_{\lambda_b}}}(\mathbf{p}_{\lambda_3})]_L \rangle \\ &= \langle [\phi_{n_{\rho_a} l_{\rho_a} m_{l_{\rho_a}}}(\mathbf{p}_{\rho_3}) \phi_{n_{\lambda_a} l_{\lambda_a} m_{l_{\lambda_a}}}(\mathbf{p}_{\lambda_3})]_L | \sqrt{\mathbf{p}_{\lambda_3}^2 + m_3^2} | [\phi_{n_{\rho_b} l_{\rho_b} m_{l_{\rho_b}}}(\mathbf{p}_{\rho_3}) \phi_{n_{\lambda_b} l_{\lambda_b} m_{l_{\lambda_b}}}(\mathbf{p}_{\lambda_3})]_L \rangle \end{aligned} \quad (47)$$

is straightforward. For the kinetic energy terms $\sqrt{\mathbf{p}_k^2 + m_k^2}_{k=1,2}$, their matrix elements can be described as,

$$\langle [\phi_{n_{\rho_a} l_{\rho_a} m_{l_{\rho_a}}}(\mathbf{p}_{\rho_3}) \phi_{n_{\lambda_a} l_{\lambda_a} m_{l_{\lambda_a}}}(\mathbf{p}_{\lambda_3})]_L | \sqrt{\mathbf{p}_{\lambda_k}^2 + m_k^2} | [\phi_{n_{\rho_b} l_{\rho_b} m_{l_{\rho_b}}}(\mathbf{p}_{\rho_3}) \phi_{n_{\lambda_b} l_{\lambda_b} m_{l_{\lambda_b}}}(\mathbf{p}_{\lambda_3})]_L \rangle_{k=1,2} \quad (48)$$

By performing the Jacobi momentum transformations, $(\mathbf{p}_{\rho_3}, \mathbf{p}_{\lambda_3}) \rightarrow (\mathbf{p}_{\rho_k}, \mathbf{p}_{\lambda_k})_{k=1,2}$ over the basis function in momentum representation, we can carry out the calculations about the matrix elements of Eq.(48). And the expression of kinetic energy matrix elements are explicitly described in **Appendix A.2**. Another problem we have to deal with is the matrix elements of the momentum-dependent factors in the Hamiltonian which are combined with spatially dependent potentials such as Eqs.20-23. This problem can be overcome by inserting complete sets of Gaussian functions between the two types of operators. Then the matrix element of the momentum-dependent factor can be evaluated just as the calculations of the kinetic energy terms in momentum space, and the position-dependent parts are obtained in the coordinate space. As for the color matrix element, the matrix elements of spin-spin and spin-orbit terms, they can easily be obtained by using the results of potential energy matrix elements. The explicit structures of these matrix elements are illustrated in **Appendixes A.3-A.4**.

Finally, it only remains to discuss how we deal with the tensor term in Hamiltonian. We first evaluate the matrix element of the tensor term in spin space,

$$\langle \chi_{s41} | \mathbf{S}_1 \cdot \hat{\mathbf{r}}_\rho \mathbf{S}_2 \cdot \hat{\mathbf{r}}_\rho | \chi_{s41} \rangle = \langle \chi_{s44} | \mathbf{S}_1 \cdot \hat{\mathbf{r}}_\rho \mathbf{S}_2 \cdot \hat{\mathbf{r}}_\rho | \chi_{s44} \rangle = \frac{\cos^2 \theta}{4} \quad (49)$$

$$\langle \chi_{s42} | \mathbf{S}_1 \cdot \hat{\mathbf{r}}_\rho \mathbf{S}_2 \cdot \hat{\mathbf{r}}_\rho | \chi_{s42} \rangle = \langle \chi_{s43} | \mathbf{S}_1 \cdot \hat{\mathbf{r}}_\rho \mathbf{S}_2 \cdot \hat{\mathbf{r}}_\rho | \chi_{s43} \rangle = \frac{1}{24}(1 - 3\cos 2\theta) \quad (50)$$

$$\langle \chi_{s21} | \mathbf{S}_1 \cdot \hat{\mathbf{r}}_\rho \mathbf{S}_2 \cdot \hat{\mathbf{r}}_\rho | \chi_{s21} \rangle = \langle \chi_{s22} | \mathbf{S}_1 \cdot \hat{\mathbf{r}}_\rho \mathbf{S}_2 \cdot \hat{\mathbf{r}}_\rho | \chi_{s22} \rangle = \frac{1}{12} \quad (51)$$

$$\langle \chi_{As21} | \mathbf{S}_1 \cdot \hat{\mathbf{r}}_\rho \mathbf{S}_2 \cdot \hat{\mathbf{r}}_\rho | \chi_{As21} \rangle = \langle \chi_{As22} | \mathbf{S}_1 \cdot \hat{\mathbf{r}}_\rho \mathbf{S}_2 \cdot \hat{\mathbf{r}}_\rho | \chi_{As22} \rangle = -\frac{1}{4} \quad (52)$$

where $\chi_{s41}, \chi_{s42}, \chi_{s43}, \chi_{s44}$ are the total spin wave functions of a baryon, which are symmetric quadruplet state, $\chi_{s21}, \chi_{s22}, \chi_{As21}$ and χ_{As22} are the mixed symmetric/antisymmetric states. These spin wave functions and a few relations used in deriving Eqs.(49)-(52) are presented in **Appendix A.5**. Finally, the remaining angular part in Eqs.(49)-(52) can be integrated together with the spatial part.

When all of the matrix elements, which are presented in **Appendixes A.1-A.4**, have been worked out, the mass spectra can be obtained by solving the generalized eigenvalue problem,

$$\sum_{j=1}^{n_{max}^2} (H_{ij} - EN_{ij}) C_j = 0, \quad (i = 1 - n_{max}^2) \quad (53)$$

Where H_{ij} denotes the matrix element in the total color-flavor-spin-spatial base, E is the eigenvalue, C_j stands for the corresponding eigenvector, and N_{ij} is the overlap matrix elements of the Gaussian functions, which arises from the nonorthogonality of the bases and can be expressed as,

$$\begin{aligned} N_{ij} &\equiv \langle \phi_{n_{\rho_a} l_{\rho_a} m_{l_{\rho_a}}} | \phi_{n_{\rho_b} l_{\rho_b} m_{l_{\rho_b}}} \rangle \times \langle \phi_{n_{\lambda_a} l_{\lambda_a} m_{l_{\lambda_a}}} | \phi_{n_{\lambda_b} l_{\lambda_b} m_{l_{\lambda_b}}} \rangle \\ &= \left(\frac{2\sqrt{\nu_{n_{\rho_a}} \nu_{n_{\rho_b}}}}{\nu_{n_{\rho_a}} + \nu_{n_{\rho_b}}} \right)^{l_{\rho_a} + 3/2} \times \left(\frac{2\sqrt{\nu_{n_{\lambda_a}} \nu_{n_{\lambda_b}}}}{\nu_{n_{\lambda_a}} + \nu_{n_{\lambda_b}}} \right)^{l_{\lambda_a} + 3/2} \end{aligned} \quad (54)$$

2.4 Mass spectra of the single heavy baryon Λ_Q, Σ_Q and Ω_Q

TABLE II: Relevant parameters of the relativized quark model

$m_u/m_d(\text{MeV})$	$m_s(\text{MeV})$	$m_c(\text{MeV})$	$m_b(\text{MeV})$	α_1	α_2
220	419	1628	4997	0.25	0.15
α_3	$\gamma_1(\text{GeV})$	$\gamma_2(\text{GeV})$	$\gamma_3(\text{GeV})$	$b(\text{GeV}^2)$	$c(\text{MeV})$
0.20	$\frac{1}{2}$	$\sqrt{10}/2$	$\sqrt{1000}/2$	0.14	-198
$\sigma_0(\text{GeV})$	s	ϵ_c	ϵ_v	ϵ_t	ϵ_s
1.8	1.55	-0.168	-0.035	0.025	0.055

Most of the parameters used in this work are taken from the original reference[18] and they are all collected in Table II for convenience. To reproduce the lowest-lying baryon mass spectra, we repair

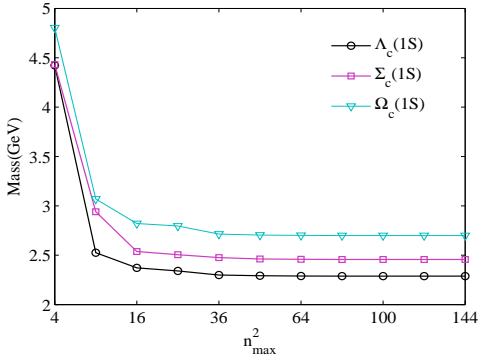


FIG. 2: Convergence of the energy of the lowest Λ_c , Σ_c and Ω_c for increasing the number of bases functions.

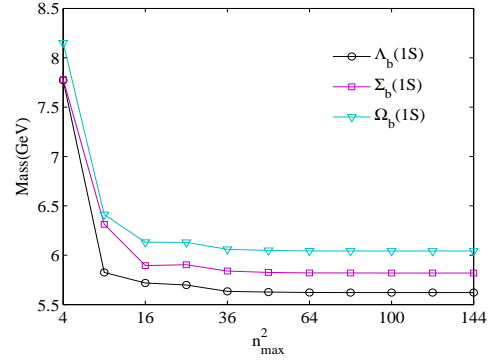


FIG. 3: Convergence of the energy of the lowest Λ_b , Σ_b and Ω_b for increasing the number of bases functions.

the values of parameters b and c in the line confining potential from 0.18 and -253 to 0.14 and -198 . In the relativized quark model, it is important to ensure the stability of the numerical results. This problem depends strongly on the number of bases. Theoretically, the number of bases should be large enough to guarantee approximate completeness, otherwise the numerical results are not reliable. In order to investigate the convergence and stability of the numerical results, we plot the eigen-energy of the lowest lying $\Lambda_Q(\frac{1}{2}^+)$, $\Sigma_Q(\frac{1}{2}^+)$ and $\Omega_Q(\frac{1}{2}^+)$ baryons in Figs.2-3. We can see that the eigenvalues decrease with the basis number and converge to a stable value when the $n_{max}^2 = 10^2$. Thus, it is enough for us to obtain the mass spectra with 10^2 Gaussian bases in present work.

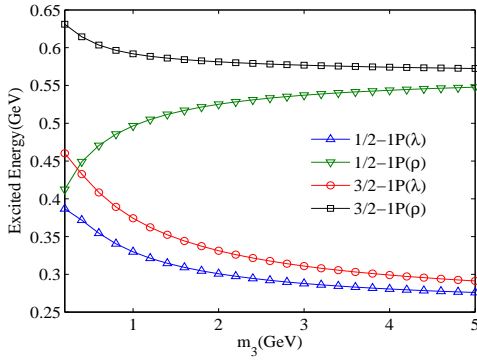


FIG. 4: Heavy quark mass dependence of excited energy of $1P \Lambda_Q(\frac{1}{2}^-, \frac{3}{2}^-)$ with λ mode and ρ mode

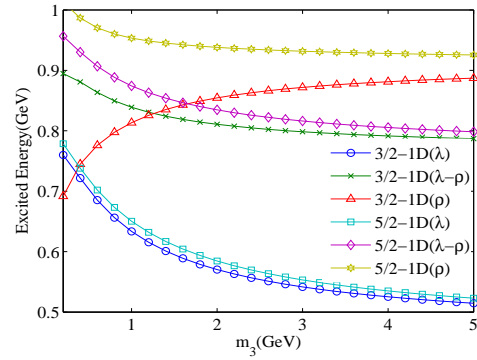


FIG. 5: Heavy quark mass dependence of excited energy of $1D \Lambda_Q(\frac{3}{2}^+, \frac{5}{2}^+)$ with λ mode, ρ mode and λ - ρ mixing mode

As discussed in Sec.2.2, the baryons have different excitation modes, λ -mode, ρ -mode and λ - ρ mixing mode. In the scheme of channel 3, the orbital angular momentum between the two light

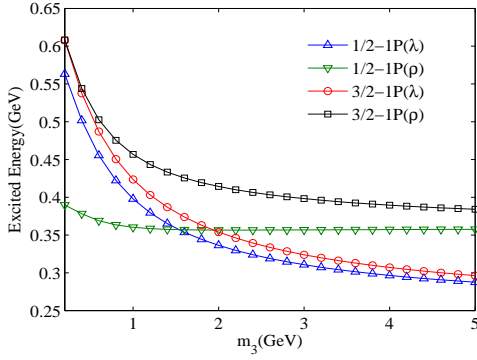


FIG. 6: Heavy quark mass dependence of excited energy of $1P \Sigma_Q(\frac{1}{2}^-, \frac{3}{2}^-)$ with λ mode and ρ mode

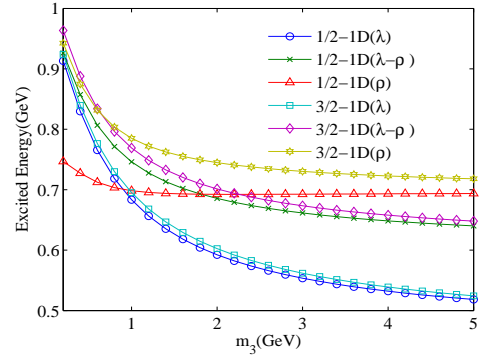


FIG. 7: Heavy quark mass dependence of excited energy of $1D \Sigma_Q(\frac{1}{2}^+, \frac{3}{2}^+)$ with λ mode, ρ mode and λ - ρ mixing mode

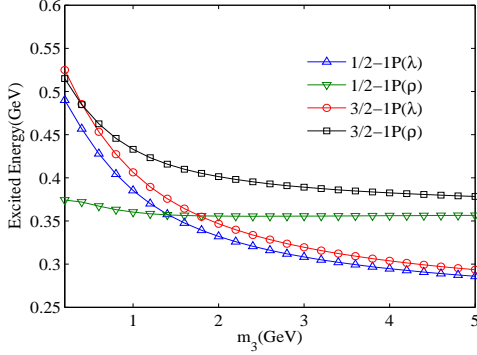


FIG. 8: Heavy quark mass dependence of excited energy of $1P \Omega_Q(\frac{1}{2}^-, \frac{3}{2}^-)$ with λ mode and ρ mode.

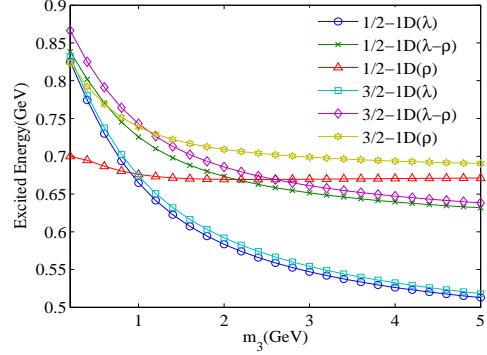


FIG. 9: Heavy quark mass dependence of excited energy of $1D \Omega_Q(\frac{1}{2}^+, \frac{3}{2}^+)$ with λ mode, ρ mode and λ - ρ mixing mode

quarks is denoted by l_ρ , while the angular momentum between the light diquarks and the heavy quark is denoted by l_λ . For P -wave baryons, there are two orbital excitation modes λ - and ρ -mode with $(l_\rho, l_\lambda) = (0, 1)$ and $(1, 0)$ respectively. While there are three excitation modes for D -wave baryon with $(l_\rho, l_\lambda) = (0, 2)$, $(2, 0)$ and $(1, 1)$, which are called the λ -mode, ρ -mode and λ - ρ mixing mode, respectively. For higher angular excited states, they are similar with the D -wave baryon, which also have three excitation modes. To investigate the mass spectra of these different excitation modes, we change the heavy quark mass m_Q , from 0.2 GeV to 5.0 GeV and analyze their excitation energies. Figs.4-9 show the spectra of Λ_Q , Σ_Q and Ω_Q systems. We can see that as m_Q becomes large, the λ -mode appears lower in excited energy than both the ρ -mode and λ - ρ mixing mode for these single heavy baryons. This indicates the lowest state becomes dominated by the λ -mode as m_Q becomes large whether for P - or D -wave baryon. In Figs.4, 5, 7 and 9, the λ dominance is seen at about $m_Q = 0.4$ GeV for

Λ_Q and $m_Q = 1.0$ GeV for D -wave Σ_Q and Ω_Q . For P -wave Σ_Q and Ω_Q systems(Figs.6 and 8), although λ and ρ excited modes are separated more slowly than the former, the λ dominance is also seen at about $m_Q \geq 1.6$ GeV. From these figures, another property which is the heavy quark spin symmetry(HQS) is clearly displayed. For P -wave Λ_Q as an example in Fig.4, when m_Q increases from 0.2 GeV to 5.0 GeV, the splitting of the spin-doublet ($\frac{1}{2}^-$, $\frac{3}{2}^-$) of λ excitation mode decreases from 80 MeV to 10 MeV. And this behavior is more obvious for P -wave Λ_Q with ρ -mode.

A. Λ_Q states

From these above discussions, we know that each state of the single heavy baryons is dominated and characterized by the λ -mode. Thus, we obtain the mass spectra of the Λ_Q , Σ_Q , and Ω_Q baryons with λ excitation mode. Our predictions for the mass spectra of the ground and excited states are shown in Tables III-VIII, while the predictions from a number of other models are also shown in these tables. In the first two columns of these tables we give the baryon quantum numbers ($l_\rho l_\lambda L s j$) and $nL(J^P)$, while in the remaining columns our results, experimental data and the results from other models are shown.

It can be seen from Tables III-IV, the available experimental data for Λ_Q states are well reproduced by the quark model in present work. There are a few observed states, $\Lambda_c(2765)$, $\Lambda_c(2940)$ and $\Lambda_b(6070)$, whose spin and parity have not been confirmed in the latest PDG[5, 6]. Our prediction for the mass of $2S(\frac{1}{2}^+)$ state is 2.764 GeV, which is very close to the experimental data for $\Lambda_c(2765)$. Thus, it is reasonable to describe $\Lambda_c(2765)$ as a $2S(\frac{1}{2}^+)$ state. In the latest PDG, the spin parity of $\Lambda_c(2940)$ was suggested to be $J^P = \frac{3}{2}^-$, but was not confirmed. Model predictions for $2P(\frac{1}{2}^-)$ and $2P(\frac{3}{2}^-)$ states are 2.988 GeV and 3.013 GeV, respectively. By comparing with the experimental data, the $2P(\frac{1}{2}^-)$ state seems to be a better candidate for $\Lambda_c(2940)$ than $2P(\frac{3}{2}^-)$. Although, the predicted mass for $2P(\frac{1}{2}^-)$ baryon is about 50 MeV higher than the experimental data, this assignment is now the best choice for $\Lambda_c(2940)$. This notable exception to this state is also seen in the predictions in Ref.[19]. For $\Lambda_b(6070)$, its quantum numbers were suggested to be $2S(\frac{1}{2}^+)$ in Refs.[76, 115]. Our prediction for this state is 6.041 GeV, which is 29 MeV lighter than the experimental data. Under the uncertainties of the model, this result is still within the realm of validity for model like these. Thus, we agree with the conclusion that $\Lambda_b(6070)$ is the first radial excitation of the Λ_b baryon with the quantum numbers $2S(\frac{1}{2}^+)$.

Besides of these above states, some other low-lying Λ_Q states are also predicted in present work, which have not been observed in experiments. First, it is the $2P$ -wave $\Lambda_c(\frac{3}{2}^-)$ state which belongs to a spin-doublet ($\frac{1}{2}^-$, $\frac{3}{2}^-$) and its model predicted mass is 3.013 GeV. In addition, there are two Λ_b model states that still remain to be found in experiments. They are the partners of the $2P$ -wave doublet ($\frac{1}{2}^-$, $\frac{3}{2}^-$) of Λ_c , and their masses are predicted to be 6.238 GeV and 6.249 GeV

TABLE III: Masses of the Λ_c heavy baryons(in MeV)

$l_\rho l_\lambda L s j$	$nL(J^P)$	M	M_{exp}	[19]	[20]	[18]	[36]	[27]	[67, 76–78]
0 0 0 0 0	$1S(\frac{1}{2}^+)$	2288	2286.46[5]	2286	2268	2265	2272	2292	2240±90[76]
	$2S(\frac{1}{2}^+)$	2764	2766.6[5]	2769	2791	2775	2769	2669	2780±80[76]
	$3S(\frac{1}{2}^+)$	3022		3130					
	$4S(\frac{1}{2}^+)$	3135		3437					
0 1 1 0 1	$1P(\frac{1}{2}^-)$	2596	2592.25[5]	2598	2625	2630	2594	2559	2610±210[77]
	$2P(\frac{1}{2}^-)$	2988	2939.3[6]	2983	2816	2780	2853	2779	
	$3P(\frac{1}{2}^-)$	3253		3303					
	$4P(\frac{1}{2}^-)$	3308		3588					
0 1 1 0 1	$1P(\frac{3}{2}^-)$	2631	2628.1[5]	2627	2636	2640	2586	2559	2620±180[78]
	$2P(\frac{3}{2}^-)$	3013		3005	2830	2840	2874	2779	
	$3P(\frac{3}{2}^-)$	3277		3322					
	$4P(\frac{3}{2}^-)$	3325		3606					
0 2 2 0 2	$1D(\frac{3}{2}^+)$	2875	2856.1[5]	2874	2887	2910	2848	2906	2830 ⁺¹⁵⁰ ₋₂₄₀ [67]
	$2D(\frac{3}{2}^+)$	3220		3189	3073	3035	3100	3061	
	$3D(\frac{3}{2}^+)$	3479		3480					
	$4D(\frac{3}{2}^+)$	3497		3747					
0 2 2 0 2	$1D(\frac{5}{2}^+)$	2891	2881.63[5]	2880	2887	2910			2880 ⁺¹⁸⁰ ₋₂₉₀ [67]
	$2D(\frac{5}{2}^+)$	3234		3209					
	$3D(\frac{5}{2}^+)$	3492		3500					
	$4D(\frac{5}{2}^+)$	3509		3767					
0 3 3 0 3	$1F(\frac{5}{2}^-)$	3104		3097	2872	2900			
	$2F(\frac{5}{2}^-)$	3429		3375					
	$3F(\frac{5}{2}^-)$	3675		3646					
	$4F(\frac{5}{2}^-)$	3692		3900					
0 3 3 0 3	$1F(\frac{7}{2}^-)$	3111		3078					
	$2F(\frac{7}{2}^-)$	3435		3393					
	$3F(\frac{7}{2}^-)$	3685		3667					
	$4F(\frac{7}{2}^-)$	3699		3922					
0 4 4 0 4	$1G(\frac{7}{2}^+)$	3304		3270					
	$2G(\frac{7}{2}^+)$	3614		3546					
	$3G(\frac{7}{2}^+)$	3868							
	$4G(\frac{7}{2}^+)$	3883							
0 4 4 0 4	$1G(\frac{9}{2}^+)$	3306		3284					
	$2G(\frac{9}{2}^+)$	3615		3564					
	$3G(\frac{9}{2}^+)$	3873							
	$4G(\frac{9}{2}^+)$	3891							

TABLE IV: Masses of the Λ_b heavy baryons(in MeV)

$l_\rho l_\lambda L s j$	$nL(J^P)$	M	M_{exp}	[19]	[20]	[18]	[27]	[116]	[76, 77]
0 0 0 0 0	$1S(\frac{1}{2}^+)$	5622	5619.60[5]	5620	5612	5585	5624	5619.6	5610 ± 120 [76]
	$2S(\frac{1}{2}^+)$	6041	6072.3[5]	6089	6107				6080 ± 90 [76]
	$3S(\frac{1}{2}^+)$	6352		6455					
	$4S(\frac{1}{2}^+)$	6388		6756					
0 1 1 0 1	$1P(\frac{1}{2}^-)$	5898	5912.19[5]	5930	5939	5912	5890		5850 ± 180 [77]
	$2P(\frac{1}{2}^-)$	6238		6326	6180	5780	5853		
	$3P(\frac{1}{2}^-)$	6544		6645					
	$4P(\frac{1}{2}^-)$	6566		6917					
0 1 1 0 1	$1P(\frac{3}{2}^-)$	5913	5920.09[5]	5942	5941	5920	5890		
	$2P(\frac{3}{2}^-)$	6249		6333	6191	5840	5874		
	$3P(\frac{3}{2}^-)$	6552		6651					
	$4P(\frac{3}{2}^-)$	6575		6922					
0 2 2 0 2	$1D(\frac{3}{2}^+)$	6137	6146.2[5, 12, 139]	6190	6181	6145	6246		6010^{+200}_{-120} [66]
	$2D(\frac{3}{2}^+)$	6432		6526	6401				
	$3D(\frac{3}{2}^+)$	6705		6811					
	$4D(\frac{3}{2}^+)$	6757		7060					
0 2 2 0 2	$1D(\frac{5}{2}^+)$	6145	6152.5[5, 12, 139]	6196	6183	6165			6010^{+200}_{-130} [66]
	$2D(\frac{5}{2}^+)$	6440		6531	6422				
	$3D(\frac{5}{2}^+)$	6709		6814					
	$4D(\frac{5}{2}^+)$	6763		7063					
0 3 3 0 3	$1F(\frac{5}{2}^-)$	6338		6408	6206	6205			
	$2F(\frac{5}{2}^-)$	6616		6705					
	$3F(\frac{5}{2}^-)$	6849		6964					
	$4F(\frac{5}{2}^-)$	6932		7196					
0 3 3 0 3	$1F(\frac{7}{2}^-)$	6343		6411					
	$2F(\frac{7}{2}^-)$	6622		6708					
	$3F(\frac{7}{2}^-)$	6852		6966					
	$4F(\frac{7}{2}^-)$	6936		7197					
0 4 4 0 4	$1G(\frac{7}{2}^+)$	6514		6598	6433				
	$2G(\frac{7}{2}^+)$	6793		6867					
	$3G(\frac{7}{2}^+)$	6986							
	$4G(\frac{7}{2}^+)$	7093							
0 4 4 0 4	$1G(\frac{9}{2}^+)$	6517		6599					
	$2G(\frac{9}{2}^+)$	6798		6868					
	$3G(\frac{9}{2}^+)$	6989							
	$4G(\frac{9}{2}^+)$	7095							

B. Σ_Q states

The lowest states of S -wave Σ_c and Σ_b baryons with the quantum numbers $J^P = \frac{1}{2}^+$ and $J^P = \frac{3}{2}^+$ have been observed and confirmed in experiments[5]. In Tables V-VI, it can be seen that the model predictions for these S -wave Σ_Q baryons also agree well with the experimental data. In addition, quark model predicts two spin doublets $(\frac{1}{2}^-, \frac{3}{2}^-)$, $(\frac{3}{2}^-, \frac{5}{2}^-)$ and a singlet $\frac{1}{2}^-$ for $1P$ -wave Σ_Q baryon. Up to now, all the $1P$ -wave Λ_Q baryons have been discovered and confirmed, however few P -wave Σ_Q baryons have been reported in experiments. The previously observed $\Sigma_c(2800)$ and $\Sigma_b(6097)$ states are good candidates for the P -wave states. We can see from Tables V-VI that the predicted masses of the lowest P -wave states are very close to each other and they are all comparable with the experimental data for $\Sigma_c(2800)$ or $\Sigma_b(6097)$. It is shown in Table V, there are two states whose masses are closer to the experimental result of $\Sigma_c(2800)$, namely, the states $1P(\frac{1}{2}^-)_{j=1}$ with a mass 2.809 GeV and $1P(\frac{3}{2}^-)_{j=2}$ with 2.802 GeV. We will see in Sec.4, if the strong decay behaviors are considered, $1P(\frac{3}{2}^-)_{j=2}$ state is a better assignment for $\Sigma_c(2800)$. In Table VI, two Σ_b states $1P(\frac{1}{2}^-)_{j=1}$ and $1P(\frac{3}{2}^-)_{j=2}$ have masses 6.107 GeV and 6.104 GeV respectively, both excellent match to the experimental state $\Sigma_b(6097)$. It is same with $\Sigma_c(2800)$, the strong decay properties in Sec.4 support assigning $\Sigma_b(6097)$ as a $1P(\frac{3}{2}^-)_{j=2}$ state.

It can be seen from Tables V-VI, more efforts are needed in searching for Σ_Q baryons in experiments because many model predicted states are still missing. If the above assignments for $\Sigma_c(2800)$ and $\Sigma_b(6097)$ are reasonable, the other low-lying P -wave states have good potentials to be observed within the mass spectra predicted in present work. On the other hand, it is shown in Tables V-VI that the splitting between the $1P$ and $2S$ state is about 100 MeV, while the splitting between the five P -wave states ranges from several to 30 MeV. We hope these informations will be helpful for searching these $2S$ and $1P$ Σ_Q states in future experiments. Finally, the $1D$ -wave Σ_Q states are most likely to be observed in forthcoming experiments as well. The predicted masses range from 3.072 GeV to 3.084 GeV for $1D$ -wave Σ_c states and from 6.338 GeV to 6.346 GeV for Σ_b ones.

C. Ω_Q states

For Ω_Q systems, there are only three states, the lowest S -wave Ω_c doublet $(\frac{1}{2}^+, \frac{3}{2}^+)$ and $1S$ -wave $\Omega_b(\frac{1}{2}^+)$, that have been discovered and confirmed[5]. In Tables VII-VIII, it can be seen that the known Ω_Q states are well reproduced by the quark model. However, the predicted $1S(\frac{3}{2}^+)$ Ω_b state with a mass of 6.069 GeV still remains to be found. In the last few years, several new Ω_c and Ω_b states were observed, they are $\Omega_c(3000)$, $\Omega_c(3050)$, $\Omega_c(3066)$, $\Omega_c(3090)$, $\Omega_c(3119)$ [16], $\Omega_b(6316)$, $\Omega_b(6330)$, $\Omega_b(6340)$ and $\Omega_b(6350)$ [15]. Model prediction for the Ω_c state of $2S(\frac{1}{2}^+)$ is 3.150 GeV, which is close to $\Omega_c(3119)$. If model uncertainties are considered, $\Omega_c(3119)$ can be interpreted as a $2S(\frac{1}{2}^+)$ state. The other four Ω_c baryons can be assigned as the lowest P -wave states because their measured masses are compatible with model predictions in Table VII. For the $1P$ -wave Ω_c doublets

TABLE V: Masses of the Σ_c heavy baryons(in MeV)

$l_\rho l_\lambda L s j$	$nL(J^P)$	M	M_{exp}	[19]	[20]	[18]	[36]	[27]	[64, 79]
0 0 0 1 1	$1S(\frac{1}{2}^+)$	2457	2453.8[5]	2443	2455	2440	2459	2448	2400±260[79]
	$2S(\frac{1}{2}^+)$	2913		2901	2958	2890	2947	2793	
	$3S(\frac{1}{2}^+)$	3088		3271					
	$4S(\frac{1}{2}^+)$	3295		3581					
0 0 0 1 1	$1S(\frac{3}{2}^+)$	2532	2518.5[5]	2519	2519	2495	2539	2505	
	$2S(\frac{3}{2}^+)$	2967		2936	2995	2985	3010	2825	
	$3S(\frac{3}{2}^+)$	3135		3293					
	$4S(\frac{3}{2}^+)$	3328		3598					
0 1 1 1 0	$1P(\frac{1}{2}^-)$	2823		2799					
	$2P(\frac{1}{2}^-)$	3196		3172					
	$3P(\frac{1}{2}^-)$	3353		3488					
	$4P(\frac{1}{2}^-)$	3511		3770					
0 1 1 1 1	$1P(\frac{1}{2}^-)$	2809		2713	2748	2765	2769	2706	2740±200[64]
	$2P(\frac{1}{2}^-)$	3185		3125	2768	2770	2817	2791	
	$3P(\frac{1}{2}^-)$	3343		3455					
	$4P(\frac{1}{2}^-)$	3501		3743					
0 1 1 1 1	$1P(\frac{3}{2}^-)$	2829		2798					
	$2P(\frac{3}{2}^-)$	3202		3172					
	$3P(\frac{3}{2}^-)$	3358		3486					
	$4P(\frac{3}{2}^-)$	3516		3768					
0 1 1 1 2	$1P(\frac{3}{2}^-)$	2802	2806[5]	2773	2763	2770	2799	2706	2740±200[64]
	$2P(\frac{3}{2}^-)$	3179		3151	2776	2805	2815	2791	
	$3P(\frac{3}{2}^-)$	3338		3469					
	$4P(\frac{3}{2}^-)$	3496		3753					
0 1 1 1 2	$1P(\frac{5}{2}^-)$	2835		2789	2790	2815			
	$2P(\frac{5}{2}^-)$	3207		3161					
	$3P(\frac{5}{2}^-)$	3362		3475					
	$4P(\frac{5}{2}^-)$	3521		3757					
0 2 2 1 1	$1D(\frac{1}{2}^+)$	3073		3041					
	$2D(\frac{1}{2}^+)$	3413		3370					
	$3D(\frac{1}{2}^+)$	3558							
	$4D(\frac{1}{2}^+)$	3696							
0 2 2 1 1	$1D(\frac{3}{2}^+)$	3084		3043					
	$2D(\frac{3}{2}^+)$	3422		3366					
	$3D(\frac{3}{2}^+)$	3567							
	$4D(\frac{3}{2}^+)$	3709							
0 2 2 1 2	$1D(\frac{3}{2}^+)$	3073		3040					
	$2D(\frac{3}{2}^+)$	3413		3364					
	$3D(\frac{3}{2}^+)$	3558							
	$4D(\frac{3}{2}^+)$	3696							
0 2 2 1 2	$1D(\frac{5}{2}^+)$	3085		3038	3003	3065			
	$2D(\frac{5}{2}^+)$	3423		3365					

$l_\rho l_\lambda L s j$	$nL(J^P)$	M	[19]	$l_\rho l_\lambda L s j$	$nL(J^P)$	M	[19]
0 2 2 1 3	$1D(\frac{5}{2}^+)$	3072	3023	0 3 3 1 4	$1F(\frac{7}{2}^-)$	3299	3227
	$2D(\frac{5}{2}^+)$	3411	3349		$2F(\frac{7}{2}^-)$	3616	
	$3D(\frac{5}{2}^+)$	3557			$3F(\frac{7}{2}^-)$	3755	
	$4D(\frac{5}{2}^+)$	3695			$4F(\frac{7}{2}^-)$	3897	
0 2 2 1 3	$1D(\frac{7}{2}^+)$	3086	3013	0 3 3 1 4	$1F(\frac{9}{2}^-)$	3305	3209
	$2D(\frac{7}{2}^+)$	3425	3342		$2F(\frac{9}{2}^-)$	3622	
	$3D(\frac{7}{2}^+)$	3569			$3F(\frac{9}{2}^-)$	3760	
	$4D(\frac{7}{2}^+)$	3712			$4F(\frac{9}{2}^-)$	3912	
0 3 3 1 2	$1F(\frac{3}{2}^-)$	3299	3288	0 4 4 1 3	$1G(\frac{5}{2}^+)$	3501	3495
	$2F(\frac{3}{2}^-)$	3617			$2G(\frac{5}{2}^+)$	3798	
	$3F(\frac{3}{2}^-)$	3755			$3G(\frac{7}{2}^+)$	3938	
	$4F(\frac{3}{2}^-)$	3898			$4G(\frac{5}{2}^+)$	4108	
0 3 3 1 2	$1F(\frac{5}{2}^-)$	3304	3283	0 4 4 1 3	$1G(\frac{7}{2}^+)$	3502	3483
	$2F(\frac{5}{2}^-)$	3621			$2G(\frac{7}{2}^+)$	3798	
	$3F(\frac{5}{2}^-)$	3759			$3G(\frac{7}{2}^+)$	3939	
	$4F(\frac{5}{2}^-)$	3910			$4G(\frac{7}{2}^+)$	4118	
0 3 3 1 3	$1F(\frac{5}{2}^-)$	3299	3254	0 4 4 1 4	$1G(\frac{7}{2}^+)$	3501	3444
	$2F(\frac{5}{2}^-)$	3617			$2G(\frac{7}{2}^+)$	3798	
	$3F(\frac{5}{2}^-)$	3755			$3G(\frac{7}{2}^+)$	3938	
	$4F(\frac{5}{2}^-)$	3898			$4G(\frac{7}{2}^+)$	4108	
0 3 3 1 3	$1F(\frac{7}{2}^-)$	3305	3253	0 4 4 1 4	$1G(\frac{9}{2}^+)$	3502	3442
	$2F(\frac{7}{2}^-)$	3621			$2G(\frac{9}{2}^+)$	3798	
	$3F(\frac{7}{2}^-)$	3760			$3G(\frac{9}{2}^+)$	3939	
	$4F(\frac{7}{2}^-)$	3911			$4G(\frac{7}{2}^+)$	4108	

$(\frac{1}{2}^-, \frac{3}{2}^-)$ and $(\frac{3}{2}^-, \frac{5}{2}^-)$, it is showed in Table VII that the splitting of these doublets are 17 MeV and 28 MeV, respectively. In comparison with the experimental data, the possible assignments for these four experimental Ω_c states are $(\Omega_c(3000), \Omega_c(3050))=(\frac{1}{2}^-, \frac{3}{2}^-)_{j=1}$ and $(\Omega_c(3066), \Omega_c(3090))=(\frac{3}{2}^-, \frac{5}{2}^-)_{j=2}$. For Ω_b baryons, quark model also predicts five $1P$ -wave states, their situation is similar with the above P -wave Ω_c baryons, the splitting of spin-doublets $(\frac{1}{2}^-, \frac{3}{2}^-)_{j=1}$ and $(\frac{3}{2}^-, \frac{5}{2}^-)_{j=2}$ are 7 MeV and 13 MeV. These four experimental Ω_b states are good candidates of these P -wave doublets, which can be assigned as $(\Omega_b(6315), \Omega_b(6330))=(\frac{1}{2}^-, \frac{3}{2}^-)_{j=1}$ and $(\Omega_b(6340), \Omega_b(6350))=(\frac{3}{2}^-, \frac{5}{2}^-)_{j=2}$. Actually, different collaborations had different conclusions about the quantum numbers of these Ω_c and Ω_b states[118–127]. For a further understanding of these Ω_Q systems, we will study their strong decay behaviors with the 3P_0 model in Sec.4.

In quark model scheme, there are two $2S$ -wave excitations whose masses are predicted to be 6.446

TABLE VI: Masses of the Σ_b heavy baryons(in MeV)

$l_\rho l_\lambda L s j$	$nL(J^P)$	M	M_{exp}	[19]	[20]	[18]	[27]	[116]	[64, 79]
0 0 0 1 1	$1S(\frac{1}{2}^+)$	5820	5815.6[5]	5808	5833	5795	5789	5815.5	5800±190[79]
	$2S(\frac{1}{2}^+)$	6225		6213	6294				
	$3S(\frac{1}{2}^+)$	6430		6575					
	$4S(\frac{1}{2}^+)$	6566		6869					
0 0 0 1 1	$1S(\frac{3}{2}^+)$	5849	5834.7[5]	5834	5858	5805	5844		
	$2S(\frac{3}{2}^+)$	6246		6226	6308				
	$3S(\frac{3}{2}^+)$	6450		6583					
	$4S(\frac{3}{2}^+)$	6579		6876					
0 1 1 1 0	$1P(\frac{1}{2}^-)$	6113		6101					
	$2P(\frac{1}{2}^-)$	6447		6440					
	$3P(\frac{1}{2}^-)$	6648		6756					
	$4P(\frac{1}{2}^-)$	6739		7024					
0 1 1 1 1	$1P(\frac{1}{2}^-)$	6107		6095	6099	6070	6039		6000±180[64]
	$2P(\frac{1}{2}^-)$	6442		6430	6106				
	$3P(\frac{1}{2}^-)$	6643		6742					
	$4P(\frac{1}{2}^-)$	6736		7008					
0 1 1 1 1	$1P(\frac{3}{2}^-)$	6116		6096	6101	6070	6039		
	$2P(\frac{3}{2}^-)$	6450		6430					
	$3P(\frac{3}{2}^-)$	6650		6742					
	$4P(\frac{3}{2}^-)$	6741		7009					
0 1 1 1 2	$1P(\frac{3}{2}^-)$	6104	6098.0[5, 117, 138]	6087	6105				6000±180[64]
	$2P(\frac{3}{2}^-)$	6439		6423					
	$3P(\frac{3}{2}^-)$	6641		6736					
	$4P(\frac{3}{2}^-)$	6734		7003					
0 1 1 1 2	$1P(\frac{5}{2}^-)$	6119		6084	6172				
	$2P(\frac{5}{2}^-)$	6452		6421					
	$3P(\frac{5}{2}^-)$	6652		6732					
	$4P(\frac{5}{2}^-)$	6743		6999					
0 2 2 1 1	$1D(\frac{1}{2}^+)$	6338		6311					
	$2D(\frac{1}{2}^+)$	6639		6636					
	$3D(\frac{1}{2}^+)$	6828		3626					
	$4D(\frac{1}{2}^+)$	6892		6647					
0 2 2 1 1	$1D(\frac{3}{2}^+)$	6344		6326					
	$2D(\frac{3}{2}^+)$	6645		6647					
	$3D(\frac{3}{2}^+)$	6833							
	$4D(\frac{3}{2}^+)$	6896							
0 2 2 1 2	$1D(\frac{3}{2}^+)$	6338		6285					
	$2D(\frac{3}{2}^+)$	6639		6612					
	$3D(\frac{3}{2}^+)$	6828							
	$4D(\frac{3}{2}^+)$	6892							
0 2 2 1 2	$1D(\frac{5}{2}^+)$	6345		6284					
	$2D(\frac{5}{2}^+)$	6646		6612					

$l_\rho l_\lambda L s j$	$nL(J^P)$	M	[19]	[20]	$l_\rho l_\lambda L s j$	$nL(J^P)$	M	[19]
0 2 2 1 3	$1D(\frac{5}{2}^+)$	6338	6270	6325	0 3 3 1 4	$1F(\frac{7}{2}^-)$	6538	6472
	$2D(\frac{5}{2}^+)$	6639		6598		$2F(\frac{7}{2}^-)$	6827	
	$3D(\frac{5}{2}^+)$	6827				$3F(\frac{7}{2}^-)$	6998	
	$4D(\frac{5}{2}^+)$	6892				$4F(\frac{7}{2}^-)$	7041	
0 2 2 1 3	$1D(\frac{7}{2}^+)$	6346	6260	6333	0 3 3 1 4	$1F(\frac{9}{2}^-)$	6542	6459
	$2D(\frac{7}{2}^+)$	6647	6590	6554		$2F(\frac{9}{2}^-)$	6833	
	$3D(\frac{7}{2}^+)$	6834				$3F(\frac{9}{2}^-)$	7002	
	$4D(\frac{7}{2}^+)$	6897				$4F(\frac{9}{2}^-)$	7045	
0 3 3 1 2	$1F(\frac{3}{2}^-)$	6538	6550		0 4 4 1 3	$1G(\frac{5}{2}^+)$	6715	6749
	$2F(\frac{3}{2}^-)$	6827				$2G(\frac{5}{2}^+)$	7006	
	$3F(\frac{3}{2}^-)$	6998				$3G(\frac{5}{2}^+)$	7155	
	$4F(\frac{3}{2}^-)$	7041				$4G(\frac{5}{2}^+)$	7187	
0 3 3 1 2	$1F(\frac{5}{2}^-)$	6542	6564		0 4 4 1 3	$1G(\frac{7}{2}^+)$	6718	6761
	$2F(\frac{5}{2}^-)$	6832				$2G(\frac{7}{2}^+)$	7009	
	$3F(\frac{5}{2}^-)$	7001				$3G(\frac{7}{2}^+)$	7158	
	$4F(\frac{5}{2}^-)$	7044				$4G(\frac{7}{2}^+)$	7190	
0 3 3 1 3	$1F(\frac{5}{2}^-)$	6538	6501		0 4 4 1 4	$1G(\frac{7}{2}^+)$	6715	6688
	$2F(\frac{5}{2}^-)$	6827				$2G(\frac{7}{2}^+)$	7006	
	$3F(\frac{5}{2}^-)$	6998				$3G(\frac{7}{2}^+)$	7155	
	$4F(\frac{5}{2}^-)$	7041				$4G(\frac{7}{2}^+)$	7187	
0 3 3 1 3	$1F(\frac{7}{2}^-)$	6542	6500		0 4 4 1 4	$1G(\frac{9}{2}^+)$	6718	6688
	$2F(\frac{7}{2}^-)$	6832				$2G(\frac{9}{2}^+)$	7009	
	$3F(\frac{7}{2}^-)$	7001				$3G(\frac{9}{2}^+)$	7158	
	$4F(\frac{7}{2}^-)$	7045				$4G(\frac{9}{2}^+)$	7190	

GeV and 6.466 GeV, respectively. The other collaborations also reported the same results as ours[19], which suggests that these Ω_b states have potentials to be observed at this mass spectra in forthcoming experiments. Finally, the $1D$ -wave Ω_Q states also have the possibilities to be found in experiments. The masses are predicted to be around 3.304 GeV \sim 3.315 GeV for $\Omega_c(1D)$ states and 6.555 GeV \sim 6.562 GeV for $\Omega_b(1D)$ ones.

TABLE VII: Masses of the Ω_c heavy baryons(in MeV)

$l_\rho l_\lambda L s j$	$nL(J^P)$	M	M_{exp}	[19]	[20]	[36]	[27]	[64, 80]
0 0 0 1 1	$1S(\frac{1}{2}^+)$	2699	2695.2[5]	2698	2718	2688	2710	
	$2S(\frac{1}{2}^+)$	3150	3119.1[5]	3088	3152	3169	3044	
	$3S(\frac{1}{2}^+)$	3308		3489				
	$4S(\frac{1}{2}^+)$	3526		3814				
0 0 0 1 1	$1S(\frac{3}{2}^+)$	2762	2765.9[5]	2768	2776	2721	2759	
	$2S(\frac{3}{2}^+)$	3197		3123	3190		3080	
	$3S(\frac{3}{2}^+)$	3346		3510				
	$4S(\frac{3}{2}^+)$	3557		3830				
0 1 1 1 0	$1P(\frac{1}{2}^-)$	3057		3055	2977		2959	3050±110[80]
	$2P(\frac{1}{2}^-)$	3426		3435	2990		3029	
	$3P(\frac{1}{2}^-)$	3562		3754				
	$4P(\frac{1}{2}^-)$	3735		4037				
0 1 1 1 1	$1P(\frac{1}{2}^-)$	3045	3000.4[5]	2966				2980±160[64]
	$2P(\frac{1}{2}^-)$	3416		3384				
	$3P(\frac{1}{2}^-)$	3554		3717				
	$4P(\frac{1}{2}^-)$	3728		4009				
0 1 1 1 1	$1P(\frac{3}{2}^-)$	3062	3050.2[5]	3054	2986		2959	3060±110[80]
	$2P(\frac{3}{2}^-)$	3431		3433	2994		3029	
	$3P(\frac{3}{2}^-)$	3566		3757				
	$4P(\frac{3}{2}^-)$	3739		4036				
0 1 1 1 2	$1P(\frac{3}{2}^-)$	3039	3065.5[5]	3029				3060±100[80]
	$2P(\frac{3}{2}^-)$	3411		3415				
	$3P(\frac{3}{2}^-)$	3550		3737				
	$4P(\frac{3}{2}^-)$	3725		4023				
0 1 1 1 2	$1P(\frac{5}{2}^-)$	3067	3090.0[5]	3051	3014			3110±100[80]
	$2P(\frac{5}{2}^-)$	3435		3427				
	$3P(\frac{5}{2}^-)$	3569		3744				
	$4P(\frac{5}{2}^-)$	3742		4028				
0 2 2 1 1	$1D(\frac{1}{2}^+)$	3304		3287				
	$2D(\frac{1}{2}^+)$	3641		3623				
	$3D(\frac{1}{2}^+)$	3764						
	$4D(\frac{1}{2}^+)$	3909						
0 2 2 1 1	$1D(\frac{3}{2}^+)$	3313		3298				
	$2D(\frac{3}{2}^+)$	3650		3627				
	$3D(\frac{3}{2}^+)$	3771						
	$4D(\frac{3}{2}^+)$	3917						
0 2 2 1 2	$1D(\frac{3}{2}^+)$	3304		3282				
	$2D(\frac{3}{2}^+)$	3641		3613				
	$3D(\frac{3}{2}^+)$	3764						
	$4D(\frac{3}{2}^+)$	3909						
0 2 2 1 2	$1D(\frac{5}{2}^+)$	3314		3297	3196			
	$2D(\frac{5}{2}^+)$	3651		3626				

		$4D(\frac{5}{2}^+)$	3918						
$l_\rho l_\lambda L s j$	$nL(J^P)$	M	[19]	[20]	$l_\rho l_\lambda L s j$	$nL(J^P)$	M	[19]	[20]
0 2 2 1 3	$1D(\frac{5}{2}^+)$	3304	3286		0 3 3 1 4	$1F(\frac{9}{2}^-)$	3529		3485
	$2D(\frac{5}{2}^+)$	3640	3614			$2F(\frac{9}{2}^-)$	3852		
	$3D(\frac{5}{2}^+)$	3764				$3F(\frac{9}{2}^-)$	3960		
	$4D(\frac{5}{2}^+)$	3908				$4F(\frac{9}{2}^-)$	4101		
0 2 2 1 3	$1D(\frac{7}{2}^+)$	3315	3283		0 4 4 1 3	$1G(\frac{5}{2}^+)$	3719	3739	
	$2D(\frac{7}{2}^+)$	3652	3611			$2G(\frac{5}{2}^+)$	4030		
	$3D(\frac{7}{2}^+)$	3773				$3G(\frac{5}{2}^+)$	4135		
	$4D(\frac{7}{2}^+)$	3919				$4G(\frac{5}{2}^+)$	4283		
0 3 3 1 2	$1F(\frac{3}{2}^-)$	3525	3533		0 4 4 1 3	$1G(\frac{7}{2}^+)$	3720	3721	
	$2F(\frac{3}{2}^-)$	3847				$2G(\frac{7}{2}^+)$	4030		
	$3F(\frac{3}{2}^-)$	3957				$3G(\frac{7}{2}^+)$	4135		
	$4F(\frac{3}{2}^-)$	4091				$4G(\frac{7}{2}^+)$	4291		
0 3 3 1 2	$1F(\frac{5}{2}^-)$	3528	3522		0 4 4 1 4	$1G(\frac{7}{2}^+)$	3719	3707	
	$2F(\frac{5}{2}^-)$	3851				$2G(\frac{7}{2}^+)$	4030		
	$3F(\frac{5}{2}^-)$	3960				$3G(\frac{7}{2}^+)$	4135		
	$4F(\frac{5}{2}^-)$	4099				$4G(\frac{7}{2}^+)$	4283		
0 3 3 1 3	$1F(\frac{5}{2}^-)$	3525	3515		0 4 4 1 4	$1G(\frac{9}{2}^+)$	3720		3705
	$2F(\frac{5}{2}^-)$	3847				$2G(\frac{9}{2}^+)$	4030		
	$3F(\frac{5}{2}^-)$	3957				$3G(\frac{9}{2}^+)$	4135		
	$4F(\frac{5}{2}^-)$	4091				$4G(\frac{9}{2}^+)$	4291		
0 3 3 1 3	$1F(\frac{7}{2}^-)$	3529	3514		0 4 4 1 5	$1G(\frac{9}{2}^+)$	3719		3685
	$2F(\frac{7}{2}^-)$	3851				$2G(\frac{9}{2}^+)$	4030		
	$3F(\frac{7}{2}^-)$	3960				$3G(\frac{9}{2}^+)$	4135		
	$4F(\frac{7}{2}^-)$	4100				$4G(\frac{9}{2}^+)$	4283		
0 3 3 1 4	$1F(\frac{7}{2}^-)$	3524	3498		0 4 4 1 5	$1G(\frac{11}{2}^+)$	3720		3665
	$2F(\frac{7}{2}^-)$	3846				$2G(\frac{11}{2}^+)$	4030		
	$3F(\frac{7}{2}^-)$	3957				$3G(\frac{11}{2}^+)$	4135		
	$4F(\frac{7}{2}^-)$	4091				$4G(\frac{11}{2}^+)$	4292		

TABLE VIII: Masses of the Ω_b heavy baryons(in MeV)

$l_\rho l_\lambda L s j$	$nL(J^P)$	M	M_{exp}	[19]	[20]	[27]	[64, 81]
0 0 0 1 1	$1S(\frac{1}{2}^+)$	6043	6046.1[5]	6064	6081	6037	
	$2S(\frac{1}{2}^+)$	6446		6450	6472		
	$3S(\frac{1}{2}^+)$	6633		6804			
	$4S(\frac{1}{2}^+)$	6790		7091			
0 0 0 1 1	$1S(\frac{3}{2}^+)$	6069		6088	6102	6090	
	$2S(\frac{3}{2}^+)$	6466		6461	6478		
	$3S(\frac{3}{2}^+)$	6650		6811			
	$4S(\frac{3}{2}^+)$	6804		7096			
0 1 1 1 0	$1P(\frac{1}{2}^-)$	6334		6339	6301	6278	6320(110)[81]
	$2P(\frac{1}{2}^-)$	6662		6710	6312		
	$3P(\frac{1}{2}^-)$	6844		7009			
	$4P(\frac{1}{2}^-)$	6969		7265			
0 1 1 1 1	$1P(\frac{1}{2}^-)$	6329	6315.64[15]	6330			6270±140[64]
	$2P(\frac{1}{2}^-)$	6658		6706			
	$3P(\frac{1}{2}^-)$	6841		7003			
	$4P(\frac{1}{2}^-)$	6966		7257			
0 1 1 1 1	$1P(\frac{3}{2}^-)$	6336	6330.30[15]	6340			6310±110[81]
	$2P(\frac{3}{2}^-)$	6664		6750			
	$3P(\frac{3}{2}^-)$	6846		7002			
	$4P(\frac{3}{2}^-)$	6970		7258			
0 1 1 1 2	$1P(\frac{3}{2}^-)$	6326	6339.71[15]	6331	6304	6278	6370±90[81]
	$2P(\frac{3}{2}^-)$	6655		6699	6311		
	$3P(\frac{3}{2}^-)$	6839		6998			
	$4P(\frac{3}{2}^-)$	6964		7250			
0 1 1 1 2	$1P(\frac{5}{2}^-)$	6339	6349.88[15]	6334	6311		6350±100[81]
	$2P(\frac{5}{2}^-)$	6666		6700			
	$3P(\frac{5}{2}^-)$	6848		6996			
	$4P(\frac{5}{2}^-)$	6972		7251			
0 2 2 1 1	$1D(\frac{1}{2}^+)$	6556		6540			
	$2D(\frac{1}{2}^+)$	6846		6857			
	$3D(\frac{1}{2}^+)$	7021					
	$4D(\frac{1}{2}^+)$	7121					
0 2 2 1 1	$1D(\frac{3}{2}^+)$	6561		6549			
	$2D(\frac{3}{2}^+)$	6852		6863			
	$3D(\frac{3}{2}^+)$	7026					
	$4D(\frac{3}{2}^+)$	7124					
0 2 2 1 2	$1D(\frac{3}{2}^+)$	6556		6530			
	$2D(\frac{3}{2}^+)$	6846		6846			
	$3D(\frac{3}{2}^+)$	7022					
	$4D(\frac{3}{2}^+)$	7121					
0 2 2 1 2	$1D(\frac{5}{2}^+)$	6561		6529			
	$2D(\frac{5}{2}^+)$	6852		6846			

$l_\rho l_\lambda L s j$	$nL(J^P)$	M	[19]		$l_\rho l_\lambda L s j$	$nL(J^P)$	M	[19]
	$4D(\frac{5}{2}^+)$	7124						
0 2 2 1 3	$1D(\frac{5}{2}^+)$	6555	6520	6492[20]	0 3 3 1 4	$1F(\frac{9}{2}^-)$	6754	6713
	$2D(\frac{5}{2}^+)$	6846	6837	6494[20]		$2F(\frac{9}{2}^-)$	7031	
	$3D(\frac{5}{2}^+)$	7021				$3F(\frac{9}{2}^-)$	7191	
	$4D(\frac{5}{2}^+)$	7121				$4F(\frac{9}{2}^-)$	7266	
0 2 2 1 3	$1D(\frac{7}{2}^+)$	6562	6517	6497[20]	0 4 4 1 3	$1G(\frac{5}{2}^+)$	6923	6952
	$2D(\frac{7}{2}^+)$	6853	6834	6667[20]		$2G(\frac{5}{2}^+)$	7201	
	$3D(\frac{7}{2}^+)$	7027				$3G(\frac{5}{2}^+)$	7342	
	$4D(\frac{7}{2}^+)$	7125				$4G(\frac{5}{2}^+)$	7398	
0 3 3 1 2	$1F(\frac{3}{2}^-)$	6751	6763	6370[81]	0 4 4 1 3	$1G(\frac{7}{2}^+)$	6925	6959
	$2F(\frac{3}{2}^-)$	7026				$2G(\frac{7}{2}^+)$	7204	
	$3F(\frac{3}{2}^-)$	7188				$3G(\frac{7}{2}^+)$	7344	
	$4F(\frac{3}{2}^-)$	7264				$4G(\frac{7}{2}^+)$	7400	
0 3 3 1 2	$1F(\frac{5}{2}^-)$	6754	6771		0 4 4 1 4	$1G(\frac{7}{2}^+)$	6923	6916
	$2F(\frac{5}{2}^-)$	7031				$2G(\frac{7}{2}^+)$	7201	
	$3F(\frac{5}{2}^-)$	7191				$3G(\frac{7}{2}^+)$	7342	
	$4F(\frac{5}{2}^-)$	7265				$4G(\frac{7}{2}^+)$	7398	
0 3 3 1 3	$1F(\frac{5}{2}^-)$	6751	6737		0 4 4 1 4	$1G(\frac{9}{2}^+)$	6925	6915
	$2F(\frac{5}{2}^-)$	7026				$2G(\frac{9}{2}^+)$	7205	
	$3F(\frac{5}{2}^-)$	7188				$3G(\frac{9}{2}^+)$	7344	
	$4F(\frac{5}{2}^-)$	7264				$4G(\frac{9}{2}^+)$	7400	
0 3 3 1 3	$1F(\frac{7}{2}^-)$	6754	6736		0 4 4 1 5	$1G(\frac{9}{2}^+)$	6922	6892
	$2F(\frac{7}{2}^-)$	7031				$2G(\frac{9}{2}^+)$	7201	
	$3F(\frac{7}{2}^-)$	7191				$3G(\frac{9}{2}^+)$	7342	
	$4F(\frac{7}{2}^-)$	7266				$4G(\frac{9}{2}^+)$	7398	
0 3 3 1 4	$1F(\frac{7}{2}^-)$	6750	6719		0 4 4 1 5	$1G(\frac{11}{2}^+)$	6925	6884
	$2F(\frac{7}{2}^-)$	7026				$2G(\frac{11}{2}^+)$	7205	
	$3F(\frac{7}{2}^-)$	7188				$3G(\frac{11}{2}^+)$	7344	
	$4F(\frac{7}{2}^-)$	7264				$4G(\frac{11}{2}^+)$	7400	

3 Regge trajectories of single heavy baryons Λ_Q , Σ_Q and Ω_Q

The well-known Regge theory was first developed by T.Regge in 1959[128, 129], which preceded the QCD. In 1961, Chew and Frautschi extended this theory and found mesons and baryons lie on linear trajectories of the (J, M^2) plane[130, 131], where J is the angular momentum and M is the mass of hadron. The Regge theory is very successful in studying the strong interactions at high energies and it is an indispensable tool in phenomenological studies. Now, it has been widely used to study the hadronic spectra and was commonly called Regge trajectory. Actually, there have been lots of studies based on QCD theory to understand the Regge trajectory[132–135]. In them, the most simple and straightforward one was proposed by Nambu in 1978[136, 137], where the relation of J and M^2 was described as,

$$J = \frac{M^2}{2\pi\sigma} + c \quad (55)$$

where, σ is the string tension and c is a constant.

In the present work, we obtained the masses of both orbitally and radially excited charmed and bottom baryons up to rather high excitation numbers, which makes it easy for us to construct the baryon Regge trajectories in (J, M^2) plane. First, both charmed and bottom baryons are classified into two groups which have natural and unnatural parities with $P = (-1)^{J-1/2}$ and $P = (-1)^{J+1/2}$ [19], respectively. Then, with the predicted mass spectra by quark model, we plot the Regge trajectories in the (J, M^2) plane for Λ_Q , Σ_Q and Ω_Q systems in Figs.10-15. Here, we use the following definition about the (J, M^2) Regge trajectories[19],

$$J = \alpha M^2 + \alpha_0 \quad (56)$$

where α and α_0 are slope and intercept. In these figures, the masses calculated in our model are denoted by diamonds and the experimental data are shown by inverted triangle with particle names. The straight lines are obtained by linear fitting of the predicted values. The fitted slopes and intercepts of the Regge trajectories are listed in Table IX.

TABLE IX: Fitted parameters α and α_0 for the slope and intercept of the (J, M^2) parent and daughter Regge trajectories for Λ_Q , Σ_Q and Ω_Q .

Trajectory	$\alpha(\text{Gev}^{-2})$	α_0	$\alpha(\text{Gev}^{-2})$	α_0
	$\Lambda_c(\frac{1}{2}^+)$		$\Lambda_c(\frac{1}{2}^-)$	
parent	0.707±0.009	-3.312±0.005	0.719±0.011	-4.393±0.033
1 daughter	0.736±0.001	-5.166±0.002	0.725±0.003	-5.998±0.018
2 daughter	0.686±0.002	-5.818±0.006	0.687±0.002	-6.790±0.013
	$\Sigma_c(\frac{1}{2}^+)$		$\Sigma_c^*(\frac{3}{2}^+)$	
parent	0.646±0.007	-3.500±0.007	0.666±0.007	-2.811±0.005
1 daughter	0.673±0.003	-5.275±0.011	0.695±0.001	-4.632±0.001
2 daughter	0.670±0.002	-5.940±0.009	0.697±0.001	-5.363±0.003
	$\Omega_c(\frac{1}{2}^+)$		$\Omega_c^*(\frac{3}{2}^+)$	
parent	0.614±0.009	-4.096±0.018	0.623±0.012	-3.306±0.003
1 daughter	0.633±0.002	-5.840±0.012	0.650±0.001	-5.158±0.003
2 daughter	0.651±0.003	-6.673±0.002	0.668±0.001	-5.999±0.005
	$\Lambda_b(\frac{1}{2}^+)$		$\Lambda_b(\frac{1}{2}^-)$	
parent	0.371±0.009	-11.364±0.196	0.393±0.011	-13.240±0.304
1 daughter	0.413±0.012	-14.594±0.012	0.415±0.010	-15.643±0.010
2 daughter	0.476±0.007	-18.843±0.232	0.502±0.003	-21.019±0.131
	$\Sigma_b(\frac{1}{2}^+)$		$\Sigma_b^*(\frac{3}{2}^+)$	
parent	0.357±0.006	-11.729±0.157	0.350±0.010	-10.535±0.202
1 daughter	0.386±0.009	-14.490±0.008	0.391±0.010	-13.775±0.010
2 daughter	0.406±0.002	-16.338±0.077	0.405±0.003	-15.370±0.095
	$\Omega_b(\frac{1}{2}^+)$		$\Omega_b^*(\frac{3}{2}^+)$	
parent	0.352±0.008	-12.517±0.214	0.342±0.012	-11.162±0.278
1 daughter	0.390±0.001	-15.739±0.017	0.393±0.051	-14.965±1.966
2 daughter	0.405±0.002	-17.382±0.087	0.401±0.003	-16.267±0.108

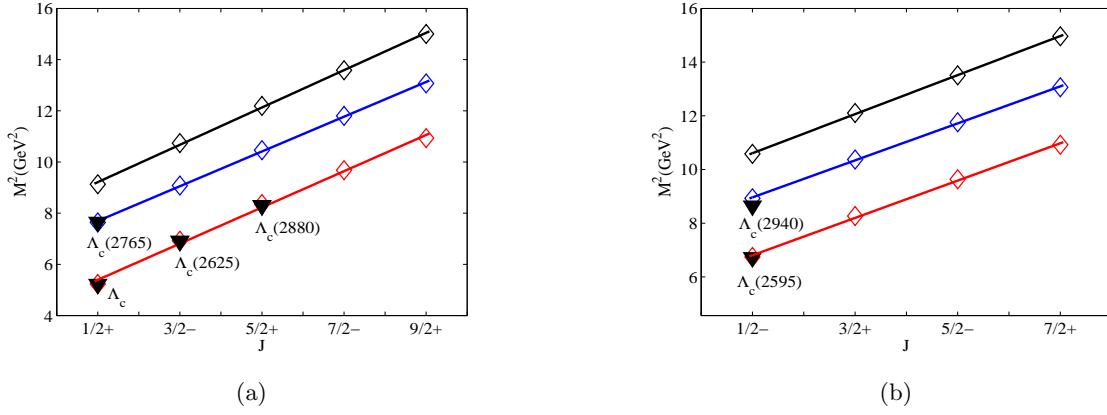


FIG. 10: Parent and daughter (J, M^2) Regge trajectories for the Λ_c baryons with natural (a) and unnatural (b) parities. Diamonds are predicted masses. Available experimental data are given by inverted triangle with particle names.

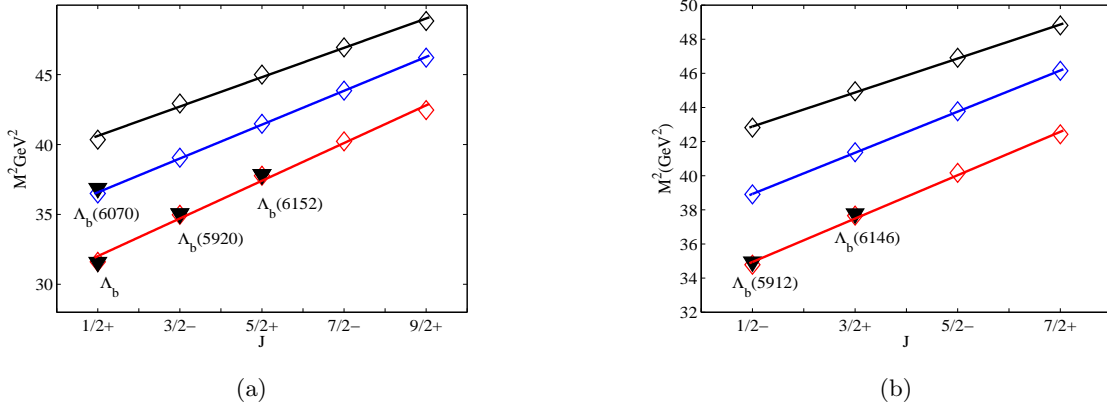


FIG. 11: Same as in FIG.10 for the Λ_b baryons

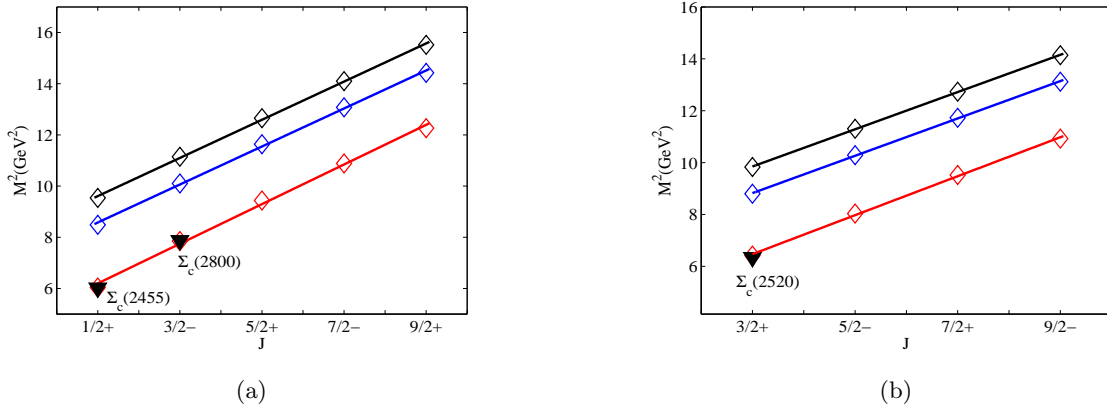
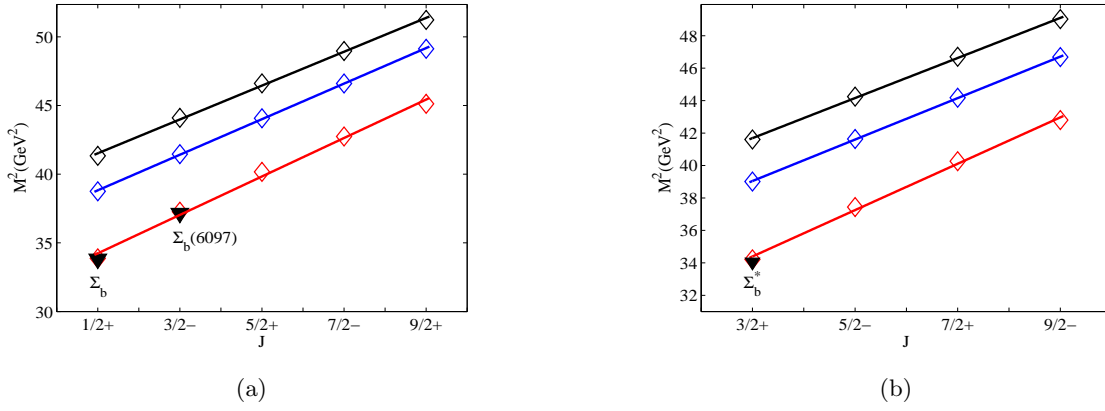
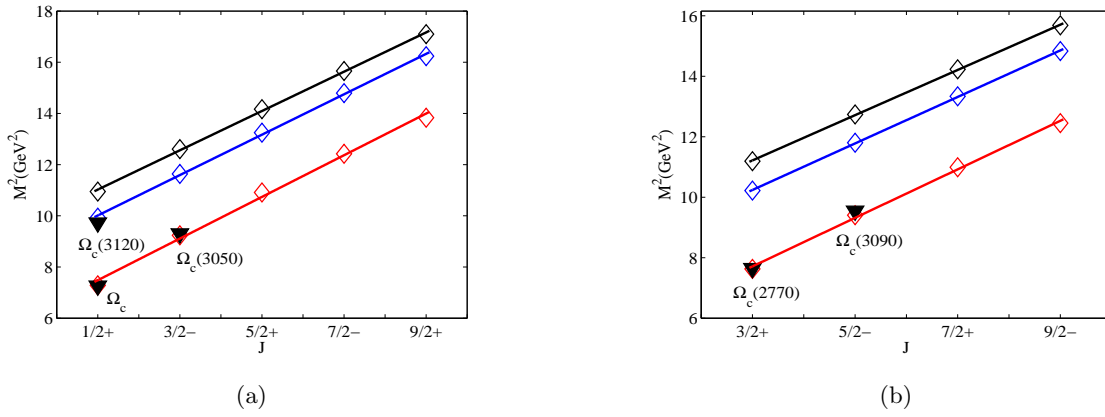
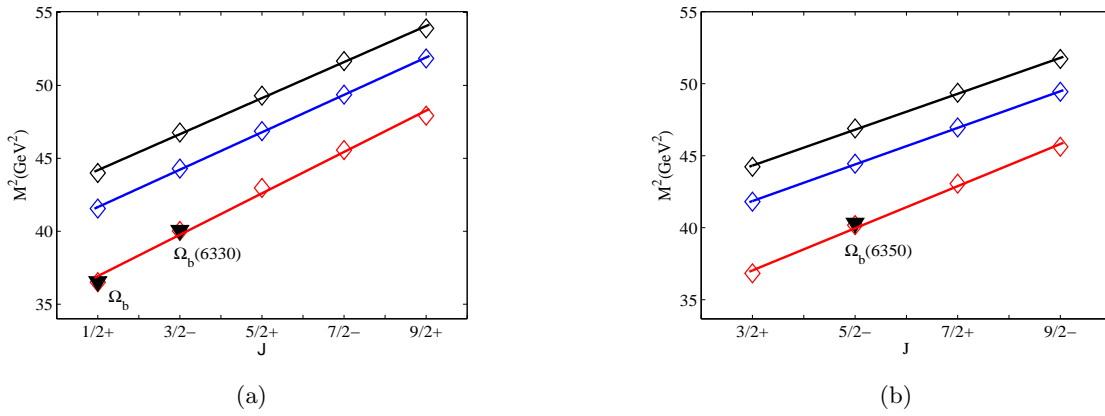


FIG. 12: Same as in FIG.10 for the Σ_c baryons

FIG. 13: Same as in FIG.10 for the Σ_b baryonsFIG. 14: Same as in FIG.10 for the Ω_c baryonsFIG. 15: Same as in FIG.10 for the Ω_b baryons

We can see from these figures that all of the predicted masses in our model fit nicely to the linear trajectories in the (J, M^2) plane. These results can help us to assign an accurate position in the mass spectra for observed baryons. There are two trajectories for which three experimental candidates are available. They are the parent trajectories for $\Lambda_c(\frac{1}{2}^+)$ in Fig.10(a) and $\Lambda_b(\frac{1}{2}^+)$ in Fig.11(a). There are several trajectories with two experimental candidates such as the parent trajectory for $\Lambda_c(\frac{1}{2}^-)$ in Fig.10(b), the parent trajectories for $\Sigma_c(2455)(\frac{1}{2}^+)$ and $\Sigma_b(\frac{1}{2}^+)$ in Figs.12(a) and 13(a), the parent trajectories for $\Omega_c(\frac{1}{2}^+)$, $\Omega_c(2770)(\frac{3}{2}^+)$ and $\Omega_b(\frac{1}{2}^+)$ in Figs.14(a), 14(b) and 15(a). All the experimental data coincide well with the corresponding Regge trajectories obtained in present work. Especially, the experimental data for $\Lambda_c(2765)$ and $\Lambda_b(6070)$ fit well with the Regge trajectories in Fig.10(a) and Fig.11(a), which suggests that they can be accommodated in the mass spectra as the $2S(\frac{1}{2}^+)$ state. We can see from Fig.10(b), if $\Lambda_c(2940)$ is interpreted as a $2P(\frac{1}{2}^-)$ state, the predicted mass is about 40 ~ 50 MeV heavier than the experimental data. On the other hand, the Regge trajectories in Fig.12(a) and Fig.13(a) show that it is reasonable to assign $\Sigma_c(2800)$ and $\Sigma_b(6097)$ as the $1P(\frac{3}{2}^-)$ state. Finally, the $\Omega_c(3120)$ can be viewed as the first radial excitations($2S$) of Ω_c with quantum numbers $\frac{1}{2}^+$ according to the first daughter Regge trajectory in Fig.14(a). As for the other four observed Ω_c states, the Regge trajectories support assigning $\Omega_c(3050)$ and $\Omega_c(3090)$ as the first orbital excited states($1P$) with quantum numbers $\frac{3}{2}^-$ and $\frac{5}{2}^-$, respectively. From Figs.15(a) and (b), we can see that the situation about $\Omega_b(6330)$ and $\Omega_b(6350)$ is similar with Ω_c . These two states can be interpreted as the $1P$ -wave partners of Ω_c with $J^P = \frac{3}{2}^-$ and $\frac{5}{2}^-$.

4 Strong decay behaviors of S -, P - and D -wave baryons

4.1 3P_0 strong decay model

In Sec.2, we have systemically analyzed the mass spectra of the single heavy baryons Λ_Q , Σ_Q and Ω_Q in the GI relativized quark model. With these results, we have also constructed the Regge trajectories in the (J, M^2) plane in Sec.3. These studies provide fruitful informations for us to determine the quantum numbers of the observed single heavy baryons. On the other hand, some low-lying excited single heavy baryons, which are still undiscovered, have also been predicted by the quark model in Sec.2.4. These predicted states have good potentials to be found in forthcoming experiments. In order to make a further confirmation about the assignments that have been given in Sec.2.4 and to provide more valuable infirmations for searching for these predicted baryons, we systematically analyze the strong decay behaviors of the $1S$, $2S$, $1P$, $2P$ and some $1D$, $2D$ states with the 3P_0 model.

Since the 3P_0 quark model was put forward in 1969, it has been widely used to study the strong decay behaviors of the mesons and baryons[138–142]. The main idea of this model is that the strong decay take place via the creation of a 3P_0 quark-antiquark pair from the vacuum. Then, this quark-antiquark pair regroups with the initial hadron A into two daughter hadrons B and C. This process is illustrated in Fig.16, In the 3P_0 model, the strong decay width for the process $A \rightarrow B + C$ can be

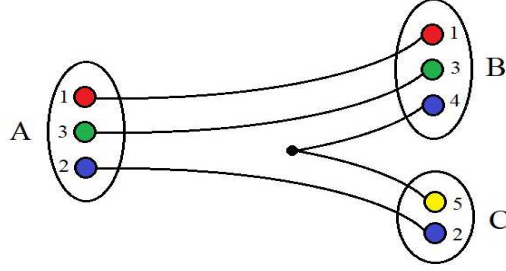


FIG. 16: The decay process of $A \rightarrow B+C$ in the 3P_0 model.

written as,

$$\Gamma = \pi^2 \frac{|\mathbf{p}|}{m_A^2} \frac{1}{2J_A + 1} \sum_{M_{J_A} M_{J_B} M_{J_C}} |M^{M_{J_A} M_{J_B} M_{J_C}}|^2 \quad (57)$$

where $|\mathbf{p}| = \frac{\sqrt{[m_A^2 - (m_B - m_C)^2][m_A^2 - (m_B + m_C)^2]}}{2m_A}$ is the momentum of the daughter hadrons in the centre-of-mass frame. The $M^{M_{J_A} M_{J_B} M_{J_C}}$ in Eq.(57) is the helicity amplitude, which reads

$$\begin{aligned} & M^{M_{J_A} M_{J_B} M_{J_C}} \\ &= -F\gamma \sqrt{8E_A E_B E_C} \sum_{M_{\rho_A}} \sum_{M_{L_A}} \sum_{M_{\rho_B}} \sum_{M_{L_B}} \sum_{M_{S_1}, M_{S_3}, M_{S_4}, m} \langle J_{l_A} M_{J_{l_A}} S_3 M_{S_3} | J_A M_{J_A} \rangle \\ & \times \langle L_{\rho_A} M_{L_{\rho_A}} L_{\lambda_A} M_{L_{\lambda_A}} | L_A M_{L_A} \rangle \langle L_A M_{L_A} S_{12} M_{S_{12}} | J_{l_A} M_{J_{l_A}} \rangle \langle S_1 M_{S_1} S_2 M_{S_2} | S_{12} M_{S_{12}} \rangle \\ & \times \langle J_{l_B} M_{J_{l_B}} S_3 M_{S_3} | J_B M_{J_B} \rangle \langle L_{\rho_B} M_{L_{\rho_B}} L_{\lambda_B} M_{L_{\lambda_B}} | L_B M_{L_B} \rangle \langle L_B M_{L_B} S_{14} M_{S_{14}} | J_{l_B} M_{J_{l_B}} \rangle \\ & \times \langle S_1 M_{S_1} S_4 M_{S_4} | S_{14} M_{S_{14}} \rangle \langle 1m; 1-m | 00 \rangle \langle S_4 M_{S_4} S_5 M_{S_5} | 1-m \rangle \\ & \times \langle L_C M_{L_C} S_C M_{S_C} | J_C M_{J_C} \rangle \langle S_2 M_{S_2} S_5 M_{S_5} | S_C M_{S_C} \rangle \times \\ & \times \langle \varphi_B^{1,4,3} \varphi_C^{2,5} | \varphi_A^{1,2,3} \varphi_0^{4,5} \rangle \times I_{M_{L_B}, M_{L_C}}^{M_{L_A}, m}(\mathbf{p}) \end{aligned} \quad (58)$$

In the above equation, $\langle \varphi_B^{1,4,3} \varphi_C^{2,5} | \varphi_A^{1,2,3} \varphi_0^{4,5} \rangle$ is the flavor matrix element, which has the following relation with the isospin matrix element[90, 110] $\langle I_B I_B^3 I_C I_C^3 | I_A I_A^3 \rangle$,

$$\langle \varphi_B^{1,4,3} \varphi_C^{2,5} | \varphi_A^{1,2,3} \varphi_0^{4,5} \rangle = \mathcal{F}^{(I^A, I^B, I^C)} \langle I_B I_B^3 I_C I_C^3 | I_A I_A^3 \rangle \quad (59)$$

where

$$\mathcal{F}^{(I^A, I^B, I^C)} = f \cdot (-1)^{I_{13} + I_C + I_A + I_2} \times \left[\frac{1}{2} (2I_C + 1)(2I_B + 1) \right]^{1/2} \times \begin{Bmatrix} I_{13} & I_B & I_4 \\ I_C & I_2 & I_A \end{Bmatrix} \quad (60)$$

Here f takes the value $f = \left(\frac{2}{3}\right)^{1/2}$ if the isospin of the created quark is $\frac{1}{2}$, and $f = -\left(\frac{1}{3}\right)^{1/2}$ for the

isospin of 0. In Eq.(58), the space integral is written as,

$$\begin{aligned}
I_{M_{L_B}, M_{L_C}}^{M_{L_A}, m}(\mathbf{p}) &= \int d\mathbf{p}_1 d\mathbf{p}_2 d\mathbf{p}_3 d\mathbf{p}_4 d\mathbf{p}_5 \delta^3(\mathbf{p}_1 + \mathbf{p}_2 + \mathbf{p}_3 - \mathbf{p}_A) \delta^3(\mathbf{p}_4 + \mathbf{p}_5) \\
&\times \delta^3(\mathbf{p}_1 + \mathbf{p}_4 + \mathbf{p}_3 - \mathbf{p}_B) \delta^3(\mathbf{p}_2 + \mathbf{p}_5 - \mathbf{p}_C) \Psi_B^*(\mathbf{p}_1, \mathbf{p}_4, \mathbf{p}_3) \Psi_C^*(\mathbf{p}_2, \mathbf{p}_5) \\
&\times \Psi_A(\mathbf{p}_1, \mathbf{p}_2, \mathbf{p}_3) y_{lm}\left(\frac{\mathbf{p}_4 - \mathbf{p}_5}{2}\right)
\end{aligned} \tag{61}$$

with the simple harmonic oscillator(SHO) wave function being chosen for the baryons,

$$\Psi(\mathbf{p}) = N \Psi_{n_\rho L_\rho M_{L_\rho}}(\mathbf{p}_\rho) \Psi_{n_\lambda L_\lambda M_{L_\lambda}}(\mathbf{p}_\lambda) \tag{62}$$

Here, N is a normalization coefficient of the wave function, and

$$\Psi_{n L M_L}(\mathbf{p}) = (-1)^n (-i)^L R^{L+\frac{3}{2}} \sqrt{\frac{2n!}{\Gamma(n+L+\frac{3}{2})}} \exp\left(-\frac{R^2 \mathbf{p}^2}{2}\right) \times L_n^{L+1/2}(R^2 \mathbf{p}^2) p^L Y_{LM_L}(\Omega_p) \tag{63}$$

4.2 Numerical results

The final results of 3P_0 model depend on some input parameters such as the quark pair ($q\bar{q}$) creation strength γ , the SHO wave function scale parameter R , and the masses of the hadrons. As for the quark pair creation strength, we take the universal value $\gamma = 13.4$. The SHO wave function scale parameter $R_{\lambda, \rho} = 1.67 \text{ GeV}^{-1}$ for $1S$ -wave baryon, $R_{\lambda, \rho} = 2.0 \text{ GeV}^{-1}$ for P -wave baryon and $R_{\lambda, \rho} = 2.5 \text{ GeV}^{-1}$ for $2S$ - and $2D$ -wave baryons[91, 143, 144]. The SHO parameter for light mesons takes the value $R = 2.5 \text{ GeV}^{-1}$. For heavier mesons, their values are different from light meson's and the values are taken as $R_B = 1.59 \text{ GeV}^{-1}$, $R_{B_s} = 1.53 \text{ GeV}^{-1}$, $R_D = 1.67 \text{ GeV}^{-1}$ and $R_{D_s} = 1.63 \text{ GeV}^{-1}$. All these parameters are consistent with those of other collaborations[91, 143, 144]. With the predicted masses in Sec.2.4, we study the OZI-allowed strong decay behaviors of the $1S$, $2S$, $1P$, $2P$ states and some of the $1D$, $2D$ states, which results are presented in Tables XIII-XXVIII. In these tables, the single heavy baryons are denoted as $\Lambda_{Qj}^{L\lambda'(\rho')}$, $\Sigma_{Qj}^{L\lambda'(\rho')}$ and $\Omega_{Qj}^{L\lambda'(\rho')}$, where the superscript L is the total orbital angular momentum with $L = l_\rho + l_\lambda$. The superscripts λ' and ρ' denote the first radial excitation with $(n_\rho, n_\lambda) = (0, 1)$ and $(1, 0)$, respectively. The subscript j represents the total angular momentum of light quarks which satisfies $j = L + s$. We also collect the available experimental information of the observed Λ_Q , Σ_Q and Ω_Q baryons in Tables X-XII[5].

A. Λ_Q states

For Λ_Q systems, we can see from Tables XIII-XVI that the predicted strong decay properties are roughly compatible with the experimental data. These results support our assignments for Λ_Q baryons which were suggested in Sec.2.4 according to their mass spectra. For example, if $\Lambda_c(2765)$ is assigned as $2S$ -wave $\Lambda_{c0}^{\lambda'(\frac{1}{2}^+)}$, its predicted total width is 25.34 MeV which is lower than the experimental

TABLE X: Masses, decay widths(MeV),and possible strong decay channels of $\Lambda_Q(Q=c,b)$

States	J^P	Mass	Width	Decay channels(experiment)
Λ_c^+	$\frac{1}{2}^+$	2286.46 ± 0.14	/	weak
$\Lambda_c(2595)^+$	$\frac{1}{2}^-$	2592.25 ± 0.28	$2.59 \pm 0.30 \pm 0.47$	$\Sigma_c^{+,0} \pi^{-,+}$
$\Lambda_c(2625)^+$	$\frac{3}{2}^-$	2628.11 ± 0.19	< 0.97	$\Sigma_c^{+,0} \pi^{-,+}$
$\Lambda_c(2765)^+$	$?^?$	2766.6 ± 2.4	50	/
$\Lambda_c(2860)^+$	$\frac{3}{2}^+$	$2856.1^{+2.0}_{-1.7} \pm 0.5^{+1.1}_{-5.6}$	$67.6^{+10.1}_{-8.1} \pm 1.4^{+5.9}_{-20.0}$	$D^0 p$
$\Lambda_c(2880)^+$	$\frac{5}{2}^+$	2881.63 ± 0.24	$5.6^{+0.8}_{-0.6}$	$\Sigma_c^{(*++)+,0} \pi^{-,+}, D^0 p$
$\Lambda_c(2940)^+$	$?^?$	$2939.6^{+1.3}_{-1.5}$	20^{+6}_{-5}	$\Sigma_c^{+,0} \pi^{-,+}$
$\Lambda_b(5912)^0$	$\frac{1}{2}^-$	5912.19 ± 0.17	< 0.25	$\Lambda_b^0 \pi^+ \pi^-$
$\Lambda_b(5920)^0$	$\frac{3}{2}^-$	5920.09 ± 0.17	< 0.25	$\Lambda_b^0 \pi^+ \pi^-$
$\Lambda_b(6070)^0$	$?^?$	6072.3 ± 2.9	72 ± 11	$\Lambda_b^0 \pi^+ \pi^-$
$\Lambda_b(6146)^0$	$\frac{3}{2}^+$	6146.17 ± 0.4	2.9 ± 1.3	$\Lambda_b^0 \pi^+ \pi^-$
$\Lambda_b(6152)^0$	$\frac{5}{2}^+$	6152.5 ± 0.4	2.1 ± 0.9	$\Lambda_b^0 \pi^+ \pi^-$

data. Considering the theoretical uncertainty, this result is acceptable. For $\Lambda_c(2940)$, although the predicted mass is about 50 MeV higher than the measured mass, the $2P(\frac{1}{2}^-)$ state is still the best assignment for it. The theoretical total widths for $2P$ -wave $\Lambda_{c1}^{\lambda'}(\frac{1}{2}^-)$ is 12.40 MeV, which is compatible with the experimental data of $\Lambda_c(2940)$. As for the $\Lambda_c(2860)$ and $\Lambda_c(2880)$, they were interpreted as a $1D$ doublet ($\frac{3}{2}^+, \frac{5}{2}^+$) by other collaborations[111]. Our predicted mass spectra in quark model also support this conclusion. Under this assignment, the theoretical total width for $\Lambda_c(2860)$ is 9.03 MeV which is consistent with the results of other collaborations[111]. However, this value is much lower than the experimental data which is about 67 MeV. We hope this divergence can be clarified in the future if more theoretical and experimental efforts were devoted into this problem.

In many references, $\Lambda_b(6146)$ and $\Lambda_b(6152)$ were suggested to be the $1D$ -wave doublet ($\frac{3}{2}^+, \frac{5}{2}^+$) which are the partners of the $\Lambda_c(2860)$ and $\Lambda_c(2880)$ [139, 141]. The predicted total widths for this doublet in this work are 5.99 MeV and 5.43 MeV, respectively. These values are comparable with the experimental measurements and consistent well with the results of other collaborations[139, 141]. However, the LHCb announced that they did not observe significant $\Lambda_b(6146) \rightarrow \Sigma_b^\pm \pi^\pm$ signals in their experiments. This result seems contradictory with theoretical predictions in Table XVI, which needs further confirmation in experiments and theories. As for the $\Lambda_b(6072)$, the LHCb Collaboration suggested that it can be assigned as the first radial excitation of the Λ_b baryon[11], the λ -mode $\Lambda_b(2S)$ state. The mass spectrum in quark model in Table IV also support this conclusion. However, the theoretical widths for the $2S$ -wave $\Lambda_{c0}^{\lambda'}$ and $\Lambda_{c0}^{\rho'}$ are 8.82 MeV and 3.59 MeV respectively, which are all significantly smaller than the experimental data. Our results are in good agreement with those of other collaborations[145]. That is, all of the theoretical works indicate that $\Lambda_b(2S)$ should be a

TABLE XI: Masses,decay widths(MeV),and possible strong decay channels of $\Sigma_Q(Q=c,b)$

States	J^P	Mass	Width	Decay channels(experiment)
$\Sigma_c(2455)^{++}$	$\frac{1}{2}^+$	2453.97±0.14	$1.89^{+0.09}_{-0.18}$	$\Lambda_c^+ \pi$
$\Sigma_c(2455)^+$	$\frac{1}{2}^+$	2452.9±0.4	<4.6	$\Lambda_c^+ \pi$
$\Sigma_c(2455)^0$	$\frac{1}{2}^+$	2453.75±0.14	$1.83^{+0.11}_{-0.19}$	$\Lambda_c^+ \pi$
$\Sigma_c(2520)^{++}$	$\frac{3}{2}^+$	$2518.41^{+0.21}_{-0.19}$	$14.78^{+0.30}_{-0.40}$	$\Lambda_c^+ \pi$
$\Sigma_c(2520)^+$	$\frac{3}{2}^+$	2517.5±2.3	<17	$\Lambda_c^+ \pi$
$\Sigma_c(2520)^0$	$\frac{3}{2}^+$	2518.48±0.20	$15.3^{+0.4}_{-0.5}$	$\Lambda_c^+ \pi$
$\Sigma_c(2800)^{++}$? [?]	2801^{+4}_{-6}	75^{+22}_{-17}	$\Lambda_c^+ \pi$
$\Sigma_c(2800)^+$? [?]	2792^{+14}_{-5}	62^{+60}_{-40}	$\Lambda_c^+ \pi$
$\Sigma_c(2800)^0$? [?]	2806^{+5}_{-7}	72^{+22}_{-15}	$\Lambda_c^+ \pi$
Σ_b^-	$\frac{1}{2}^+$	5815.64±0.27	5.3±0.5	$\Lambda_b^0 \pi$
Σ_b^+	$\frac{1}{2}^+$	5810.56±0.25	5.0±0.5	$\Lambda_b^0 \pi$
Σ_b^{*+}	$\frac{3}{2}^+$	5830.32±0.27	9.4±0.5	$\Lambda_b^0 \pi$
Σ_b^{*-}	$\frac{3}{2}^+$	5834.74±0.30	10.4±0.8	$\Lambda_b^0 \pi$
$\Sigma_b(6097)^-$? [?]	6098.0±1.8	29±4	$\Lambda_b \pi, \Sigma_b \pi, \Sigma_b^* \pi$
$\Sigma_b(6097)^+$? [?]	6095.8±1.7	31±6	$\Lambda_b \pi, \Sigma_b \pi, \Sigma_b^* \pi$

TABLE XII: Masses,decay widths(MeV),and possible strong decay channels of $\Omega_Q(Q=c,b)$

States	J^P	Mass	Width	Decay channels(experiment)
Ω_c^0	$\frac{1}{2}^+$	2695.2±1.7	-	-
$\Omega_c(2770)^0$	$\frac{3}{2}^+$	2765.9±2.0	-	-
$\Omega_c(3000)^0$? [?]	3000.4±0.2±0.1±0.3	4.5±0.6±0.3	$\Xi_c^+ K^-$
$\Omega_c(3050)^0$? [?]	3050.2±0.1±0.1±0.3	< 1.2	$\Xi_c^+ K^-$
$\Omega_c(3065)^0$? [?]	3065.6±0.1±0.3±0.3	3.5±0.4±0.2	$\Xi_c^+ K^-$
$\Omega_c(3090)^0$? [?]	3090.2±0.3±0.5±0.3	8.7±1.0±0.8	$\Xi_c^+ K^-$
$\Omega_c(3120)^0$? [?]	3119.1±0.3±0.9±0.3	< 2.6	$\Xi_c^+ K^-$
$\Omega_b(6316)^-$	$\frac{3}{2}^-$	6315.64±0.31±0.07±0.50	< 2.8(4.2)	$\Xi_b^0 K^-$
$\Omega_b(6330)^-$	$\frac{1}{2}^-$	6330.30±0.28±0.07±0.50	< 3.1(4.7)	$\Xi_b^0 K^-$
$\Omega_b(6340)^-$	$\frac{5}{2}^-$	6339.71±0.26±0.05±0.50	< 1.5(1.8)	$\Xi_b^0 K^-$
$\Omega_b(6350)^-$	$\frac{3}{2}^-$	6349.88±0.35±0.05±0.50	< 2.8(3.2)	$\Xi_b^0 K^-$

narrow state.

It is also shown in Tables XIII-XVI, the predicted total widths for $2P$ -wave states $\Lambda_{c1}^{1\lambda'}(\frac{3}{2}^-)$, $\Lambda_{b1}^{1\lambda'}(\frac{1}{2}^-)$ and $\Lambda_{b1}^{1\lambda'}(\frac{3}{2}^-)$ are 13.31 MeV, 5.97 MeV and 5.81 MeV, respectively. These widths are relatively narrow, which indicates these states have good potentials to be discovered in the future.

To be more specific, the main decay channels are $\Sigma_c^{*+,0}\pi^{0,+}$, $D^{*0}p$ and $D^{*+}n$ for $\Lambda_{c1}^{1\lambda'}(\frac{3}{2}^-)$, while $\Sigma_b^{+,0,-}\pi^{-,0,+}$ and $\Sigma_b^{*+,0,-}\pi^{-,0,+}$ are the main decay modes for $\Lambda_{b1}^{1\lambda'}(\frac{1}{2}^-)$ and $\Lambda_{b1}^{1\lambda'}(\frac{3}{2}^-)$, respectively.

TABLE XIII: Decay widths of $\Lambda_c(\text{MeV})$

N	1	2	3	4	5	6	7
Notations	$\Lambda_{c0}^{0\lambda'}$	$\Lambda_{c0}^{0\rho'}$	Λ_{c1}^1	$\Lambda_{c1}^{1\lambda'}$	$\Lambda_{c1}^{1\rho'}$	Λ_{c1}^1	$\Lambda_{c1}^{1\lambda'}$
Assignments	$\frac{1}{2}^+$ (2S)	$\frac{1}{2}^+$ (2S)	$\frac{1}{2}^-$ (1P)	$\frac{1}{2}^-$ (2P)	$\frac{1}{2}^-$ (2P)	$\frac{3}{2}^-$ (1P)	$\frac{3}{2}^-$ (2P)
Mass	2764	2764	2592	2988	2988	2628	3013
$\Sigma_c^{++}\pi^-$	5.04	1.49	2.72	2.34	6.84	3.09×10^{-3}	8.50×10^{-2}
$\Sigma_c^+\pi^0$	5.14	1.50	6.00	2.34	6.77	3.93×10^{-3}	8.70×10^{-2}
$\Sigma_c^0\pi^+$	5.04	1.49	2.72	2.34	6.84	3.09×10^{-3}	8.50×10^{-2}
$\Sigma_c^{*++}\pi^-$	3.33	1.26	-	5.20×10^{-2}	5.74	-	2.17
$\Sigma_c^{*+}\pi^0$	3.46	1.30	-	5.70×10^{-2}	5.80	-	2.17
$\Sigma_c^{*0}\pi^+$	3.33	1.26	-	0.052	5.74	-	2.17
$D^{*0}p$	-	-	-	2.67	2.81	-	3.31
$D^{*+}n$	-	-	-	2.55	2.80	-	3.23
Γ_{total}	25.34	8.30	11.44	12.40	43.34	1.00×10^{-3}	13.31
$\frac{\Sigma_c^*\pi^\pm}{\Sigma_c\pi^\pm}$	0.66	0.85	-	0.023	0.84	-	25.33

B. Σ_Q states

As for the Σ_Q baryons, the lowest S -wave states $\frac{1}{2}^+$ and $\frac{3}{2}^+$ have been observed and confirmed[5, 6], while the spin-parities of recently observed $\Sigma_c(2800)$ and $\Sigma_b(6097)$ need confirmation in more ways[41, 70, 110, 138]. According to the predictions by quark model, both $\Sigma_c(2800)$ and $\Sigma_b(6097)$ can be accommodated in the mass spectra as lowest-lying P -wave states. However, as illustrated in Tables V-VI, there are five $1P$ -wave states, where their masses are close to each other. In Sec.2.4, $\Sigma_b(6097)$ is proposed to be a $1P(\frac{3}{2}^-)_{j=2}$ state and so does $\Sigma_c(2800)$. From Tables XVII-XXII, it is indicated that both the $\Sigma_c(2800)$ and $\Sigma_b(6097)$ are impossible the spin singlet $J^P = \frac{1}{2}^-$ or the spin doublet $(\frac{1}{2}^-, \frac{3}{2}^-)_{j=1}$ because of their large theoretical widths. For Σ_b baryons, the predicted total widths for $\Sigma_{b2}^1(\frac{3}{2}^-)$ or $\Sigma_{b2}^1(\frac{5}{2}^-)$ are 15.64 MeV and 18.65 MeV respectively, which are close to each other and at the same order of magnitude as the experimental data. Because the predicted mass for $\Sigma_{b2}^1(\frac{3}{2}^-)$ in quark model is closer to the measured results, the $\Sigma_{b2}^1(\frac{3}{2}^-)$ is a better candidate for $\Sigma_b(6097)$. As for $\Sigma_c(2800)$, its situation is very similar with that of $\Sigma_b(6097)$ [146–148] and the possible assignment for it is $\Sigma_{c2}^1(\frac{3}{2}^-)$. If these assignments for $\Sigma_c(2800)$ and $\Sigma_b(6097)$ are true, their predicted total widths are still lower than measured values. Especially for $\Sigma_c(2800)$, its theoretical width is 19.13 MeV, which is much lower than experimental data. The first interpretation of this deviation is the uncertainties of

TABLE XIV: Decay widths of $\Lambda_c(\text{MeV})$

N	1	2	3	4	5	6	7
Notations	$\Lambda_{c1}^{1\rho'}$	Λ_{c2}^2	$\Lambda_{c2}^{2\lambda'}$	$\Lambda_{c2}^{2\rho'}$	Λ_{c2}^2	$\Lambda_{c2}^{2\lambda'}$	$\Lambda_{c2}^{2\rho'}$
Assignments	$\frac{3}{2}^-$ (2P)	$\frac{3}{2}^+$ (1D)	$\frac{3}{2}^+$ (2D)	$\frac{3}{2}^+$ (2D)	$\frac{5}{2}^+$ (1D)	$\frac{5}{2}^+$ (2D)	$\frac{5}{2}^+$ (2D)
Mass	3013	2856	3220	3220	2882	3234	3234
$\Sigma_c^{++}\pi^-$	6.47	2.69	3.10	8.90×10^{-2}	5.60×10^{-2}	8.40×10^{-1}	7.47×10^{-1}
$\Sigma_c^+\pi^0$	6.51	2.71	3.11	8.70×10^{-2}	5.70×10^{-2}	8.43×10^{-1}	7.50×10^{-1}
$\Sigma_c^0\pi^+$	6.47	2.69	3.10	8.90×10^{-2}	5.60×10^{-2}	8.39×10^{-1}	7.47×10^{-1}
$\Sigma_c^{*++}\pi^-$	12.4	0.313	1.36	8.98×10^{-1}	2.34	3.93	6.53×10^{-1}
$\Sigma_c^{*+}\pi^0$	12.4	0.318	1.37	9.01×10^{-2}	2.37	3.93	6.52×10^{-1}
$\Sigma_c^{*0}\pi^+$	12.4	0.313	1.36	8.98×10^{-2}	2.34	3.93	6.53×10^{-1}
$\Lambda_c\omega$	-	-	2.53	2.57	-	2.81	2.70
$\Xi_c'^+K^0$	-	-	1.58×10^{-1}	7.50×10^{-2}	-	2.67×10^{-3}	4.84×10^{-3}
$\Xi_c'^0K^+$	-	-	1.58×10^{-1}	7.50×10^{-2}	-	2.67×10^{-3}	4.84×10^{-3}
$D^{*0}p$	2.69	-	2.90	1.37×10^{-1}	-	3.04	1.66×10^{-1}
$D^{*+}n$	2.73	-	2.87	1.30×10^{-1}	-	3.00	1.58×10^{-1}
$\Xi_c'^{*+}K^0$	-	-	1.30×10^{-2}	8.84×10^{-3}	-	9.90×10^{-2}	6.00×10^{-2}
$\Xi_c'^{*0}K^+$	-	-	1.30×10^{-2}	8.84×10^{-3}	-	9.90×10^{-2}	6.00×10^{-2}
Γ_{total}	62.07	9.03	22.04	5.97	7.22	23.37	7.36
$\frac{\Sigma_c^*\pi^\pm}{\Sigma_c\pi^\pm}$	1.91	0.12	0.44	10.18	41.72	4.67	0.87

the 3P_0 model. In the following, we will see that the result from the 3P_0 model may be a factor of $3 \sim 4$ off the experimental width. Another interpretation of this problem is the mixing mechanism of the quark model states. We know that the physical resonances can be the mixing of the quark model states with the same J^P [125],

$$\begin{pmatrix} |1P_{\frac{1}{2}}^{1-}\rangle_1 \\ |1P_{\frac{1}{2}}^{1-}\rangle_2 \end{pmatrix} = \begin{pmatrix} \cos\theta & \sin\theta \\ -\sin\theta & \cos\theta \end{pmatrix} \begin{pmatrix} |\frac{1}{2}^-, j=0\rangle \\ |\frac{1}{2}^-, j=1\rangle \end{pmatrix} \quad (64)$$

$$\begin{pmatrix} |1P_{\frac{3}{2}}^{3-}\rangle_1 \\ |1P_{\frac{3}{2}}^{3-}\rangle_2 \end{pmatrix} = \begin{pmatrix} \cos\theta & \sin\theta \\ -\sin\theta & \cos\theta \end{pmatrix} \begin{pmatrix} |\frac{3}{2}^-, j=1\rangle \\ |\frac{3}{2}^-, j=2\rangle \end{pmatrix} \quad (65)$$

That is to say, state mixing can occur between $|\frac{3}{2}^-, j=1\rangle$ and $|\frac{3}{2}^-, j=2\rangle$ as in Eq.(65). Considering the mixing mechanism, we plot the total decay widths of the mixing states $|1P_{\frac{3}{2}}^{3-}\rangle_1$ and $|1P_{\frac{3}{2}}^{3-}\rangle_2$ versus the mixing angle θ in the range $0^\circ \sim 30^\circ$ in Figs.17-18. When the mixing angle θ is constrained in $10^\circ \sim 15^\circ$ in Fig.18, the total width of $|1P_{\frac{3}{2}}^{3-}\rangle_2$ can reach about 30 MeV, which is consistent with the experimental data. Thus, $\Sigma_b(6097)$ can be interpreted as a mixing state of $|\frac{3}{2}^-, j=1\rangle$ and

TABLE XV: Decay widths of $\Lambda_b(\text{MeV})$

N	1	2	3	4	5	6
Notations	$\Lambda_{b0}^{1\lambda'}$	$\Lambda_{b0}^{1\rho'}$	$\Lambda_{b1}^{1\lambda'}$	$\Lambda_{b1}^{1\rho'}$	$\Lambda_{b1}^{1\lambda'}$	$\Lambda_{b1}^{1\rho'}$
Assignments	$\frac{1}{2}^+(2S)$	$\frac{1}{2}^+(2S)$	$\frac{1}{2}^-(2P)$	$\frac{1}{2}^-(2P)$	$\frac{3}{2}^-(2P)$	$\frac{3}{2}^-(2P)$
Mass	6072	6072	6238	6238	6249	6249
$\Sigma_b^+ \pi^-$	1.39	5.50×10^{-1}	1.98	11.5	2.40×10^{-2}	2.76
$\Sigma_b^0 \pi^0$	1.39	5.40×10^{-1}	1.97	11.5	2.40×10^{-2}	2.73
$\Sigma_b^- \pi^+$	1.23	4.90×10^{-1}	1.94	11.7	2.20×10^{-2}	2.60
$\Sigma_b^{*+} \pi^-$	1.68	7.00×10^{-1}	2.80×10^{-2}	3.76	1.93	14.0
$\Sigma_b^{*0} \pi^0$	1.69	7.00×10^{-1}	2.80×10^{-2}	3.71	1.92	14.0
$\Sigma_b^{*-} \pi^+$	1.44	6.10×10^{-1}	2.60×10^{-2}	3.51	1.89	14.0
Γ_{total}	8.82	3.59	5.97	45.68	5.81	50.09
$\frac{\Sigma_b^* \pi^\pm}{\Sigma_b \pi^\pm}$	1.2	1.27	0.014	0.32	82	5.19

TABLE XVI: Decay widths of $\Lambda_b(\text{MeV})$

N	1	2	3	4	5	6
Notations	Λ_{b2}^2	$\Lambda_{b2}^{2\lambda'}$	$\Lambda_{b2}^{2\rho'}$	Λ_{b2}^2	$\Lambda_{b2}^{2\lambda'}$	$\Lambda_{b2}^{2\rho'}$
Assignments	$\frac{3}{2}^+(1D)$	$\frac{3}{2}^+(2D)$	$\frac{3}{2}^+(2D)$	$\frac{5}{2}^+(1D)$	$\frac{5}{2}^+(2D)$	$\frac{5}{2}^+(2D)$
Mass	6146	6432	6432	6153	6440	6440
$\Sigma_b^+ \pi^-$	1.75	2.95	3.70×10^{-1}	1.30×10^{-2}	3.50×10^{-1}	4.20×10^{-1}
$\Sigma_b^0 \pi^0$	1.74	2.94	3.80×10^{-1}	1.30×10^{-2}	3.50×10^{-1}	4.10×10^{-1}
$\Sigma_b^- \pi^+$	1.65	2.91	3.90×10^{-1}	1.10×10^{-2}	3.30×10^{-1}	4.00×10^{-1}
$\Sigma_b^{*+} \pi^-$	2.90×10^{-1}	1.02	6.70×10^{-1}	1.84	3.67	7.60×10^{-1}
$\Sigma_b^{*0} \pi^0$	2.90×10^{-1}	1.01	6.60×10^{-1}	1.82	3.65	7.60×10^{-1}
$\Sigma_b^{*-} \pi^+$	2.70×10^{-1}	0.99	6.40×10^{-1}	1.73	3.60	7.70×10^{-1}
$\Lambda_b \omega$	-	4.50×10^{-1}	5.30×10^{-1}	-	6.40×10^{-1}	7.20×10^{-1}
$B^{*-} p$	-	2.72	8.80×10^{-2}	-	2.85	1.10×10^{-1}
$B^{*0} n$	-	2.71	8.70×10^{-2}	-	2.84	1.10×10^{-1}
Γ_{total}	5.99	17.7	3.82	5.43	18.28	4.46
$\frac{\Sigma_b^* \pi^\pm}{\Sigma_b \pi^\pm}$	0.17	0.34	1.73	145.68	10.6	1.86

$|\frac{3}{2}^-, j=2\rangle$. It is same for $\Sigma_c(2800)$, if the mixing angle equals to 30° in Fig.17, the total width of $|1P_{\frac{3}{2}}^-\rangle_2$ can reach $60 \text{ MeV} \sim 70 \text{ MeV}$, which indicates $\Sigma_c(2800)$ is possibly a mixing state of $|\frac{3}{2}^-, j=1\rangle$ and $|\frac{3}{2}^-, j=2\rangle$.

For Σ_Q baryons that have good possibility to be discovered in experiments, we predict the total

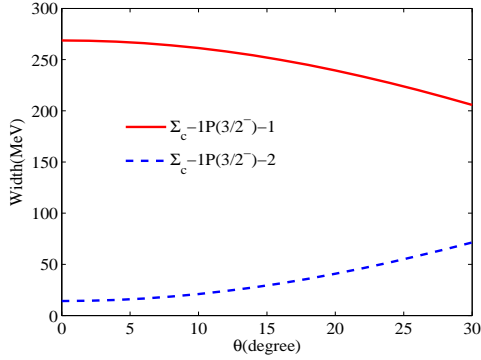


FIG. 17: The total decay widths of $|1P_{\frac{3}{2}}^{-}\rangle_1$ and $|1P_{\frac{3}{2}}^{-}\rangle_2$ as functions of the mixing angle θ in the range $0^\circ \sim 30^\circ$.

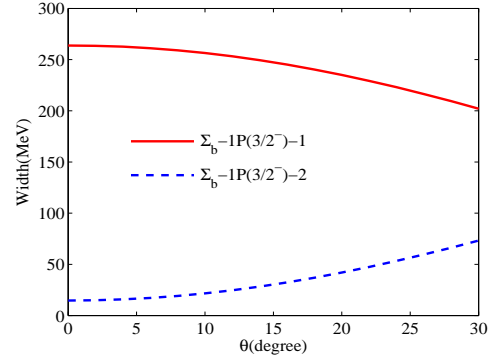


FIG. 18: The total decay widths of $|1P_{\frac{3}{2}}^{-}\rangle_1$ and $|1P_{\frac{3}{2}}^{-}\rangle_2$ as functions of the mixing angle θ in the range $0^\circ \sim 30^\circ$.

widths of $1P$ -wave $\Sigma_c(\frac{5}{2}^-)$ and $\Sigma_b(\frac{5}{2}^-)$ to be 22.42 MeV and 18.65 MeV, respectively. We can see in Tables XIX and XXII, the $\Lambda_c\pi^+$ and $\Lambda_b\pi^+$ are the ideal channels to search for these two states. As mentioned in Sec.2.4, the $2S$ -wave $\Sigma_Q(\frac{1}{2}^+)$ and $\Sigma_Q(\frac{3}{2}^+)$ are also expected to be observed in the near future. The theoretical total widths for the states $\Sigma_{c1}^{0\rho'}(\frac{1}{2}^+)$, $\Sigma_{c1}^{0\rho'}(\frac{3}{2}^+)$, $\Sigma_{b1}^{0\rho'}(\frac{1}{2}^+)$, and $\Sigma_{b1}^{0\rho'}(\frac{3}{2}^+)$ are about $11 \sim 13$ MeV, which are relatively narrow. These narrow total widths suggest that these states may be easily observed in future experiments. The decay modes $\Sigma_c^{++,+}\pi^{0,+}$ and $\Sigma_c^{*++,+}\pi^{0,+}$ provide dominating contributions to the total widths of $\Sigma_{c1}^{0\rho'}(\frac{1}{2}^+)$ and $\Sigma_{c1}^{0\rho'}(\frac{3}{2}^+)$, while $\Sigma_b^{+,0}\pi^{0,+}$, and $\Sigma_b^{*+,0}\pi^{0,+}$ are the dominating decay channels for $\Sigma_{b1}^{0\rho'}(\frac{1}{2}^+)$ and $\Sigma_{b1}^{0\rho'}(\frac{3}{2}^+)$ states.

C. Ω_Q states

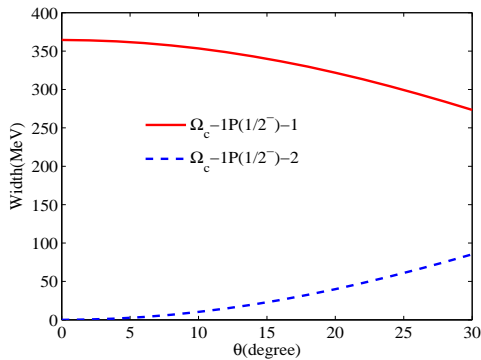


FIG. 19: The total decay widths of $|1P_{\frac{1}{2}}^{-}\rangle_1$ and $|1P_{\frac{1}{2}}^{-}\rangle_2$ as functions of the mixing angle θ in the range $0^\circ \sim 30^\circ$.

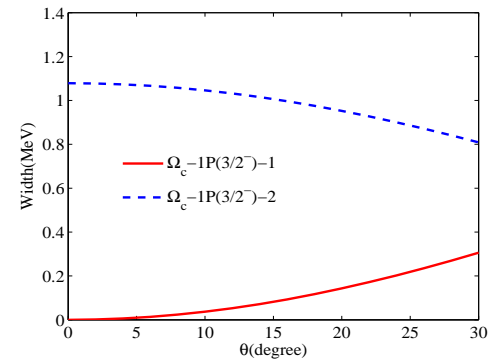


FIG. 20: The total decay widths of $|1P_{\frac{3}{2}}^{-}\rangle_1$ and $|1P_{\frac{3}{2}}^{-}\rangle_2$ as functions of the mixing angle θ in the range $0^\circ \sim 30^\circ$.

TABLE XVII: Decay widths (MeV) of Σ_c

N	1	2	3	4	5	6	7
Notations	$\Sigma_{c1}^{0\lambda'}$	$\Sigma_{c1}^{0\rho'}$	Σ_{c1}^0	$\Sigma_{c1}^{0\lambda'}$	$\Sigma_{c1}^{0\rho'}$	Σ_{c0}^1	$\Sigma_{c0}^{1\lambda'}$
Assignments	$\frac{1}{2}^+$ (2S)	$\frac{1}{2}^+$ (2S)	$\frac{3}{2}^+$ (1S)	$\frac{3}{2}^+$ (2S)	$\frac{3}{2}^+$ (2S)	$\frac{1}{2}^-$ (1P)	$\frac{1}{2}^-$ (2P)
Mass	2913	2913	2518	2967	2967	2823	3196
$\Lambda_c\pi^+$	71.70	5.38×10^{-1}	12.90	93.70	1.75×10^{-4}	282.70	6.96
$\Lambda_c\rho^+$	-	-	-	-	-	-	1.26×10^{-9}
$\Sigma_c^{++}\pi^0$	33.00	3.80	-	12.40	8.26×10^{-1}	1.23×10^{-10}	8.93×10^{-10}
$\Sigma_c^+\pi^+$	32.70	3.81	-	12.30	8.33×10^{-1}	1.13×10^{-10}	3.03×10^{-9}
$\Sigma_c^{*++}\pi^0$	9.28	1.73	-	38.00	4.78	1.08×10^{-11}	3.55×10^{-9}
$\Sigma_c^{*+}\pi^+$	9.28	1.73	-	38.00	4.78	1.08×10^{-11}	3.55×10^{-9}
$\Xi_c'^+K^+$	-	-	-	-	-	-	1.50×10^{-10}
$\Xi_c^+K^+$	-	-	-	2.74×10^{-3}	1.35×10^{-3}	-	2.31
$\Xi_c^{*+}K^+$	-	-	-	-	-	-	1.41×10^{-10}
D^+p	10.20	3.50×10^{-1}	-	18.80	1.26	100.30	8.09
$D^{*+}p$	-	-	-	1.77	1.71×10^{-3}	-	1.38×10^{-8}
$D^0\Delta^{++}$	-	-	-	-	-	-	7.91×10^{-9}
$D^+\Delta^+$	-	-	-	-	-	-	2.36×10^{-9}
$D_s\Sigma^+$	-	-	-	-	-	-	1.51×10^{-11}
Γ_{total}	166.16	11.96	12.90	214.97	12.48	383	17.36
$\frac{\Sigma_c^*\pi}{\Sigma_c\pi}$	0.28	0.45	-	3.08	5.76	0.1	1.81

We have also seen that the available experimental data for Ω_Q baryons are well reproduced by the quark model. And the spin-parities of these experimental states have also been tentatively determined by comparing their measured masses with model predictions. The $(\Omega_c(3000), \Omega_c(3050))$ and $(\Omega_c(3065), \Omega_c(3090))$ were interpreted as the $1P$ doublets $(\frac{1}{2}^-, \frac{3}{2}^-)_{j=1}$ and $(\frac{3}{2}^-, \frac{5}{2}^-)_{j=2}$, respectively. The $\Omega_c(3120)$ was described as the $2S(\frac{1}{2}^+)$ state. From Table XXIII, one can see that the theoretical width of $2S(\Omega_{c1}^{0\rho'})$ is 5.95 MeV, which is larger than the experimental data. Under the theoretical uncertainty, our assignment for $\Omega_c(3120)$ is possible. We can also see that the predicted widths for the five $1P$ -wave states, $\Omega_{c0}^1(\frac{1}{2}^-)$, $\Omega_{c1}^1(\frac{1}{2}^-)$, $\Omega_{c1}^1(\frac{3}{2}^-)$, $\Omega_{c2}^1(\frac{3}{2}^-)$ and $\Omega_{c2}^1(\frac{5}{2}^-)$ are 364 MeV, 2.18×10^{-11} MeV, 2.85×10^{-10} MeV, 1.08 MeV and 2.50 MeV, respectively. In comparison with the experimental data, the assignments for $\Omega_c(3065)$ and $\Omega_c(3090)$ as a doublet $(\frac{3}{2}^-, \frac{5}{2}^-)_{j=2}$ is reasonable. However, the predicted widths of the doublet $(\frac{1}{2}^-, \frac{3}{2}^-)_{j=1}$ are very tiny, which means our assignments for $\Omega_c(3000)$ and $\Omega_c(3050)$ is contradictory with experiments. In Ref.[118], these two Ω_c baryons were suggested to be the $1D$ -wave states. However, the predicted masses in quark model for $1D$ -wave Ω_c are much larger than the experimental data, which indicates $1D$ -wave states are not good candidates for $\Omega_c(3000)$ and

TABLE XVIII: Decay widths (MeV) of Σ_c

N	1	2	3	4	5	6	7
Notations	$\Sigma_{c0}^{1\rho'}$	Σ_{c1}^1	$\Sigma_{c1}^{1\lambda'}$	$\Sigma_{c1}^{1\rho'}$	Σ_{c1}^1	$\Sigma_{c1}^{1\lambda'}$	$\Sigma_{c1}^{1\rho'}$
Assignments	$\frac{1}{2}^-$ (2P)	$\frac{1}{2}^-$ (1P)	$\frac{1}{2}^-$ (2P)	$\frac{1}{2}^-$ (2P)	$\frac{3}{2}^-$ (1P)	$\frac{3}{2}^-$ (2P)	$\frac{3}{2}^-$ (2P)
Mass	3196	2809	3185	3185	2829	3202	3202
$\Lambda_c \pi^+$	16.30	5.85×10^{-11}	4.53×10^{-9}	7.91×10^{-10}	2.22×10^{-10}	4.45×10^{-9}	4.27×10^{-10}
$\Lambda_c \rho^+$	3.15×10^{-9}	-	3.42	57.8	-	3.69	52.80
$\Sigma_c^{++} \pi^0$	1.25×10^{-10}	157	5.85	2.90×10^{-2}	9.92×10^{-1}	2.97×10^{-1}	9.50
$\Sigma_c^+ \pi^+$	2.36×10^{-10}	157	5.85	3.20×10^{-2}	9.71×10^{-1}	2.95×10^{-1}	9.48
$\Sigma_c^{*++} \pi^0$	8.65×10^{-10}	3.90×10^{-1}	2.84×10^{-1}	13.20	134	5.99	8.42
$\Sigma_c^{*+} \pi^+$	8.65×10^{-10}	3.90×10^{-1}	2.84×10^{-1}	13.20	134	5.99	8.42
$\Xi_c'^+ K^+$	1.40×10^{-11}	-	1.02	9.56	-	1.36×10^{-3}	2.07×10^{-1}
$\Xi_c^+ K^+$	6.68	-	3.82×10^{-10}	7.40×10^{-11}	-	1.54×10^{-10}	1.25×10^{-10}
$\Xi_c^{*+} K^+$	3.04×10^{-11}	-	1.07×10^{-4}	2.60×10^{-2}	-	7.15×10^{-1}	9.69
$D^+ p$	8.23	1.26×10^{-12}	8.45×10^{-11}	4.65×10^{-11}	7.76×10^{-12}	6.24×10^{-9}	1.80×10^{-10}
$D^{*+} p$	7.51×10^{-13}	-	6.33	1.68	-	6.34	2.08
$D^0 \Delta^{++}$	1.88×10^{-11}	-	6.30×10^{-2}	5.38×10^{-1}	-	10.4	6.60×10^{-1}
$D^+ \Delta^+$	2.52×10^{-11}	-	1.90×10^{-2}	1.63×10^{-1}	-	3.42	2.50×10^{-1}
$D_s \Sigma^+$	1.40×10^{-11}	-	2.95	1.68	-	1.58×10^{-3}	1.90×10^{-2}
Γ_{total}	31.21	314.78	26.07	97.91	269.96	37.14	101.53
$\frac{\Sigma_c^* \pi}{\Sigma_c \pi}$	4.79	0.002	0.049	432.79	136.53	20.24	0.89

$\Omega_c(3050)$. Again, if we consider the mixing of the quark model states as in Eqs.(64)-(65), $\Omega_c(3000)$ and $\Omega_c(3050)$ still can be described as the $1P$ -wave states.

We plot the total widths of the mixing states versus the mixing angle θ in the range $0^\circ \sim 30^\circ$ in Figs.19-20. After considering the mixing of the pure quark model states, three mixing states $|1P\frac{1}{2}^- \rangle_2$, $|1P\frac{3}{2}^- \rangle_1$, and $|1P\frac{3}{2}^- \rangle_2$ belong to the narrow resonances. If the mixing angle θ is constrained in a small value in Fig.19, the total width of $|1P\frac{1}{2}^- \rangle_2$ reaches a magnitude of MeV. In addition, the values for $|1P\frac{3}{2}^- \rangle_1$ and $|1P\frac{3}{2}^- \rangle_2$ in Fig.20 are all lower than 1 MeV. Considering the uncertainties of the model, these results are compatible with the experimental data. Thus, we tentatively assign the $\Omega_c(3000)$, $\Omega_c(3050)$, and $\Omega_c(3065)$ as the mixing states $|1P\frac{1}{2}^- \rangle_2$, $|1P\frac{3}{2}^- \rangle_1$ and $|1P\frac{3}{2}^- \rangle_2$, respectively and assign $\Omega_c(3090)$ as a pure $1P(\frac{5}{2}^-)$ state.

As for the narrow resonances, $\Omega_b(6316)$, $\Omega_b(6330)$, $\Omega_b(6340)$, and $\Omega_b(6350)$, their situation is very similar with the $1P$ -wave Ω_c states. After considering the mixing of the quark model states, the total width are plotted in Figs.21-22. From these figures, we can obtain the similar conclusions with Ω_c baryons, that $\Omega_b(6316)$, $\Omega_b(6330)$, $\Omega_b(6340)$, and $\Omega_b(6350)$ can be respectively described as three

TABLE XIX: Decay widths (MeV) of Σ_c

N	1	2	3	4	5	6
Notations	Σ_{c2}^1	$\Sigma_{c2}^{1\lambda'}$	$\Sigma_{c2}^{1\rho'}$	Σ_{c2}^1	$\Sigma_{c2}^{1\lambda'}$	$\Sigma_{c2}^{1\rho'}$
Assignments	$\frac{3}{2}^-$ (1P)	$\frac{3}{2}^-$ (2P)	$\frac{3}{2}^-$ (2P)	$\frac{5}{2}^-$ (1P)	$\frac{5}{2}^-$ (2P)	$\frac{5}{2}^-$ (2P)
Mass	2806	3179	3179	2835	3207	3207
$\Lambda_c \pi^+$	13.60	2.06	33.40	18.70	2.49	35.0
$\Lambda_c \rho^+$	-	1.70×10^{-2}	8.99	-	3.70×10^{-2}	14.5
$\Sigma_c^{++} \pi^0$	1.13	4.36×10^{-1}	15.57	8.70×10^{-1}	2.46×10^{-1}	7.75
$\Sigma_c^+ \pi^+$	1.11	4.33×10^{-1}	5.53	8.50×10^{-1}	2.46×10^{-1}	7.74
$\Sigma_c^{*++} \pi^0$	2.95×10^{-1}	2.41×10^{-1}	11.51	9.70×10^{-1}	4.93×10^{-1}	20.70
$\Sigma_c^{*+} \pi^+$	2.95×10^{-1}	2.41×10^{-1}	11.51	9.70×10^{-1}	4.93×10^{-1}	20.70
$\Xi_c'^+ K^+$	-	1.29×10^{-3}	2.30×10^{-1}	-	1.24×10^{-3}	1.83×10^{-1}
$\Xi_c^+ K^+$	-	1.90×10^{-2}	1.75	-	3.00×10^{-2}	2.33
$\Xi_c^{*+} K^+$	-	6.28×10^{-5}	1.6×10^{-2}	-	4.96×10^{-4}	1.07×10^{-1}
$D^+ p$	-	0.854	1.95	5.70×10^{-2}	1.05	1.99
$D^{*+} p$	-	3.60×10^{-1}	2.66	-	4.98×10^{-1}	3.16
$D^0 \Delta^{++}$	-	4.80×10^{-2}	4.30×10^{-1}	-	1.43×10^{-1}	1.08
$D^+ \Delta^+$	-	1.40×10^{-2}	1.30×10^{-1}	-	4.30×10^{-2}	3.40×10^{-1}
$D_s \Sigma^+$	-	4.55×10^{-4}	6.25×10^{-3}	-	1.67×10^{-3}	2.00×10^{-2}
Γ_{total}	19.13	4.72	93.68	22.42	5.77	115.60
$\frac{\Sigma_c^* \pi}{\Sigma_c \pi}$	0.26	0.55	1.09	1.13	2	2.67

mixing states $|1P_{\frac{1}{2}}^{1-}\rangle_2$, $|1P_{\frac{3}{2}}^{3-}\rangle_1$, $|1P_{\frac{3}{2}}^{3-}\rangle_2$, and a pure quark state $1P(\frac{5}{2}^-)$. In Refs.[125, 126], they also obtained the same conclusions as ours.

If $\Omega_c(3119)$ is assigned as a $2S(\frac{1}{2}^+)$ state, the $2S(\frac{3}{2}^+)$ state still remain to be found. In Table XXIII, we can see the theoretical width for $\Omega_{c1}^{0\rho'}(\frac{3}{2}^+)$ is 6.33 MeV and its main decay channels are $\Xi_c^+ K^-$, $\Xi_c^0 K^0$ and $\Xi_c^{*+} K^-$. Thus, the $2S(\frac{3}{2}^+)$ state have good potentials to be observed in these above decay channels. Finally, another valuable clues for experiments are the predictions for $2S$ -wave $\Omega_b(\frac{1}{2}^+)$ and $\Omega_b(\frac{3}{2}^+)$ which are still missing in experiments. The results in Table XXVI show that the radial excited mode of these two states may be the ρ' excitations with $(n_\rho, n_\lambda)=(1, 0)$. Theoretical predicting widths for these two states are 5.06 MeV and 4.63 MeV, respectively. They have the similar decay behaviors with each other, both of them dominantly decay into $\Xi_b^0 K^-$ and $\Xi_b^- K^0$.

Finally, let us take a short discussion about the uncertainties of the results based on the 3P_0 decay model. Since this model is a simplified model of a complicated theory, it is not surprising that the prediction is not very accurate. Especially, the input parameter R has a significant influence on the shapes of the radial wave functions, the spatial integral in Eq.(61) is sensitive to the parameter R ,

TABLE XX: Decay widths (MeV) of Σ_b

N	1	2	3	4	5	6	7
Notations	$\Sigma_{b1}^{0\lambda'}$	$\Sigma_{b1}^{0\rho'}$	Σ_{b1}^0	$\Sigma_{b1}^{0\lambda'}$	$\Sigma_{b1}^{0\rho'}$	Σ_{b0}^1	$\Sigma_{b0}^{1\lambda'}$
Assignments	$\frac{1}{2}^+$ (2S)	$\frac{1}{2}^+$ (2S)	$\frac{3}{2}^+$ (1S)	$\frac{3}{2}^+$ (2S)	$\frac{3}{2}^+$ (2S)	$\frac{1}{2}^-$ (1P)	$\frac{1}{2}^-$ (2P)
Mass	6225	6225	5835	6246	6246	6113	6447
$\Lambda_b \pi^+$	88.80	3.05×10^{-1}	14.0	100	4.50×10^{-2}	316	8.23
$\Lambda_b \rho^+$	-	-	-	-	-	-	3.42×10^{-9}
$\Sigma_b^+ \pi^0$	28.40	4.09	-	8.67	1.04	3.64×10^{-12}	2.60×10^{-9}
$\Sigma_b^0 \pi^+$	28.20	4.09	-	8.59	1.04	6.54×10^{-12}	2.56×10^{-9}
$\Sigma_b^{*+} \pi^0$	11.80	1.96	-	36.3	5.13	6.60×10^{-13}	1.62×10^{-9}
$\Sigma_b^{*0} \pi^+$	11.80	1.96	-	36.3	5.13	6.60×10^{-13}	1.62×10^{-9}
$\Xi_b'^+ K^+$	-	-	-	-	-	-	-
$\Xi_b^+ K^+$	-	-	-	-	-	-	2.31
$\overline{B}^0 p$	3.06×10^{-1}	3.19×10^{-3}	-	2.46	4.70×10^{-2}	-	12.4
$\overline{B}^{*0} p$	-	-	-	-	-	-	7.11×10^{-11}
Γ_{total}	169.31	12.41	14.00	189.91	12.43	316.00	22.94
$\frac{\Sigma_b^* \pi}{\Sigma_b \pi}$	0.42	0.48	-	4.21	4.93	0.13	0.63

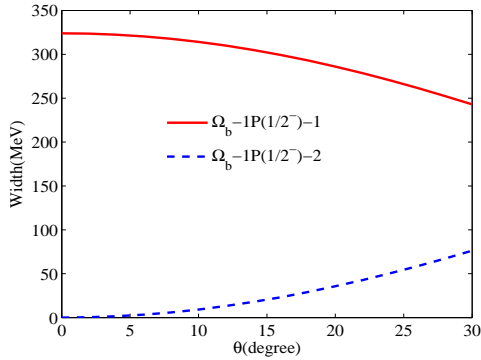


FIG. 21: The total decay widths of $|1P_{\frac{1}{2}}^{-}\rangle_1$ and $|1P_{\frac{1}{2}}^{-}\rangle_2$ as functions of the mixing angle θ in the range $0^\circ \sim 30^\circ$.

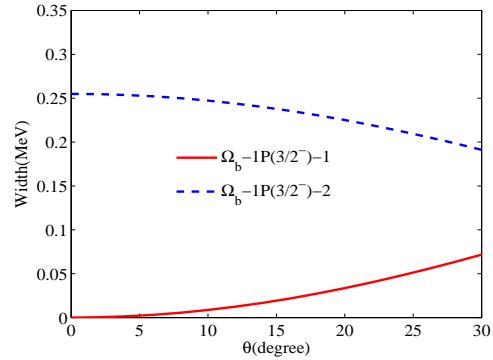
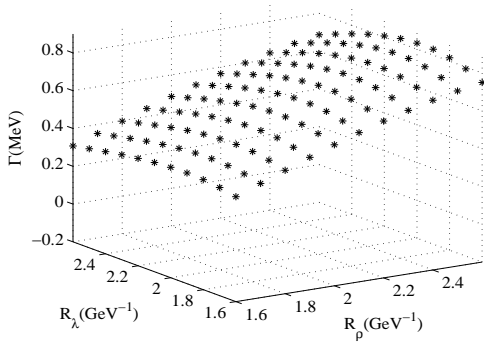
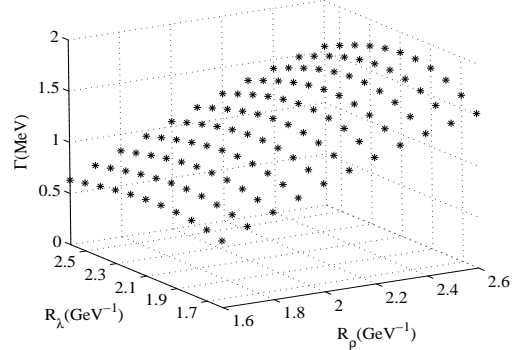


FIG. 22: The total decay widths of $|1P_{\frac{3}{2}}^{-}\rangle_1$ and $|1P_{\frac{3}{2}}^{-}\rangle_2$ as functions of the mixing angle θ in the range $0^\circ \sim 30^\circ$.

therefore the decay width based on the 3P_0 decay model is sensitive to the parameter R . Taking the decay channels $\Omega_{c2}^1(\frac{3}{2}^-) \rightarrow \Xi_c^+ K^-$ and $\Omega_{c2}^1(\frac{5}{2}^-) \rightarrow \Xi_c^+ K^-$ as examples, we plot the decay widths versus the R_ρ and R_λ of the Ω_c states in Figs.23-24. From these figures, we can see that the predicted width changes 3 ~ 4 times when the parameters R_ρ and R_λ of Ω_{c2}^1 are changed from 1.6 GeV^{-1} to 2.6 GeV^{-1} . Even with the above uncertainty, the 3P_0 model is still the most systematic, effective, and

TABLE XXI: Decay widths (MeV) of Σ_b

N	1	2	3	4	5	6	7
Notations	$\Sigma_{b0}^{1\rho'}$	Σ_{b1}^1	$\Sigma_{b1}^{1\lambda'}$	$\Sigma_{b1}^{1\rho'}$	Σ_{b1}^1	$\Sigma_{b1}^{1\lambda'}$	$\Sigma_{b1}^{1\rho'}$
Assignments	$\frac{1}{2}^-$ (2P)	$\frac{1}{2}^-$ (1P)	$\frac{1}{2}^-$ (2P)	$\frac{1}{2}^-$ (2P)	$\frac{3}{2}^-$ (1P)	$\frac{3}{2}^-$ (2P)	$\frac{3}{2}^-$ (2P)
Mass	6447	6107	6442	6442	6116	6450	6450
$\Lambda_b \pi^+$	16.70	9.39×10^{-11}	5.50×10^{-9}	1.06×10^{-9}	-	6.05×10^{-9}	1.37×10^{-9}
$\Lambda_b \rho^+$	1.87×10^{-10}	-	2.47	83.4	-	2.71	83.3
$\Sigma_b^+ \pi^0$	4.47×10^{-10}	139	6.45	2.08	3.52×10^{-1}	1.80×10^{-1}	7.89
$\Sigma_b^0 \pi^+$	4.82×10^{-10}	138	6.45	2.14	3.40×10^{-1}	1.79×10^{-1}	7.86
$\Sigma_b^{*+} \pi^0$	6.71×10^{-10}	3.59×10^{-1}	2.66×10^{-1}	13.4	132	6.53	9.90
$\Sigma_b^{*0} \pi^+$	6.71×10^{-10}	3.59×10^{-1}	2.66×10^{-1}	13.4	132	6.53	9.90
$\Xi_b'^+ K^+$	1.40×10^{-12}	-	9.70×10^{-2}	1.92	-	1.43×10^{-6}	3.77×10^{-4}
$\Xi_b^+ K^+$	12.40	-	1.54×10^{-10}	1.84×10^{-11}	-	1.87×10^{-7}	2.56×10^{-11}
$\overline{B}^0 p$	4.60	-	2.62×10^{-10}	1.51×10^{-10}	-	4.69×10^{-10}	5.82×10^{-11}
$\overline{B}^{*0} p$	7.65×10^{-11}	-	8.39	1.67	-	8.41	1.96
Γ_{total}	33.70	277.72	24.39	118.01	264.69	24.54	120.81
$\frac{\Sigma_b^* \pi}{\Sigma_b \pi}$	1.44	0.002	0.04	6.35	381.5	36.38	1.26

FIG. 23: The variation of the decay width of $\Omega_{c2}^1(\frac{3}{2}^-) \rightarrow \Xi_c^+ K^-$ with R_ρ and R_λ .FIG. 24: The variation of the decay width of $\Omega_{c2}^1(\frac{5}{2}^-) \rightarrow \Xi_c^+ K^-$ with R_ρ and R_λ .

widely used framework to study the baryon strong decays.

5 Conclusions

In this work, we have systematically investigate the mass spectra and strong decay behaviors of the single heavy baryons Λ_Q , Σ_Q , and Ω_Q . The first feature of this work in studying the mass spectra is that the baryons are regarded as a real three-body systems of quarks and all quarks contribute fully to the dynamics in the baryon. This is very different with the heavy-quark-light-diquark approximations

TABLE XXII: Decay widths (MeV) of Σ_b

N	1	2	3	4	5	6
Notations	Σ_{b2}^1	$\Sigma_{b2}^{1\lambda'}$	$\Sigma_{b2}^{1\rho'}$	Σ_{b2}^1	$\Sigma_{b2}^{1\lambda'}$	$\Sigma_{b2}^{1\rho'}$
Assignments	$\frac{3}{2}^-$ (1P)	$\frac{3}{2}^-$ (2P)	$\frac{3}{2}^-$ (2P)	$\frac{5}{2}^-$ (1P)	$\frac{5}{2}^-$ (2P)	$\frac{5}{2}^-$ (2P)
Mass	6098	6439	6439	6119	6452	6452
$\Lambda_b \pi^+$	14.10	2.34	38.6	16.7	2.60	39.7
$\Lambda_b \rho^+$	-	1.15×10^{-3}	1.53	-	2.62×10^{-3}	2.86
$\Sigma_b^+ \pi^0$	4.81×10^{-1}	2.87×10^{-1}	13.30	3.00×10^{-1}	1.47×10^{-1}	6.39
$\Sigma_b^0 \pi^+$	4.62×10^{-1}	2.84×10^{-1}	13.20	2.91×10^{-1}	1.46×10^{-1}	6.36
$\Sigma_b^{*+} \pi^0$	2.99×10^{-1}	2.31×10^{-1}	11.8	6.80×10^{-1}	4.19×10^{-1}	20.00
$\Sigma_b^{*0} \pi^+$	2.99×10^{-1}	2.31×10^{-1}	11.8	6.80×10^{-1}	4.19×10^{-1}	20.00
$\Xi_b'^+ K^+$	-	-	-	-	8.88×10^{-7}	5.02×10^{-4}
$\Xi_b^+ K^+$	-	8.11×10^{-3}	1.00	-	1.10×10^{-2}	1.24
$\overline{B}^0 p$	-	5.13×10^{-1}	1.51	-	6.03×10^{-1}	1.61
$\overline{B}^{*0} p$	-	4.09×10^{-1}	2.42	-	5.00×10^{-1}	2.71
Γ_{total}	15.64	4.30	95.16	18.65	4.85	100.87
$\frac{\Sigma_b^{*+} \pi}{\Sigma_b^+ \pi}$	0.63	0.81	0.89	2.3	2.86	3.14

where the three-body problem was reduced to two-body calculations. Second, all parameters of our relativistic quark model such as quark masses and parameters of the interquark potential were determined previously according to the ground states of the baryons. Third, this is the first time that the masses of ground, orbitally and radially excited single heavy baryons up to rather excitations are systematically studied (in Tables III-VIII).

In addition, with the predicted mass spectra, we construct the Regge trajectories in (J, M^2) plane. It is found that the available experimental data nicely fit to the Regge trajectories, which suggests our assignments for the excited heavy baryons are reasonable. Finally, to make a further confirmation about the quantum numbers of the experimental states and to provide more valuable infirmations for searching for the missing baryon states in experiments, we systematically study the strong decay behaviors in the 3P_0 quark model. In summary, we have obtained the followings:

(1) We have studied the dependencies on the heavy quark mass m_Q of the λ -mode, ρ -mode and λ - ρ mixing mode to see the features of the single heavy baryons. The results show that mixing of these different excited modes is suppressed and only λ -mode dominates. Basing on this mechanism, we obtained the mass spectra of the Λ_Q , Σ_Q , and Ω_Q baryons with λ excitations. It is found that all currently available experimental data can be well reproduced.

(2) With the predicted masses, we construct the Regge trajectories in (J, M^2) plane and also obtain

TABLE XXIII: Decay widths (MeV) of Ω_c

N	1	2	3	4	5	6
Notations	$\Omega_{c1}^{0\lambda'}$	$\Omega_{c1}^{0\rho'}$	$\Omega_{c1}^{0\lambda'}$	$\Omega_{c1}^{0\rho'}$	Ω_{c0}^1	$\Omega_{c0}^{1\lambda'}$
Assignments	$\frac{1}{2}^+$ (2S)	$\frac{1}{2}^+$ (2S)	$\frac{3}{2}^+$ (2S)	$\frac{3}{2}^+$ (2S)	$\frac{1}{2}^-$ (1P)	$\frac{1}{2}^-$ (2P)
Mass	3120	3120	3197	3197	3057	3426
$\Xi_c^+ K^-$	14.40	2.03	28.9	1.38	183	4.79
$\Xi_c^+ K^{*-}$	-	-	-	-	-	1.11×10^{-8}
$\Xi_c^0 K^0$	13.50	2.04	27.81	1.47	181	4.83
$\Xi_c^0 K^{*0}$	-	-	-	-	-	3.54×10^{-9}
$\Xi_c^{*+} K^-$	2.77	1.01	3.28	6.40×10^{-1}	-	7.45×10^{-10}
$\Xi_c^{*+} K^-$	-	-	3.17	1.18	-	1.15×10^{-10}
$\Xi_c^{\prime 0} K^0$	2.29	8.70×10^{-1}	3.07	6.30×10^{-1}	-	1.51×10^{-9}
$\Xi_c^{*0} K^0$	-	-	2.69	1.03	-	5.34×10^{-10}
$\Xi^0 D^0$	-	-	5.60×10^{-1}	2.31×10^{-3}	-	9.90×10^{-10}
$\Xi^- D^+$	-	-	9.00×10^{-2}	1.67×10^{-4}	-	3.80×10^{-10}
$\Xi^0 D^{*0}$	-	-	-	-	-	1.85
$\Xi^- D^{*+}$	-	-	-	-	-	1.77
Γ_{total}	32.96	5.95	78.16	6.33	364.00	13.24
$\frac{\Xi_c^0 K^0}{\Xi_c^+ K^-}$	0.94	1.00	0.96	1.07	0.99	1.01

the slopes and intercepts of the Regge trajectories. Both the predicted masses and the experimental data fit nicely to the linear trajectories in (J, M^2) plane.

(3) According to the predicted mass spectra as well as the strong decay properties obtained by 3P_0 model, a number of experimental states without spin-parity assignments are successfully distinguished. For example, the $\Lambda_c(2940)$, $\Lambda_c(2860)$, $\Lambda_c(2880)$, $\Lambda_b(6070)$ are suggested to be the $2P(\frac{1}{2}^-)$, $1D(\frac{1}{2}^+)$, $1D(\frac{3}{2}^+)$ and $2S(\frac{1}{2}^+)$ respectively. The $\Sigma_c(2800)$ and $\Sigma_b(6097)$ may be the pure quark model state $1P(\frac{3}{2}^-)_{j=2}$. Another possible interpretation is that each of them is the mixing state of $|\frac{3}{2}^-, j=1\rangle$ and $|\frac{3}{2}^-, j=2\rangle$. At present, it is difficult for us to make a further confirmation with current calculations. The $\Omega_c(3120)$ and $\Omega_c(3090)$ are assigned as the pure quark model states $2S(\frac{1}{2}^+)$ and $1P(\frac{5}{2}^-)$, respectively, while $\Omega_c(3000)$, $\Omega_c(3050)$ and $\Omega_c(3065)$ can be interpreted as the mixing states $|1P(\frac{1}{2}^-)_{j=2}\rangle$, $|1P(\frac{3}{2}^-)_{j=1}\rangle$, $|1P(\frac{3}{2}^-)_{j=2}\rangle$. The $\Omega_b(6316)$, $\Omega_b(6330)$, $\Omega_b(6340)$, and $\Omega_b(6350)$ can be described as the mixing states $|1P(\frac{1}{2}^-)_{j=2}\rangle$, $|1P(\frac{3}{2}^-)_{j=1}\rangle$, $|1P(\frac{3}{2}^-)_{j=2}\rangle$, and a pure quark model state $1P(\frac{5}{2}^-)$, respectively.

(4) A number of single heavy baryons which have good potentials to be discovered in forthcoming experiments are predicted by quark model. Some valuable clues for searching for these missing baryons are suggested by 3P_0 decay model. For Λ_Q systems, we suggest to search for the $2P$ -wave state

TABLE XXIV: Decay widths (MeV) of Ω_c

N	1	2	3	4	5	6	7
Notations	$\Omega_{c0}^{1\rho'}$	Ω_{c1}^1	$\Omega_{c1}^{1\lambda'}$	$\Omega_{c1}^{1\rho'}$	Ω_{c1}^1	$\Omega_{c1}^{1\lambda'}$	$\Omega_{c1}^{1\rho'}$
Assignments	$\frac{1}{2}^-$ (2P)	$\frac{1}{2}^-$ (1P)	$\frac{1}{2}^-$ (2P)	$\frac{1}{2}^-$ (2P)	$\frac{3}{2}^-$ (1P)	$\frac{3}{2}^-$ (2P)	$\frac{3}{2}^-$ (2P)
Mass	3426	3000	3416	3416	3050	3431	3431
$\Xi_c^+ K^-$	2.25	1.30×10^{-11}	1.38×10^{-9}	2.89×10^{-9}	2.06×10^{-10}	7.89×10^{-10}	2.27×10^{-9}
$\Xi_c^+ K^{*-}$	7.90×10^{-10}	-	1.21	39.60	-	1.41	38.9
$\Xi_c^0 K^0$	1.95	8.76×10^{-12}	1.25×10^{-9}	9.24×10^{-11}	7.88×10^{-11}	4.80×10^{-10}	2.49×10^{-9}
$\Xi_c^0 K^{*0}$	1.60×10^{-9}	-	1.18	39.6	-	1.38	39.10
$\Xi_c'^+ K^-$	9.67×10^{-11}	-	3.52	8.94×10^{-1}	-	1.14×10^{-1}	4.61
$\Xi_c^{*'+} K^-$	5.67×10^{-10}	-	7.25×10^{-2}	4.95	-	3.44	7.30
$\Xi_c'^0 K^0$	3.15×10^{-10}	-	3.53	1.05	-	1.09×10^{-1}	4.53
$\Xi_c^{*'0} K^0$	4.88×10^{-10}	-	6.94×10^{-2}	4.83	-	3.43	7.51
$\Xi^0 D^0$	9.84×10^{-12}	-	11.0	2.602	-	3.40×10^{-1}	1.19
$\Xi^- D^+$	5.07×10^{-11}	-	11.1	2.012	-	3.02×10^{-1}	1.14
$\Xi^0 D^{*0}$	2.69	-	1.56×10^{-1}	2.097	-	1.16×10^{-1}	1.42
$\Xi^- D^{*+}$	2.38	-	1.18×10^{-1}	1.67	-	9.10×10^{-2}	1.18
Γ_{total}	9.27	2.18×10^{-11}	31.96	99.31	2.85×10^{-10}	10.73	106.88
$\frac{\Xi_c^0 K^0}{\Xi_c^+ K^-}$	8.70×10^{-1}	6.70×10^{-1}	9.10×10^{-1}	3.00×10^{-2}	3.80	6.10×10^{-1}	1.1

$\Lambda_{c1}^{1\lambda'}(\frac{3}{2}^-)$ in the decay channels $\Sigma_c^{*+,0}\pi^{0,+}$, $D^{*0}p$ and $D^{*+}n$. For Λ_b spin-doublet $(\frac{1}{2}^-, \frac{3}{2}^-)_{j=1}$, they are most likely to be found in decay channels $\Sigma_b^{+,0,-}\pi^{-,0,+}$ and $\Sigma_b^{*+,0,-}\pi^{-,0,+}$, respectively.

As mentioned in Sec.4, $\Lambda_c\pi^+$ and $\Lambda_b\pi^+$ are the ideal decay channels to find the $1P$ -wave $\Sigma_c(\frac{5}{2}^-)$ and $\Sigma_b(\frac{5}{2}^-)$ states. The $2S$ -wave $\Sigma_{c1}^{0\rho'}(\frac{1}{2}^+)$ and $\Sigma_{c1}^{0\rho'}(\frac{3}{2}^+)$ have good potentials to be observed in the $\Sigma_c^{+,+}\pi^{0,+}$ and $\Sigma_c^{*+,+}\pi^{0,+}$ decay channels, while $\Sigma_b^{+,0}\pi^{0,+}$, and $\Sigma_b^{*+,0}\pi^{0,+}$ are the dominating decay modes for $\Sigma_{b1}^{0\rho'}(\frac{1}{2}^+)$ and $\Sigma_{b1}^{0\rho'}(\frac{3}{2}^+)$ states.

Finally, we suggest to hunt for the $2S$ -wave $\Omega_c(\frac{3}{2}^+)$ state in the $\Xi_c^+ K^-$, $\Xi_c^0 K^0$ and $\Xi_c^{*+} K^-$ decay channels. Our suggestions for searching the $2S$ -wave $\Omega_b(\frac{1}{2}^+)$ and $\Omega_b(\frac{3}{2}^+)$ states are in the $\Xi_b^0 K^-$ and $\Xi_b^- K^0$ decay channels.

-
- [1] H. Albrecht *et al.* [ARGUS Collaboration], Phys. Lett. B 317, 227 (1993).
 - [2] P. L. Frabetti *et al.* [E687 Collaboration], Phys. Rev. Lett. 72, 961(1994).
 - [3] R. Aaij *et al.* (LHCb Collaboration), Phys. Rev. Lett. 109, 172003 (2012).
 - [4] T. A. Aaltonen *et al.* (CDF Collaboration), Phys. Rev. D 88, 071101 (2013).

TABLE XXV: Decay widths (MeV) of Ω_c

N	1	2	3	4	5	6
Notations	Ω_{c2}^1	$\Omega_{c2}^{1\lambda'}$	$\Omega_{c2}^{1\rho'}$	Ω_{c2}^1	$\Omega_{c2}^{1\lambda'}$	$\Omega_{c2}^{1\rho'}$
Assignments	$\frac{3}{2}^-$ (1P)	$\frac{3}{2}^-$ (2P)	$\frac{3}{2}^-$ (2P)	$\frac{5}{2}^-$ (1P)	$\frac{5}{2}^-$ (2P)	$\frac{5}{2}^-$ (2P)
Mass	3066	3411	3411	3090	3435	3435
$\Xi_c^+ K^-$	5.99×10^{-1}	0.634	15.80	1.35	7.80×10^{-1}	17.0
$\Xi_c^+ K^{*-}$	-	5.81×10^{-4}	7.68×10^{-1}	-	2.29×10^{-3}	2.04
$\Xi_c^0 K^0$	4.80×10^{-1}	6.10×10^{-1}	15.6	1.15	7.51×10^{-1}	16.8
$\Xi_c^0 K^{*0}$	-	5.07×10^{-4}	6.92×10^{-1}	-	2.15×10^{-3}	1.91
$\Xi_c'^+ K^-$	-	1.64×10^{-1}	7.43	-	9.50×10^{-2}	3.77
$\Xi_c^{*+} K^-$	-	6.10×10^{-2}	4.27	-	1.32×10^{-1}	8.08
$\Xi_c'^0 K^0$	-	1.57×10^{-1}	7.27	-	910×10^{-2}	3.70
$\Xi_c^{*0} K^0$	-	5.80×10^{-2}	4.16	-	1.26×10^{-1}	7.90
$\Xi^0 D^0$	-	4.88×10^{-1}	1.95	-	2.84×10^{-1}	9.67×10^{-1}
$\Xi^- D^+$	-	4.28×10^{-1}	1.84	-	2.52×10^{-1}	9.26×10^{-1}
$\Xi^0 D^{*0}$	-	16.0	6.67	-	5.10×10^{-2}	6.12×10^{-1}
$\Xi^- D^{*+}$	-	15.4	7.62	-	4.00×10^{-2}	5.12×10^{-1}
Γ_{total}	1.08	34.00	74.07	2.50	2.61	64.22
$\frac{\Xi_c^0 K^0}{\Xi_c^+ K^-}$	0.8	0.96	0.99	0.85	0.96	0.99

- [5] P. A. Zyla *et al.*(Particle Data Group), Prog. Theor. Exp. Phys. 2020, 083C01(2020) and 2021 update.
- [6] K. Nakamura *et al.*(Particle Data Group), J.Phys.G 37, 075021(2010).
- [7] A. Abdesselam *et al.* [Belle Collaboration], arXiv:1908.06235.
- [8] B. Aubert *et al.* [BaBar Collaboration], Phys. Rev. Lett. 98, 012001 (2007).
- [9] K. Abe *et al.* [Belle Collaboration], Phys. Rev. Lett. 98, 262001 (2007).
- [10] R. Aaij *et al.* [LHCb Collaboration], JHEP 1705, 030 (2017).
- [11] R. Aaij *et al.* [LHCb Collaboration], J. High Energy Phys. 06, 136(2020).
- [12] R. Aaij *et al.* (LHCb Collaboration), Phys. Rev. Lett. 123, 152001(2019).
- [13] R. Mizuket *et al.* [Belle Collaboration], Phys. Rev. Lett. 94, 122002 (2005).
- [14] R. Aaij *et al.* (LHCb Collaboration), Phys. Rev. Lett. 122, 012001(2019).
- [15] R. Aaij *et al.*(LHCb Collaboration), Phys. Rev. Lett. 124, 082002(2020).
- [16] R. Aaij *et al.* [LHCb Collaboration], arXiv:1703.04639[hep-ex].
- [17] S. Godfrey and N. Isgur, Phys. Rev. D 32, 189(1985).
- [18] S. Capstick and N. Isgur, Phys. Rev. D 34, 2809 (1986); AIPConf. Proc. 132, 267(1985).
- [19] D. Ebert, R. N. Faustov, and V. O. Galkin, Phys. Rev. D 84, 014025(2011).
- [20] W. Roberts and M. Pervin, Int. J. Mod. Phys. A 23, 2817(2008).
- [21] T. Yoshida, E. Hiyama, A. Hosaka, *et al.*, Phys. Rev. D 92, 114029(2015).

TABLE XXVI: Decay widths (MeV) of Ω_b

N	1	2	3	4	5	6
Notations	$\Omega_{b1}^{0\lambda'}$	$\Omega_{b1}^{0\rho'}$	$\Omega_{b1}^{0\lambda'}$	$\Omega_{b1}^{0\rho'}$	Ω_{b0}^1	$\Omega_{b0}^{1\lambda'}$
Assignments	$\frac{1}{2}^+$ (2S)	$\frac{1}{2}^+$ (2S)	$\frac{3}{2}^+$ (2S)	$\frac{3}{2}^+$ (2S)	$\frac{1}{2}^-$ (1P)	$\frac{1}{2}^-$ (2P)
Mass	6446	6446	6466	6466	6334	6662
$\Xi_b^0 K^-$	258	2.23	25.30	2.03	169	5.83
$\Xi_b^- K^0$	235	2.29	23.00	2.16	155	5.91
$\Xi_b^{\prime 0} K^-$	11.30	3.30×10^{-1}	6.00×10^{-1}	2.30×10^{-1}	-	2.21×10^{-10}
$\Xi_b^{*\prime 0} K^-$	-	-	3.30×10^{-2}	1.60×10^{-2}	-	8.14×10^{-10}
$\Xi_b^{\prime -} K^0$	7.03	2.10×10^{-1}	4.87×10^{-1}	1.90×10^{-1}	-	9.17×10^{-11}
$\Xi_b^{*\prime -} K^0$	-	-	-	-	-	1.19×10^{-9}
$\Xi_b^0 B^-$	-	-	-	0	-	9.04×10^{-11}
$\Xi_b^- \bar{B}^0$	-	-	-	0	-	4.98×10^{-9}
$\Xi_b^0 B^{*-}$	-	-	-	-	-	1.45
$\Xi_b^- \bar{B}^{*0}$	-	-	-	-	-	1.22
Γ_{total}	511.30	5.06	49.42	4.63	324	14.41
$\frac{\Xi_b^- K^0}{\Xi_b^0 K^-}$	0.91	0.98	0.91	1.06	0.92	1.01

- [22] K. L. Wang, Q. F. Lü, and X. H. Zhong, Phys. Rev. D 100, 114035(2019).
- [23] L. A. Copley, N. Isgur, and G. Karl, Phys. Rev. D 20, 768(1979); 23, 817(E)(1981).
- [24] K. Maltman and N. Isgur, Phys. Rev. D 22, 1701(1980).
- [25] D. Ebert, R. N. Faustov, and V. O. Galkin, Phys. Rev. D 72, 034026(2005).
- [26] D. Ebert, R. N. Faustov, and V. O. Galkin, Phys. Lett. B 659, 612(2008).
- [27] H. Garcilazo, J. Vijande, and A. Valcarce, J. Phys. G 34, 961(2007).
- [28] M. Karliner and J. L. Rosner, Phys. Rev. D 92, 074026(2015).
- [29] K. Thakkar, Z. Shah, A. K. Rai, *et al.*, Nucl. Phys. A 965, 57(2017).
- [30] Z. Shah, K. Thakkar, A. K. Rai, *et al.*, Chin. Phys. C 40, 123102(2016).
- [31] Z. Shah, K. Thakkar, A. Kumar Rai, *et al.*, Eur. Phys. J. A 52, 313(2016).
- [32] F. Hussain, J. G. Korner, and S. Tawfiq, Phys. Rev. D 61, 114003(2000).
- [33] M. A. Ivanov, J. G. Korner, and V. E. Lyubovitskij, Phys.Lett. B 448, 143(1999).
- [34] M. A. Ivanov, J. G. Korner, V. E. Lyubovitskij, *et al.*, Phys. Rev. D 60, 094002(1999).
- [35] C. Albertus, E. Hernandez, J. Nieves, *et al.*, Phys. Rev. D 72, 094022(2005).
- [36] S. Migura, D. Merten, B. Metsch, *et al.*, Eur. Phys. J.A 28, 41(2006).
- [37] X. H. Zhong and Q. Zhao, Phys. Rev. D 77, 074008(2008).
- [38] E. Hernandez and J. Nieves, Phys. Rev. D 84, 057902(2011).
- [39] L. H. Liu, L. Y. Xiao, and X. H. Zhong, Phys. Rev. D 86, 034024(2012).
- [40] B. Chen, K. W. Wei, X. Liu, and T. Matsuki, Eur. Phys. J. C 77, 154(2017).

TABLE XXVII: Decay widths (MeV) of Ω_b

N	1	2	3	4	5	6	7
Notations	$\Omega_{b0}^{1\rho'}$	Ω_{b1}^1	$\Omega_{b1}^{1\lambda'}$	$\Omega_{b1}^{1\rho'}$	Ω_{b1}^1	$\Omega_{b1}^{1\lambda'}$	$\Omega_{b1}^{1\rho'}$
Assignments	$\frac{1}{2}^-$ (2P)	$\frac{1}{2}^-$ (1P)	$\frac{1}{2}^-$ (2P)	$\frac{1}{2}^-$ (2P)	$\frac{3}{2}^-$ (1P)	$\frac{3}{2}^-$ (2P)	$\frac{3}{2}^-$ (2P)
Mass	6662	6316	6658	6658	6330	6664	6664
$\Xi_b^0 K^-$	5.60×10^{-1}	2.76×10^{-11}	6.27×10^{-8}	8.94×10^{-11}	6.08×10^{-12}	1.43×10^{-9}	1.27×10^{-10}
$\Xi_b^- K^0$	2.50×10^{-1}	1.13×10^{-11}	1.55×10^{-8}	1.78×10^{-10}	2.35×10^{-11}	2.83×10^{-9}	1.69×10^{-10}
$\Xi_b^{\prime 0} K^-$	1.68×10^{-10}	-	3.69	7.33	-	3.90×10^{-2}	2.73
$\Xi_b^{*\prime 0} K^-$	1.56×10^{-10}	-	3.80×10^{-2}	3.44	-	3.47	12.70
$\Xi_b^{\prime -} K^0$	2.04×10^{-10}	-	3.68	7.76	-	3.70×10^{-2}	2.65
$\Xi_b^{*\prime -} K^0$	2.25×10^{-10}	-	3.60×10^{-2}	3.30	-	3.46	13.10
$\Xi^0 B^-$	1.18×10^{-11}	-	13.90	7.70×10^{-1}	-	3.50×10^{-2}	2.50×10^{-1}
$\Xi^- \bar{B}^0$	3.01×10^{-12}	-	13.30	1.16	-	2.60×10^{-2}	1.90×10^{-1}
$\Xi^0 B^{*-}$	1.11	-	6.25×10^{-3}	9.50×10^{-2}	-	6.51×10^{-3}	9.50×10^{-2}
$\Xi^- \bar{B}^{*0}$	1.01	-	1.82×10^{-3}	2.90×10^{-2}	-	2.75×10^{-3}	4.80×10^{-2}
Γ_{total}	2.93	3.89×10^{-11}	34.65	23.88	2.96×10^{-11}	7.08	31.76
$\frac{\Xi_b^- K^0}{\Xi_b^0 K^-}$	0.45	0.41	0.25	1.99	3.87	1.98	1.33

- [41] B. Chen and X. Liu, Phys. Rev. D 98, 074032(2018).
- [42] H. Nagahiro, S. Yasui, A. Hosaka, M. Oka, and H. Noumi, Phys. Rev. D 95, 014023(2017).
- [43] Y. X. Yao, K. L. Wang, and X. H. Zhong, Phys. Rev. D 98, 076015(2018).
- [44] A. Valcarce, H. Garcilazo, and J. Vijande, Eur. Phys. J. A37, 217(2008).
- [45] M. Q. Huang, Y. B. Dai, and C. S. Huang, Phys. Rev. D 52, 3986(1995); 55, 7317(E)(1997).
- [46] M. C. Banuls, A. Pich, and I. Scimemi, Phys. Rev. D 61, 094009(2000).
- [47] H. Y. Cheng and C. K. Chua, Phys. Rev. D 75, 014006(2007).
- [48] N. Jiang, X. L. Chen, and S. L. Zhu, Phys. Rev. D 92, 054017(2015).
- [49] H. Y. Cheng and C. K. Chua, Phys. Rev. D 92, 074014(2015).
- [50] Y. Kawakami and M. Harada, Phys. Rev. D 99, 094016(2019).
- [51] M. Padmanath, R. G. Edwards, N. Mathur, and M. Peardon, arXiv:1311.4806(2013).
- [52] H. Bahtiyar, K. U. Can, G. Erkol, and M. Oka, Phys. Lett. B747, 281(2015).
- [53] P. Perez-Rubio, S. Collins, and G. S. Bali, Phys. Rev. D 92,034504(2015).
- [54] H. Bahtiyar, K. U. Can, G. Erkol, M. Oka, and T. T.Takahashi, Phys. Lett. B 772, 121(2017).
- [55] S. L. Zhu and Y. B. Dai, Phys. Rev. D 59, 114015(1999).
- [56] S. S. Agaev, K. Azizi, and H. Sundu, Phys. Rev. D 96, 094011(2017).
- [57] H. X. Chen, Q. Mao, W. Chen, A. Hosaka, X. Liu, and S. L.Zhu, Phys. Rev. D 95, 094008(2017).
- [58] Z. G. Wang, Phys. Rev. D 81, 036002(2010).
- [59] Z. G. Wang, Eur. Phys. J. A 44, 105(2010).

TABLE XXVIII: Decay widths (MeV) of Ω_b

N	1	2	3	4	5	6
Notations	Ω_{b2}^1	$\Omega_{b2}^{1\lambda'}$	$\Omega_{b2}^{1\rho'}$	Ω_{b2}^1	$\Omega_{b2}^{1\lambda'}$	$\Omega_{b2}^{1\rho'}$
Assignments	$\frac{3}{2}^-$ (1P)	$\frac{3}{2}^-$ (2P)	$\frac{3}{2}^-$ (2P)	$\frac{5}{2}^-$ (1P)	$\frac{5}{2}^-$ (2P)	$\frac{5}{2}^-$ (2P)
Mass	6340	6655	6655	6350	6666	6666
$\Xi_b^0 K^-$	1.70×10^{-1}	5.60×10^{-1}	16.50	3.50×10^{-1}	6.30×10^{-1}	17.30
$\Xi_b^- K^0$	8.10×10^{-2}	5.10×10^{-1}	15.90	2.00×10^{-1}	5.70×10^{-1}	16.70
$\Xi_b^{\prime 0} K^-$	-	6.10×10^{-2}	4.49	-	3.30×10^{-2}	2.23
$\Xi_b^{*\prime 0} K^-$	-	3.20×10^{-2}	2.98	-	6.20×10^{-2}	5.31
$\Xi_b^{\prime -} K^0$	-	5.80×10^{-2}	4.35	-	3.10×10^{-2}	2.16
$\Xi_b^{*\prime -} K^0$	-	3.00×10^{-2}	2.86	-	5.80×10^{-2}	5.11
$\Xi^0 B^-$	-	4.40×10^{-2}	3.30×10^{-1}	-	3.00×10^{-2}	2.10×10^{-1}
$\Xi^- \bar{B}^0$	-	3.10×10^{-2}	2.0×10^{-1}	-	2.30×10^{-2}	1.70×10^{-1}
$\Xi^0 B^{*-}$	-	12.10	9.58	-	3.19×10^{-3}	4.60×10^{-2}
$\Xi^- \bar{B}^{*0}$	-	9.00	8.23	-	1.46×10^{-3}	2.20×10^{-2}
Γ_{total}	2.50×10^{-1}	22.43	65.47	5.50×10^{-1}	1.44	49.26
$\frac{\Xi_b^- K^0}{\Xi_b^0 K^-}$	4.80×10^{-1}	9.10×10^{-1}	9.60×10^{-1}	5.70×10^{-1}	9.00×10^{-1}	9.70×10^{-1}

- [60] T. M. Aliev, K. Azizi, and H. Sundu, Eur. Phys. J. C 75, 14(2015).
- [61] T. M. Aliev, T. Barakat, and M. Savci, Phys. Rev. D 93, 056007(2016).
- [62] T. M. Aliev, K. Azizi, Y. Sarac, and H. Sundu, Phys. Rev. D 99, 094003(2019).
- [63] S. L. Zhu, Phys. Rev. D 61, 114019(2000).
- [64] Z. G. Wang, Eur. Phys. J. A 47, 81(2011).
- [65] Q. Mao, H. X. Chen, W. Chen, A. Hosaka, X. Liu, and S. L. Zhu, Phys. Rev. D 92, 114007(2015).
- [66] H. X. Chen, Q. Mao, A. Hosaka, X. Liu, and S. L. Zhu, Phys. Rev. D 94, 114016(2016).
- [67] Z. G. Wang, Nucl. Phys. B 926, 467(2018).
- [68] Q. Mao, H. X. Chen, A. Hosaka, X. Liu, and S. L. Zhu, Phys. Rev. D 96, 074021(2017).
- [69] T. M. Aliev, K. Azizi, Y. Sarac, and H. Sundu, Phys. Rev. D 98, 094014(2018).
- [70] E. L. Cui, H. M. Yang, H. X. Chen, and A. Hosaka, Phys. Rev. D 99, 094021(2019).
- [71] K. Azizi, Y. Sarac, and H. Sundu, Phys. Rev. D 101, 074026(2020).
- [72] X. Liu, H. X. Chen, Y. R. Liu, A. Hosaka and S. L. Zhu, Phys. Rev. D 77, 014031(2008).
- [73] Francisco O. Duraes, Marina Nielsen, Phys. Lett. B 658, 40(2007).
- [74] J. R. Zhang, M. Q. Huang, Phys. Rev. D 77, 094002(2008).
- [75] J. R. Zhang, M. Q. Huang, Phys. Rev. D 78, 094015(2008).
- [76] Z. G. Wang, Chin. Phys. C 45, 013109(2021).
- [77] Z. G. Wang, Eur. Phys. J. C 68, 479(2010).
- [78] Z. G. Wang, Eur. Phys. J. C 75, 359(2015).

- [79] Z. G. Wang, Phys. Lett. B 685, 59(2010).
- [80] Z. G. Wang, Eur. Phys. J. C 77, 325(2017).
- [81] Z. G. Wang, Int. J. Mod. Phys. A 35, 2050043(2020).
- [82] G. L. Yu, Z. G. Wang, arXiv:2109.02217(2021).
- [83] B. Chen, K.W. Wei and A. Zhang, Eur. Phys. J. A 51, 82(2015).
- [84] Q. F. Lü, D. Y. Chen, and Y. B. Dong, Eur. Phys. J. C 80, 871 (2020).
- [85] Q. F. Lü, D. Y. Chen, and Y. B. Dong, *et al.* Phys. Rev. D 104, 054026 (2021)
- [86] Q. F. Lü, D. Y. Chen, and Y. B. Dong, Phys. Rev. D 102, 074021 (2020)
- [87] L.Micu, Nucl. Phys. B10, 521 (1969).
- [88] A. Le Yaouanc, L. Oliver, O. Pene, J-C. Raynal, Phys. Rev. D 8, 2223 (1973); Phys. Rev. D9, 1415(1974); Phys. Rev. D11, 1272 (1975); Phys. Lett. B71, 397 (1977).
- [89] A. Le Yaouanc, L. Oliver, O. Pene, and J. C. Raynal, Phys. Lett. 71 B, 397 (1977); 72B, 57 (1977).
- [90] A. Le Yaouanc, L. Oliver, O. Pene, and J. C. Raynal, Hadron Transitions in the Quark Model (Gordon and Breach Science Publishers, New York, 1987).
- [91] H. G. Blundell, hep-ph/9608473; H. G. Blundell, S. Godfrey, Phys. Rev. D 53, 3700(1996); H. G. Blundell, S. Godfrey, B. Phelps, Phys. Rev. D 53, 3712(1996).
- [92] E. S. Ackleh, T. Barnes and E. S. Swanson, Phys. Rev. D 54, 6811(1996);
- [93] T. Barnes, N. Black and P. R. Page, Phys. Rev. D 68, 054014(2003);
- [94] F. E. Close, E. S. Swanson, Phys. Rev. D 72, 094004(2005);
- [95] F. E. Close, C. E. Thomas, O. Lakhina, E. S. Swanson, Phys. Lett. B647, 159 (2007);
- [96] H. Q. Zhou, R. G. Ping, B. S. Zou, Phys. Lett. B 611, 123 (2005); G. J. Ding, M. L. Yan, Phys. Lett. B657, 49 (2007).
- [97] B. Chen, D. X. Wang and A. L. Zhang, Phys. Rev. D 80, 071502 (2009).
- [98] D. M. Li, S. Zhou, Phys. Rev. D78, 054013 (2008); D. M. Li, P. F. Ji, B. Ma, Eur. Phys. J. C71, 1582(2011)
- [99] D. M. Li, B. Ma, Phys. Rev. D81, 014021 (2010)
- [100] B. Zhang, X. Liu, W. Z. Deng, S. L. Zhu, Eur. Phys. J. C50, 617 (2007);
- [101] Y. Sun, Q. T. Song, D. Y. Chen, X. Liu and S. L. Zhu, arXiv:1401.1595 [hep-ph](2013).
- [102] Y. C. Yang, Z. R. Xia, J. L. Ping, Phys. Rev. D81, 094003 (2010).
- [103] G. L. Yu, Z. G. Wang, Z. Y. Li, Phys. Rev. D 94, 074024(2016).
- [104] G. L. Yu, Z. G. Wang, Z. Y. Li, Chin. Phys. C, 36(6), 063101(2015); Chin. Phys. C 42(4), 043107(2018).
- [105] G. L. Yu, Z. G. Wang, Chin. Phys. C 44(3), 033103(2020).
- [106] C. Chen, X. L. Chen, X. Liu, W. Z. Deng, and S. L. Zhu, Phys. Rev. D 75, 094017(2007).
- [107] D. D. Ye, Z. Zhao, and A. Zhang, Phys. Rev. D 96, 114009(2017).
- [108] D. D. Ye, Z. Zhao, and A. Zhang, Phys. Rev. D 96, 114003(2017).
- [109] B. Chen, X. Liu, and A. Zhang, Phys. Rev. D 95, 074022(2017).
- [110] P. Yang, J. J. Guo, and A. Zhang, Phys. Rev. D 99, 034018(2019).
- [111] J. J. Guo, P. Yang, and A. L. Zhang, Phys. Rev. D 100, 014001(2019).
- [112] Q. F. Lü and X. H. Zhong, Phys. Rev. D 101, 014017(2020).
- [113] X. W. Liu, H. W. Ke, X. Liu, *et al.* Eur. Phys. J. C 76, 549 (2016).
- [114] E. Hiyama, Y. Kin, and M. Kamimura, Prog. Part. Nucl. Phys. 51, 223(2003)

- [115] K. Azizi, Y. Sarac, H. Sundu, Phys. Rev. D 102, 034007(2020).
- [116] Y. Huang, C.J. Xiao, L.S. Geng, *et al.*, Phys. Rev. D 99, 014008(2019).
- [117] R. Aaij *et al.*(LHCb Collaboration), Phys. Rev. Lett. 122, 012001(2019).
- [118] Z. Zhao, D. D. Ye, A. Zhang, Phys. Rev. D 95, 114024 (2017).
- [119] B. Chen, X. Liu, Phys. Rev. D 96, 094015 (2017).
- [120] M. Padmanath, Nilmani Mathur, Phys. Rev. Lett. 119, 042001 (2017).
- [121] K. L. Wang, L. Y. Xiao, X. H. Zhong, *et al.*, Phys. Rev. D 95, 116010 (2017).
- [122] H. X. Chen, Q. Mao, W. Chen, *et al.*, Phys. Rev. D 95, 094008 (2017)
- [123] G. Yang, J. L. Ping, Phys. Rev. D 97, 034023 (2018).
- [124] H. M. Yang, H. X. Chen, Phys. Rev. D 104, 034037 (2021).
- [125] W. Liang, Q. F. Lü, arXiv:2001.02221(2020).
- [126] L. Y. Xiao, K. L. Wang, M. S. Liu, *et al.*, arXiv:2001.05110(2020).
- [127] Halil Mutuk, Eur. Phys. J. A 56, 146 (2020).
- [128] T. Regge, Nuovo Cim. 14, 951(1959).
- [129] T. Regge, Nuovo Cim. 18, 947(1960).
- [130] G. F. Chew, S. C. Frautschi, Phys. Rev. Lett. 7, 394(1961).
- [131] G. F. Chew, S. C. Frautschi, Phys. Rev. Lett. 8, 41 (1962).
- [132] G. S. Bali, Phys. Rept. 343, 1, arXiv:hep-ph/0001312(2001).
- [133] D. V. Bugg, Four sorts of meson, Phys. Rept. 397, 257, arXiv:hep-ex/0412045(2004).
- [134] E. Klempt, A. Zaitsev, Phys. Rept. 454, 1, arXiv:0708.4016(2007).
- [135] W. Lucha, F. F. Schoberl, D. Gromes, Phys. Rept. 200, 127(1991).
- [136] Y. Nambu, Phys. Rev. D 10, 4262(1974).
- [137] Y. Nambu, Phys. Lett. B 80, 372(1979).
- [138] K. L. Wang, Q. F. Lü and X. H. Zhong, Rev. D 99, 014011 (2019).
- [139] B. Chen, S. Q. Luo, X. Liu, *et al.*, Phys. Rev. D 100, 094032(2019).
- [140] Q. F. Lü, L. Y. Xiao, Z. Y. Wang and X. H. Zhong, Eur. Phys. J. C 78,599(2018).
- [141] W. Liang, Q. F. Lü and X. H. Zhong, Phys. Rev. D 100, 054013(2019).
- [142] Q. F. Lü and X. H. Zhong, arXiv:1910.06126(2019).
- [143] S. Godfrey and K. Moats, Phys. Rev. D 93, 034035(2016).
- [144] S. Godfrey, K. Moats, and E. S. Swanson, Phys. Rev. D 94, 054025(2016).
- [145] W. Liang, Q. F. Lü, arXiv:2004.13568(2020).
- [146] H. M. Yang, H. X. Chen, Phys. Rev. D 104, 034037(2021).
- [147] K. L. Wang, Y. X. Yao, X. H. Zhong, *et al.*, Phys. Rev. D 96, 116016(2017).
- [148] H. X. Chen, Q. Mao, W. Chen, *et al.*, Phys. Rev. D 95, 094008 (2017).

Appendix

A.1 Three-body matrix elements of the potential energy

$$\begin{aligned}
& \langle [\phi_{n_{\rho_a} l_{\rho_a} m_{l_{\rho_a}}}(\mathbf{r}_{\rho_3}) \phi_{n_{\lambda_a} l_{\lambda_a} m_{l_{\lambda_a}}}(\mathbf{r}_{\lambda_3})]_{Lm_L} | \tilde{G}(\mathbf{r}_{\rho_k}) | [\phi_{n_{\rho_b} l_{\rho_b} m_{l_{\rho_b}}}(\mathbf{r}_{\rho_3}) \phi_{n_{\lambda_b} l_{\lambda_b} m_{l_{\lambda_b}}}(\mathbf{r}_{\lambda_3})]_{Lm_L} \rangle_{k=1,2} \\
&= N_{n_{\rho_a} l_{\rho_a}} N_{n_{\lambda_a} l_{\lambda_a}} N_{n_{\rho_b} l_{\rho_b}} N_{n_{\lambda_b} l_{\lambda_b}} \frac{1}{(\nu_{n_{\rho_a}})^{l_{\rho_a}} (\nu_{n_{\lambda_a}})^{l_{\lambda_a}} (\nu_{n_{\rho_b}})^{l_{\rho_b}} (\nu_{n_{\lambda_b}})^{l_{\lambda_b}}} 4\pi \left(\frac{\pi}{B_{r_k}}\right)^{\frac{3}{2}} \\
&\times \sum_{m_{l_{\rho_a}} m_{l_{\lambda_a}}} (l_{\rho_a} m_{l_{\rho_a}} l_{\lambda_a} m_{l_{\lambda_a}} | Lm_L) \sum_{m_{l_{\rho_b}} m_{l_{\lambda_b}}} (l_{\rho_b} m_{l_{\rho_b}} l_{\lambda_b} m_{l_{\lambda_b}} | Lm_L) \\
&\times \sum_{m=0}^{Lsum} \frac{m!}{(2m+1)!} \int_0^\infty V(r_{\rho_k}) \text{Exp}(-\alpha_{r_k} r_{\rho_k}^2) r_{\rho_k}^{2m+2} dr_{\rho_k} \\
&\times \sum_{k_a K_a k_b K_b} C_{l_{\rho_a} m_{l_{\rho_a}} k_a} C_{l_{\lambda_a} m_{l_{\lambda_a}} K_a} C_{l_{\rho_b} m_{l_{\rho_b}} k_b} C_{l_{\lambda_b} m_{l_{\lambda_b}} K_b} \tag{66} \\
&\times \sum_{n_{12}=0}^{Lsum-m} \sum_{n_{13}=0}^{Lsum-m} \sum_{n_{14}=0}^{Lsum-m} \sum_{n_{23}=0}^{Lsum-m} \sum_{n_{24}=0}^{Lsum-m} \sum_{n_{34}=0}^{Lsum-m} \sum_{m_{12}=0}^m \sum_{m_{13}=0}^m \sum_{m_{14}=0}^m \sum_{m_{23}=0}^m \sum_{m_{24}=0}^m \sum_{m_{34}=0}^m \\
&\times \frac{\tilde{g}_{12}^{m_{12}} \tilde{g}_{13}^{m_{13}} \tilde{g}_{14}^{m_{14}} \tilde{g}_{23}^{m_{23}} \tilde{g}_{24}^{m_{24}} \tilde{g}_{34}^{m_{34}} \hat{g}_{12}^{n_{12}} \hat{g}_{13}^{n_{13}} \hat{g}_{14}^{n_{14}} \hat{g}_{23}^{n_{23}} \hat{g}_{24}^{n_{24}} \hat{g}_{34}^{n_{34}}}{n_{12}! n_{13}! n_{14}! n_{23}! n_{24}! n_{34}! m_{12}! m_{13}! m_{14}! m_{23}! m_{24}! m_{34}!} \\
&\times (\mathbf{D}_1 \cdot \mathbf{D}_2)^{n_{12}+m_{12}} (\mathbf{D}_1 \cdot \mathbf{D}_3)^{n_{13}+m_{13}} (\mathbf{D}_1 \cdot \mathbf{D}_4)^{n_{14}+m_{14}} \\
&\times (\mathbf{D}_2 \cdot \mathbf{D}_3)^{n_{23}+m_{23}} (\mathbf{D}_2 \cdot \mathbf{D}_4)^{n_{24}+m_{24}} (\mathbf{D}_3 \cdot \mathbf{D}_4)^{n_{34}+m_{34}} \\
&\times \delta(n_{12} + n_{13} + n_{14} + n_{23} + n_{24} + n_{34} - (Lsum - m)) \delta(m_{12} + m_{13} + m_{14} + m_{23} + m_{24} + m_{34} - m) \\
&\times \delta(n_{12} + n_{13} + n_{14} + m_{12} + m_{13} + m_{14} - l_{\rho_a}) \delta(n_{12} + n_{23} + n_{24} + m_{12} + m_{23} + m_{24} - l_{\lambda_a}) \\
&\times \delta(n_{13} + n_{23} + n_{34} + m_{13} + m_{23} + m_{34} - l_{\rho_b}) \delta(n_{14} + n_{24} + n_{34} + m_{14} + m_{24} + m_{34} - l_{\lambda_b})
\end{aligned}$$

$$\begin{aligned}
A_{r_k} &= \nu_{n_{\rho_a}} \alpha_{3k}^{r2} + \nu_{n_{\lambda_a}} \gamma_{3k}^{r2} + \nu_{n_{\rho_b}} \alpha_{3k}^{r2} + \nu_{n_{\lambda_b}} \gamma_{3k}^{r2} \\
B_{r_k} &= \nu_{n_{\rho_a}} \beta_{3k}^{r2} + \nu_{n_{\lambda_a}} \delta_{3k}^{r2} + \nu_{n_{\rho_b}} \beta_{3k}^{r2} + \nu_{n_{\lambda_b}} \delta_{3k}^{r2} \\
C_{r_1} &= 2\nu_{n_{\rho_a}} \alpha_{3k}^r \beta_{3k}^r + 2\nu_{n_{\lambda_a}} \gamma_{3k}^r \delta_{3k}^r + 2\nu_{n_{\rho_b}} \alpha_{3k}^r \beta_{3k}^r + 2\nu_{n_{\lambda_b}} \gamma_{3k}^r \delta_{3k}^r
\end{aligned} \tag{67}$$

$$\alpha_{r_k} = \left(A_{r_k} - \frac{C_{r_k}^2}{4B_{r_k}} \right), \tag{68}$$

$$\mathbf{D}_1 = \mathbf{D}_{l_{\rho_a} m_{l_{\rho_a}}, k_a}, \quad \mathbf{D}_2 = \mathbf{D}_{l_{\lambda_a} m_{l_{\lambda_a}}, K_a}, \quad \mathbf{D}_3 = \mathbf{D}_{l_{\rho_b} m_{l_{\rho_b}}, k_b}, \quad \mathbf{D}_4 = \mathbf{D}_{l_{\lambda_b} m_{l_{\lambda_b}}, K_b} \tag{69}$$

$$\tilde{g}_{ij} = \frac{C_{r_k}^2}{2B_{r_k}^2} c_i c_j + 2d_i d_j - \frac{C_{r_k}}{B_{r_k}} (c_i d_j + c_j d_i), \quad \hat{g}_{ij} = \frac{1}{2B_{r_k}} c_i c_j \tag{70}$$

$$\begin{aligned}
c_1 &= 2\nu_{n_{\rho_a}} \beta_{3k}^r, & c_2 &= 2\nu_{n_{\lambda_a}} \delta_{3k}^r, & c_3 &= 2\nu_{n_{\rho_b}} \beta_{3k}^r, & c_4 &= 2\nu_{n_{\lambda_b}} \delta_{3k}^r, \\
d_1 &= 2\nu_{n_{\rho_a}} \alpha_{3k}^r, & d_2 &= 2\nu_{n_{\lambda_a}} \gamma_{3k}^r, & d_3 &= 2\nu_{n_{\rho_b}} \alpha_{3k}^r, & d_4 &= 2\nu_{n_{\lambda_b}} \gamma_{3k}^r
\end{aligned} \tag{71}$$

$$L_{sum} = \frac{l_{\rho_a} + l_{\lambda_a} + l_{\rho_b} + l_{\lambda_b}}{2} \tag{72}$$

$$\begin{aligned}
& \langle [\phi_{n_{\rho_a} l_{\rho_a} m_{l_{\rho_a}}}(\mathbf{r}_{\rho_3}) \phi_{n_{\lambda_a} l_{\lambda_a} m_{l_{\lambda_a}}}(\mathbf{r}_{\lambda_3})]_{Lm_L} | \tilde{G}(\mathbf{r}_{\rho_3}) | [\phi_{n_{\rho_b} l_{\rho_b} m_{l_{\rho_b}}}(\mathbf{r}_{\rho_3}) \phi_{n_{\lambda_b} l_{\lambda_b} m_{l_{\lambda_b}}}(\mathbf{r}_{\lambda_3})]_{Lm_L} \rangle \\
&= N_{n_{\rho_a} l_{\rho_a}} N_{n_{\lambda_a} l_{\lambda_a}} N_{n_{\rho_b} l_{\rho_b}} N_{n_{\lambda_b} l_{\lambda_b}} \frac{1}{(\nu_{n_{\rho_a}})^{l_{\rho_a}} (\nu_{n_{\lambda_a}})^{l_{\lambda_a}} (\nu_{n_{\rho_b}})^{l_{\rho_b}} (\nu_{n_{\lambda_b}})^{l_{\lambda_b}}} \\
&\times \sum_{m_{l_{\rho_a}} m_{l_{\lambda_a}}} (l_{\rho_a} m_{l_{\rho_a}} l_{\lambda_a} m_{l_{\lambda_a}} | Lm_L) \sum_{m_{l_{\rho_b}} m_{l_{\lambda_b}}} (l_{\rho_b} m_{l_{\rho_b}} l_{\lambda_b} m_{l_{\lambda_b}} | Lm_L) \\
&\times 4\pi \left(\frac{\pi}{B_{r_3}}\right)^{\frac{3}{2}} \sum_{k_a K_a k_b K_b} C_{l_{\rho_a} m_{l_{\rho_a}} k_a} C_{l_{\lambda_a} m_{l_{\lambda_a}} K_a} C_{l_{\rho_b} m_{l_{\rho_b}} k_b} C_{l_{\lambda_b} m_{l_{\lambda_b}} K_b} \\
&\times \frac{1}{(2l_{\rho_a} + 1)!} \int_0^\infty V(r_{\rho_3}) \text{Exp}(-A_{r_3} r_{\rho_3}^2) r_{\rho_3}^{2l_{\rho_a} + 2} dr_{\rho_3} \frac{\hat{g}_{24}^{l_{\lambda_a}} \tilde{g}_{13}^{l_{\rho_a}}}{l_{\lambda_a}!} (\mathbf{D}_1 \cdot \mathbf{D}_3)^{l_{\rho_a}} (\mathbf{D}_2 \cdot \mathbf{D}_4)^{l_{\lambda_a}} \quad (73)
\end{aligned}$$

$$\begin{aligned}
A_{r_3} &= \nu_{n_{\rho_a}} + \nu_{n_{\rho_b}} \\
B_{r_3} &= \nu_{n_{\lambda_a}} + \nu_{n_{\lambda_b}} \quad (74)
\end{aligned}$$

$$\tilde{g}_{13} = 2d_1 d_3, \quad \hat{g}_{24} = \frac{1}{2B_{r_3}} \times c_2 c_4 \quad (75)$$

$$c_2 = 2\nu_{n_{\lambda_a}}, \quad c_4 = 2\nu_{n_{\lambda_b}}, \quad d_1 = 2\nu_{n_{\rho_a}}, \quad d_3 = 2\nu_{n_{\rho_b}}, \quad (76)$$

A.2 Three-body matrix elements of the kinetic-energy operators

$$\begin{aligned}
& \langle [\phi_{n_{\rho_a} l_{\rho_a} m_{l_{\rho_a}}}(\mathbf{p}_{\rho_3}) \phi_{n_{\lambda_a} l_{\lambda_a} m_{l_{\lambda_a}}}(\mathbf{p}_{\lambda_3})]_{Lm_L} | \sqrt{\mathbf{p}_{\lambda_k}^2 + m_k^2} | [\phi_{n_{\rho_b} l_{\rho_b} m_{l_{\rho_b}}}(\mathbf{p}_{\rho_3}) \phi_{n_{\lambda_b} l_{\lambda_b} m_{l_{\lambda_b}}}(\mathbf{p}_{\lambda_3})]_{Lm_L} \rangle_{k=1,2} \\
&= N_{n_{\rho_a} l_{\rho_a}} N_{n_{\lambda_a} l_{\lambda_a}} N_{n_{\rho_b} l_{\rho_b}} N_{n_{\lambda_b} l_{\lambda_b}} (4\nu_{n_{\rho_a}})^{l_{\rho_a}} (4\nu_{n_{\lambda_a}})^{l_{\lambda_a}} (4\nu_{n_{\rho_b}})^{l_{\rho_b}} (4\nu_{n_{\lambda_b}})^{l_{\lambda_b}} 4\pi \left(\frac{\pi}{A_{p_k}}\right)^{\frac{3}{2}} \\
&\times \sum_{m_{l_{\rho_a}} m_{l_{\lambda_a}}} (l_{\rho_a} m_{l_{\rho_a}} l_{\lambda_a} m_{l_{\lambda_a}} | Lm_L) \sum_{m_{l_{\rho_b}} m_{l_{\lambda_b}}} (l_{\rho_b} m_{l_{\rho_b}} l_{\lambda_b} m_{l_{\lambda_b}} | Lm_L) \\
&\times \sum_{m=0}^{Lsum} \frac{m!}{(2m+1)!} \int_0^\infty \sqrt{p_{\lambda_k}^2 + m_k^2} \text{Exp}(-\alpha_{p_k} p_{\lambda_k}^2) p_{\lambda_k}^{2m+2} dp_{\lambda_k} \\
&\times \sum_{k_a K_a k_b K_b} C_{l_{\rho_a} m_{l_{\rho_a}} k_a} C_{l_{\lambda_a} m_{l_{\lambda_a}} K_a} C_{l_{\rho_b} m_{l_{\rho_b}} k_b} C_{l_{\lambda_b} m_{l_{\lambda_b}} K_b} \quad (77) \\
&\times \sum_{n_{12}=0}^{Lsum-m} \sum_{n_{13}=0}^{Lsum-m} \sum_{n_{14}=0}^{Lsum-m} \sum_{n_{23}=0}^{Lsum-m} \sum_{n_{24}=0}^{Lsum-m} \sum_{n_{34}=0}^{Lsum-m} \sum_{m_{12}=0}^m \sum_{m_{13}=0}^m \sum_{m_{14}=0}^m \sum_{m_{23}=0}^m \sum_{m_{24}=0}^m \sum_{m_{34}=0}^m \\
&\times \frac{\tilde{g}_{12}^{m_{12}} \tilde{g}_{13}^{m_{13}} \tilde{g}_{14}^{m_{14}} \tilde{g}_{23}^{m_{23}} \tilde{g}_{24}^{m_{24}} \tilde{g}_{34}^{m_{34}} \hat{g}_{12}^{n_{12}} \hat{g}_{13}^{n_{13}} \hat{g}_{14}^{n_{14}} \hat{g}_{23}^{n_{23}} \hat{g}_{24}^{n_{24}} \hat{g}_{34}^{n_{34}}}{n_{12}! n_{13}! n_{14}! n_{23}! n_{24}! n_{34}! m_{12}! m_{13}! m_{14}! m_{23}! m_{24}! m_{34}!} \\
&\times (\mathbf{D}_1 \cdot \mathbf{D}_2)^{n_{12} + m_{12}} (\mathbf{D}_1 \cdot \mathbf{D}_3)^{n_{13} + m_{13}} (\mathbf{D}_1 \cdot \mathbf{D}_4)^{n_{14} + m_{14}} \\
&\times (\mathbf{D}_2 \cdot \mathbf{D}_3)^{n_{23} + m_{23}} (\mathbf{D}_2 \cdot \mathbf{D}_4)^{n_{24} + m_{24}} (\mathbf{D}_3 \cdot \mathbf{D}_4)^{n_{34} + m_{34}} \\
&\times \delta(n_{12} + n_{13} + n_{14} + n_{23} + n_{24} + n_{34} - (Lsum - m)) \delta(m_{12} + m_{13} + m_{14} + m_{23} + m_{24} + m_{34} - m) \\
&\times \delta(n_{12} + n_{13} + n_{14} + m_{12} + m_{13} + m_{14} - l_{\rho_a}) \delta(n_{12} + n_{23} + n_{24} + m_{12} + m_{23} + m_{24} - l_{\lambda_a}) \\
&\times \delta(n_{13} + n_{23} + n_{34} + m_{13} + m_{23} + m_{34} - l_{\rho_b}) \delta(n_{14} + n_{24} + n_{34} + m_{14} + m_{24} + m_{34} - l_{\lambda_b}) \quad (78)
\end{aligned}$$

$$\alpha_{p_k} = \left(B_{p_k} - \frac{C_{p_k}^2}{4A_{p_k}} \right), \quad (79)$$

$$\begin{aligned}
A_{p_k} &= \frac{\alpha_{3k}^{p^2}}{4\nu_{n_{\rho_a}}} + \frac{\gamma_{3k}^{p^2}}{4\nu_{n_{\lambda_a}}} + \frac{\alpha_{3k}^{p^2}}{4\nu_{n_{\rho_b}}} + \frac{\gamma_{3k}^{p^2}}{4\nu_{n_{\lambda_b}}} \\
B_{p_k} &= \frac{\beta_{3k}^{p^2}}{4\nu_{n_{\rho_a}}} + \frac{\delta_{3k}^{p^2}}{4\nu_{n_{\lambda_a}}} + \frac{\beta_{3k}^{p^2}}{4\nu_{n_{\rho_b}}} + \frac{\delta_{3k}^{p^2}}{4\nu_{n_{\lambda_b}}} \\
C_{p_k} &= \frac{\alpha_{3k}^p \beta_{3k}^p}{2\nu_{n_{\rho_a}}} + \frac{\gamma_{3k}^p \delta_{3k}^p}{2\nu_{n_{\lambda_a}}} + \frac{\alpha_{3k}^p \beta_{3k}^p}{2\nu_{n_{\rho_b}}} + \frac{\gamma_{3k}^p \delta_{3k}^p}{2\nu_{n_{\lambda_b}}}
\end{aligned} \tag{80}$$

$$\tilde{g}_{ij} = \frac{C_{p_k}^2}{2B_{p_k}^2} d_i d_j + 2c_i c_j - \frac{C_{p_k}}{B_{p_k}} (c_i d_j + c_j d_i), \quad \hat{g}_{ij} = \frac{1}{2A_{p_k}} d_i d_j \tag{81}$$

$$\begin{aligned}
c_1 &= \frac{\beta_{3k}^p}{2\nu_{n_{\rho_a}}}, c_2 = \frac{\delta_{3k}^p}{2\nu_{n_{\lambda_a}}}, c_3 = \frac{\beta_{3k}^p}{2\nu_{n_{\rho_b}}}, c_4 = \frac{\delta_{3k}^p}{2\nu_{n_{\lambda_b}}}, \\
d_1 &= \frac{\alpha_{3k}^p}{2\nu_{n_{\rho_a}}}, d_2 = \frac{\gamma_{3k}^p}{2\nu_{n_{\lambda_a}}}, d_3 = \frac{\alpha_{3k}^p}{2\nu_{n_{\rho_b}}}, d_4 = \frac{\gamma_{3k}^p}{2\nu_{n_{\lambda_b}}}
\end{aligned} \tag{82}$$

$$\begin{aligned}
&\langle [\phi_{n_{\rho_a} l_{\rho_a} m_{l_{\rho_a}}}(\mathbf{p}_{\rho_3}) \phi_{n_{\lambda_a} l_{\lambda_a} m_{l_{\lambda_a}}}(\mathbf{p}_{\lambda_3})]_{Lm_L} | \sqrt{p_{\lambda_3}^2 + m_3^2} | [\phi_{n_{\rho_b} l_{\rho_b} m_{l_{\rho_b}}}(\mathbf{p}_{\rho_3}) \phi_{n_{\lambda_b} l_{\lambda_b} m_{l_{\lambda_b}}}(\mathbf{p}_{\lambda_3})]_{Lm_L} \rangle \\
&= N_{n_{\rho_a} l_{\rho_a}} N_{n_{\lambda_a} l_{\lambda_a}} N_{n_{\rho_b} l_{\rho_b}} N_{n_{\lambda_b} l_{\lambda_b}} (4\nu_{n_{\rho_a}})^{l_{\rho_a}} (4\nu_{n_{\lambda_a}})^{l_{\lambda_a}} (4\nu_{n_{\rho_b}})^{l_{\rho_b}} (4\nu_{n_{\lambda_b}})^{l_{\lambda_b}} \\
&\times \sum_{m_{l_{\rho_a}} m_{l_{\lambda_a}}} (l_{\rho_a} m_{l_{\rho_a}} l_{\lambda_a} m_{l_{\lambda_a}} | Lm_L) \sum_{m_{l_{\rho_b}} m_{l_{\lambda_b}}} (l_{\rho_b} m_{l_{\rho_b}} l_{\lambda_b} m_{l_{\lambda_b}} | Lm_L) \\
&\times \sum_{k_a K_a k_b K_b} C_{l_{\rho_a} m_{l_{\rho_a}} k_a} C_{l_{\lambda_a} m_{l_{\lambda_a}} K_a} C_{l_{\rho_b} m_{l_{\rho_b}} k_b} C_{l_{\lambda_b} m_{l_{\lambda_b}} K_b} \frac{1}{l_{\rho_a}} (\mathbf{D}_1 \cdot \mathbf{D}_3)^{l_{\rho_a}} (\mathbf{D}_2 \cdot \mathbf{D}_4)^{l_{\lambda_a}} \\
&\times 4\pi \left(\frac{\pi}{A_{p_3}}\right)^{\frac{3}{2}} \frac{\hat{g}_{13}^{l_{\rho_a}} \tilde{g}_{24}^{l_{\lambda_a}}}{(2m+1)!} \int_0^\infty \sqrt{p_{\lambda_3}^2 + m_3^2} \text{Exp}(-B_{p_3} p_{\lambda_3}^2) p_{\lambda_3}^{2m+2} dp_{\lambda_3}
\end{aligned} \tag{83}$$

$$\begin{aligned}
A_{p_3} &= \frac{1}{4\nu_{n_{\rho_a}}} + \frac{1}{4\nu_{n_{\rho_b}}} \\
B_{p_3} &= \frac{1}{4\nu_{n_{\lambda_a}}} + \frac{1}{4\nu_{n_{\lambda_b}}}
\end{aligned} \tag{84}$$

$$\hat{g}_{13} = \frac{1}{2A} \times d_1 d_3, \quad \tilde{g}_{24} = 2c_2 c_4, \tag{85}$$

$$\begin{aligned}
c_2 &= \frac{1}{2\nu_{n_{\lambda_a}}}, \quad c_4 = \frac{1}{2\nu_{n_{\lambda_b}}}, \\
d_1 &= \frac{1}{2\nu_{n_{\rho_a}}}, \quad d_3 = \frac{1}{2\nu_{n_{\rho_b}}}
\end{aligned} \tag{86}$$

A.3 Three-body matrix elements of momentum-dependent factors in the

potential energy

$$\begin{aligned}
& \langle [\phi_{n_{\rho_a} l_{\rho_a} m_{l_{\rho_a}}}(\mathbf{p}_{\rho_3}) \phi_{n_{\lambda_a} l_{\lambda_a} m_{l_{\lambda_a}}}(\mathbf{p}_{\lambda_3})]_{Lm_L} | F(\mathbf{p}_{\rho_k}) | [\phi_{n_{\rho_b} l_{\rho_b} m_{l_{\rho_b}}}(\mathbf{p}_{\rho_3}) \phi_{n_{\lambda_b} l_{\lambda_b} m_{l_{\lambda_b}}}(\mathbf{p}_{\lambda_3})]_{Lm_L} \rangle_{k=1,2} \\
& = N_{n_{\rho_a} l_{\rho_a}} N_{n_{\lambda_a} l_{\lambda_a}} N_{n_{\rho_b} l_{\rho_b}} N_{n_{\lambda_b} l_{\lambda_b}} (4\nu_{n_{\rho_a}})^{l_{\rho_a}} (4\nu_{n_{\lambda_a}})^{l_{\lambda_a}} (4\nu_{n_{\rho_b}})^{l_{\rho_b}} (4\nu_{n_{\lambda_b}})^{l_{\lambda_b}} 4\pi \left(\frac{\pi}{B_{p_1}}\right)^{\frac{3}{2}} \\
& \times \sum_{m_{l_{\rho_a}} m_{l_{\lambda_a}}} (l_{\rho_a} m_{l_{\rho_a}} l_{\lambda_a} m_{l_{\lambda_a}} | Lm_L) \sum_{m_{l_{\rho_b}} m_{l_{\lambda_b}}} (l_{\rho_b} m_{l_{\rho_b}} l_{\lambda_b} m_{l_{\lambda_b}} | Lm_L) \\
& \times \sum_{m=0}^{Lsum} \frac{m!}{(2m+1)!} \int_0^\infty F(p_{\rho_k}) \text{Exp}(-\alpha'_{p_k} p_{\rho_k}^2) p_{\rho_k}^{2m+2} dp_{\rho_k} \\
& \times \sum_{k_a K_a k_b K_b} C_{l_{\rho_a} m_{l_{\rho_a}} k_a} C_{l_{\lambda_a} m_{l_{\lambda_a}} K_a} C_{l_{\rho_b} m_{l_{\rho_b}} k_b} C_{l_{\lambda_b} m_{l_{\lambda_b}} K_b} \tag{87} \\
& \times \sum_{n_{12}=0}^{Lsum-m} \sum_{n_{13}=0}^{Lsum-m} \sum_{n_{14}=0}^{Lsum-m} \sum_{n_{23}=0}^{Lsum-m} \sum_{n_{24}=0}^{Lsum-m} \sum_{n_{34}=0}^{Lsum-m} \sum_{m_{12}=0}^m \sum_{m_{13}=0}^m \sum_{m_{14}=0}^m \sum_{m_{23}=0}^m \sum_{m_{24}=0}^m \sum_{m_{34}=0}^m \\
& \times \frac{\tilde{g}_{12}^{m_{12}} \tilde{g}_{13}^{m_{13}} \tilde{g}_{14}^{m_{14}} \tilde{g}_{23}^{m_{23}} \tilde{g}_{24}^{m_{24}} \tilde{g}_{34}^{m_{34}} \hat{g}_{12}^{n_{12}} \hat{g}_{13}^{n_{13}} \hat{g}_{14}^{n_{14}} \hat{g}_{23}^{n_{23}} \hat{g}_{24}^{n_{24}} \hat{g}_{34}^{n_{34}}}{n_{12}! n_{13}! n_{14}! n_{23}! n_{24}! n_{34}! m_{12}! m_{13}! m_{14}! m_{23}! m_{24}! m_{34}!} \\
& \times (\mathbf{D}_1 \cdot \mathbf{D}_2)^{n_{12}+m_{12}} (\mathbf{D}_1 \cdot \mathbf{D}_3)^{n_{13}+m_{13}} (\mathbf{D}_1 \cdot \mathbf{D}_4)^{n_{14}+m_{14}} \\
& \times (\mathbf{D}_2 \cdot \mathbf{D}_3)^{n_{23}+m_{23}} (\mathbf{D}_2 \cdot \mathbf{D}_4)^{n_{24}+m_{24}} (\mathbf{D}_3 \cdot \mathbf{D}_4)^{n_{34}+m_{34}} \\
& \times \delta(n_{12} + n_{13} + n_{14} + n_{23} + n_{24} + n_{34} - (Lsum - m)) \delta(m_{12} + m_{13} + m_{14} + m_{23} + m_{24} + m_{34} - m) \\
& \times \delta(n_{12} + n_{13} + n_{14} + m_{12} + m_{13} + m_{14} - l_{\rho_a}) \delta(n_{12} + n_{23} + n_{24} + m_{12} + m_{23} + m_{24} - l_{\lambda_a}) \\
& \times \delta(n_{13} + n_{23} + n_{34} + m_{13} + m_{23} + m_{34} - l_{\rho_b}) \delta(n_{14} + n_{24} + n_{34} + m_{14} + m_{24} + m_{34} - l_{\lambda_b})
\end{aligned}$$

$$F(\mathbf{p}_{\rho_k}) = \sqrt{\beta(\mathbf{p}_{\rho_k})} \quad \text{or} \quad F(\mathbf{p}_{\rho_k}) = \sqrt{\delta(\mathbf{p}_{\rho_k})} \tag{88}$$

$$\begin{aligned}
\beta(\mathbf{p}_{\rho_k}) & = 1 + \frac{\mathbf{p}_{\rho_k}^2}{\sqrt{\mathbf{p}_{\rho_k}^2 + m_l^2} \sqrt{\mathbf{p}_{\rho_k}^2 + m_n^2}} \\
\delta(\mathbf{p}_{\rho_k}) & = \frac{m_l m_n}{\sqrt{\mathbf{p}_{\rho_k}^2 + m_l^2} \sqrt{\mathbf{p}_{\rho_k}^2 + m_n^2}} \tag{89}
\end{aligned}$$

$$(k, l, n) = (1, 2, 3), \quad (2, 1, 3) \quad \text{and} \quad (3, 2, 1)$$

$$\alpha'_{p_k} = \left(A_{p_k} - \frac{C_{p_k}^2}{4B_{p_k}} \right), \tag{90}$$

$$\tilde{g}_{ij} = \frac{C_{p_k}^2}{2B_{p_k}^2} c_i c_j + 2d_i d_j - \frac{C_{p_k}}{B_{p_k}} (c_i d_j + c_j d_i), \quad \hat{g}_{ij} = \frac{1}{2B_{p_k}} c_i c_j \tag{91}$$

$$\begin{aligned}
& \langle [\phi_{n_{\rho_a} l_{\rho_a} m_{l_{\rho_a}}}(\mathbf{p}_{\rho_3}) \phi_{n_{\lambda_a} l_{\lambda_a} m_{l_{\lambda_a}}}(\mathbf{p}_{\lambda_3})]_{Lm_L} | F(p_{\rho_3}) | [\phi_{n_{\rho_b} l_{\rho_b} m_{l_{\rho_b}}}(\mathbf{p}_{\rho_3}) \phi_{n_{\lambda_b} l_{\lambda_b} m_{l_{\lambda_b}}}(\mathbf{p}_{\lambda_3})]_{Lm_L} \rangle \\
&= N_{n_{\rho_a} l_{\rho_a}} N_{n_{\lambda_a} l_{\lambda_a}} N_{n_{\rho_b} l_{\rho_b}} N_{n_{\lambda_b} l_{\lambda_b}} (4\nu_{n_{\rho_a}})^{l_{\rho_a}} (4\nu_{n_{\lambda_a}})^{l_{\lambda_a}} (4\nu_{n_{\rho_b}})^{l_{\rho_b}} (4\nu_{n_{\lambda_b}})^{l_{\lambda_b}} \\
&\times \sum_{m_{l_{\rho_a}} m_{l_{\lambda_a}}} (l_{\rho_a} m_{l_{\rho_a}} l_{\lambda_a} m_{l_{\lambda_a}} | Lm_L) \sum_{m_{l_{\rho_b}} m_{l_{\lambda_b}}} (l_{\rho_b} m_{l_{\rho_b}} l_{\lambda_b} m_{l_{\lambda_b}} | Lm_L) \\
&\times \sum_{k_a K_a k_b K_b} C_{l_{\rho_a} m_{l_{\rho_a}} k_a} C_{l_{\lambda_a} m_{l_{\lambda_a}} K_a} C_{l_{\rho_b} m_{l_{\rho_b}} k_b} C_{l_{\lambda_b} m_{l_{\lambda_b}} K_b} \frac{1}{l_{\lambda_a}!} (\mathbf{D}_1 \cdot \mathbf{D}_3)^{l_{\rho_a}} (\mathbf{D}_2 \cdot \mathbf{D}_4)^{l_{\lambda_a}} \\
&\times 4\pi \left(\frac{\pi}{B_{p_3}} \right)^{\frac{3}{2}} \frac{\hat{g}_{13}^{l_{\rho_a}} \hat{g}_{24}^{l_{\lambda_a}}}{(2l_{\rho_a} + 1)!} \int_0^\infty F(p_{\rho_3}) \text{Exp}(-A_{p_3} p_{\rho_3}^2) p_{\rho_3}^{2m+2} dp_{\rho_3}
\end{aligned}$$

$$\begin{aligned}
\tilde{g}_{13} &= 2d_1 d_3, \quad \hat{g}_{24} = \frac{1}{2B_{p_3}} c_2 c_4, \\
c_2 &= \frac{1}{2\nu_{n_{\lambda_a}}}, \quad c_4 = \frac{1}{2\nu_{n_{\lambda_b}}}, \quad d_1 = \frac{1}{2\nu_{n_{\rho_a}}}, \quad d_3 = \frac{1}{2\nu_{n_{\rho_b}}},
\end{aligned} \tag{92}$$

A.4 Three-body matrix elements of the potential energy with spin-orbit interactions

$$\begin{aligned}
& \langle [\phi_{n_{\rho_a} l_{\rho_a} m_{l_{\rho_a}}}(\mathbf{r}_{\rho_3}) \phi_{n_{\lambda_a} l_{\lambda_a} m_{l_{\lambda_a}}}(\mathbf{r}_{\lambda_3})]_{Lm_L} [\chi_{s'_1 m_{s'_1}} \chi_{s'_2 m_{s'_2}}]_{sm_s} | \tilde{G}(r_{\rho_3}) \mathbf{s}_i \cdot \mathbf{l}_{\rho} | \\
& [\phi_{n_{\rho_b} l_{\rho_b} m_{l_{\rho_b}}}(\mathbf{r}_{\rho_3}) \phi_{n_{\lambda_b} l_{\lambda_b} m_{l_{\lambda_b}}}(\mathbf{r}_{\lambda_3})]_{Lm_L} [\chi_{s_1 m_{s_1}} \chi_{s_2 m_{s_2}}]_{sm_s} \rangle_{i=1,2} \\
&= \sum_{m_{s_1}=-1/2}^{1/2} \sum_{m_{s'_1}=-1/2}^{1/2} \sum_{m_{l_{\rho_a}}=-l_{\rho_a}}^{l_{\rho_a}} \sum_{m_{l_{\rho_b}}=-l_{\rho_b}}^{l_{\rho_b}} (l_{\rho_a} m_{l_{\rho_a}} l_{\lambda_a} m_{l_{\lambda_a}} | Lm_L) (l_{\rho_b} m_{l_{\rho_b}} l_{\lambda_b} m_{l_{\lambda_b}} | Lm_L) \\
&\times (s'_1 m_{s'_1} s'_2 m_{s'_2} | sm_s) (s_1 m_{s_1} s_2 m_{s_2} | sm_s) \times \\
&\left[\langle \phi_{n_{\rho_a} l_{\rho_a} m_{l_{\rho_a}}}(\mathbf{r}_{\rho_3}) \phi_{n_{\lambda_a} l_{\lambda_a} m_{l_{\lambda_a}}}(\mathbf{r}_{\lambda_3}) | \tilde{G}(r_{\rho_3}) | \phi_{n_{\rho_b} l_{\rho_b} m_{l_{\rho_b}+1}}(\mathbf{r}_{\rho_3}) \phi_{n_{\lambda_b} l_{\lambda_b} m_{l_{\lambda_b}}}(\mathbf{r}_{\lambda_3}) \rangle \right. \\
&\times \frac{1}{2} \sqrt{(l_{\rho_b} - m_{l_{\rho_b}})(l_{\rho_b} + m_{l_{\rho_b}} + 1)} \sqrt{(s_i + m_{s_i})(s_i - m_{s_i} + 1)} \delta_{s'_i s_i} \delta_{m_{s'_i} m_{s_i} - 1} \\
&+ \langle \phi_{n_{\rho_a} l_{\rho_a} m_{l_{\rho_a}}}(\mathbf{r}_{\rho_3}) \phi_{n_{\lambda_a} l_{\lambda_a} m_{l_{\lambda_a}}}(\mathbf{r}_{\lambda_3}) | \tilde{G}(r_{\rho_3}) | \phi_{n_{\rho_b} l_{\rho_b} m_{l_{\rho_b}-1}}(\mathbf{r}_{\rho_3}) \phi_{n_{\lambda_b} l_{\lambda_b} m_{l_{\lambda_b}}}(\mathbf{r}_{\lambda_3}) \rangle \\
&\times \frac{1}{2} \sqrt{(l_{\rho_b} + m_{l_{\rho_b}})(l_{\rho_b} - m_{l_{\rho_b}} + 1)} \sqrt{(s_i - m_{s_i})(s_i + m_{s_i} + 1)} \delta_{s'_i s_i} \delta_{m_{s'_i} m_{s_i} + 1} \\
&\left. + \langle \phi_{n_{\rho_a} l_{\rho_a} m_{l_{\rho_a}}}(\mathbf{r}_{\rho_3}) \phi_{n_{\lambda_a} l_{\lambda_a} m_{l_{\lambda_a}}}(\mathbf{r}_{\lambda_3}) | \tilde{G}(r_{\rho_3}) | \phi_{n_{\rho_b} l_{\rho_b} m_{l_{\rho_b}}}(\mathbf{r}_{\rho_3}) \phi_{n_{\lambda_b} l_{\lambda_b} m_{l_{\lambda_b}}}(\mathbf{r}_{\lambda_3}) \rangle m_{l_{\rho_b}} m_{s_i} \delta_{m_{s'_i} m_{s_i}} \right]
\end{aligned} \tag{93}$$

$$\begin{aligned}
& \left\langle \left[\left[\left[\phi_{n_{\rho_a} l_{\rho_a} m_{i_{\rho_a}}}(\mathbf{r}_{\rho_3}) \phi_{n_{\lambda_a} l_{\lambda_a} m_{i_{\lambda_a}}}(\mathbf{r}_{\lambda_3}) \right]_{Lm_L} [\chi_{s'_1 m_{s'_1}} \chi_{s'_2 m_{s'_2}}]_{sm_s} \right]_{jm_j} \chi_{s'_3 m_{s'_3}} \right]_{JM} | \tilde{G}(r_{\lambda_3}) \mathbf{s}_3 \cdot \mathbf{l}_{\lambda} | \right. \\
& \left. \left[\left[\left[\phi_{n_{\rho_b} l_{\rho_b} m_{i_{\rho_b}}}(\mathbf{r}_{\rho_3}) \phi_{n_{\lambda_b} l_{\lambda_b} m_{i_{\lambda_b}}}(\mathbf{r}_{\lambda_3}) \right]_{Lm_L} [\chi_{s_1 m_{s_1}} \chi_{s_2 m_{s_2}}]_{sm_s} \right]_{jm_j} \chi_{s_3 m_{s_3}} \right]_{JM} \right\rangle \\
& = \sum_{m_{s_3}=-1/2}^{1/2} \sum_{m_{s'_3}=-1/2}^{1/2} \sum_{m_{i_{\rho_a}}=-l_{\rho_a}}^{l_{\rho_a}} \sum_{m_{i_{\rho_b}}=-l_{\rho_b}}^{l_{\rho_b}} \sum_{m_s=-s}^s \sum_{m_{s'}=-s'}^{s'} (l_{\rho_a} m_{i_{\rho_a}} l_{\lambda_a} m_{i_{\lambda_a}} | Lm_L) \\
& \times (l_{\rho_b} m_{i_{\rho_b}} l_{\lambda_b} m_{i_{\lambda_b}} | Lm_L) (s' m_{s'} Lm_L | jm_j) (sm_s Lm_L | jm_j) (jm_j s'_3 m_{s'_3} | JM) (jm_j s_3 m_{s_3} | JM) \\
& \times \left[\langle \phi_{n_{\rho_a} l_{\rho_a} m_{i_{\rho_a}}}(\mathbf{r}_{\rho_3}) \phi_{n_{\lambda_a} l_{\lambda_a} m_{i_{\lambda_a}}}(\mathbf{r}_{\lambda_3}) | \tilde{G}(r_{\lambda_3}) | \phi_{n_{\rho_b} l_{\rho_b} m_{i_{\rho_b}}}(\mathbf{r}_{\rho_3}) \phi_{n_{\lambda_b} l_{\lambda_b} m_{i_{\lambda_b}+1}}(\mathbf{r}_{\lambda_3}) \rangle \right. \\
& \times \frac{1}{2} \sqrt{(l_{\lambda_b} - m_{i_{\lambda_b}})(l_{\lambda_b} + m_{i_{\lambda_b}} + 1)} \sqrt{(s_3 + m_{s_3})(s_3 - m_{s_3} + 1)} \delta_{m_{s'_3} m_{s_3} - 1} \\
& + \langle \phi_{n_{\rho_a} l_{\rho_a} m_{i_{\rho_a}}}(\mathbf{r}_{\rho_3}) \phi_{n_{\lambda_a} l_{\lambda_a} m_{i_{\lambda_a}}}(\mathbf{r}_{\lambda_3}) | \tilde{G}(r_{\lambda_3}) | \phi_{n_{\rho_b} l_{\rho_b} m_{i_{\rho_b}}}(\mathbf{r}_{\rho_3}) \phi_{n_{\lambda_b} l_{\lambda_b} m_{i_{\lambda_b} - 1}}(\mathbf{r}_{\lambda_3}) \rangle \\
& \times \frac{1}{2} \sqrt{(l_{\lambda_b} + m_{i_{\lambda_b}})(l_{\lambda_b} - m_{i_{\lambda_b}} + 1)} \sqrt{(s_3 - m_{s_3})(s_3 + m_{s_3} + 1)} \delta_{m_{s'_3} m_{s_3} + 1} \\
& \left. + \langle \phi_{n_{\rho_a} l_{\rho_a} m_{i_{\rho_a}}}(\mathbf{r}_{\rho_3}) \phi_{n_{\lambda_a} l_{\lambda_a} m_{i_{\lambda_a}}}(\mathbf{r}_{\lambda_3}) | \tilde{G}(r_{\lambda_3}) | \phi_{n_{\rho_b} l_{\rho_b} m_{i_{\rho_b}}}(\mathbf{r}_{\rho_3}) \phi_{n_{\lambda_b} l_{\lambda_b} m_{i_{\lambda_b}}}(\mathbf{r}_{\lambda_3}) \rangle m_{i_{\lambda_b}} m_{s_3} \delta_{m_{s'_3} m_{s_3}} \right]
\end{aligned} \tag{94}$$

$$\begin{aligned}
& \langle [\phi_{n_{\rho_a} l_{\rho_a} m_{i_{\rho_a}}}(\mathbf{r}_{\rho_3}) \phi_{n_{\lambda_a} l_{\lambda_a} m_{i_{\lambda_a}}}(\mathbf{r}_{\lambda_3})]_{Lm_L} | \tilde{G}(r_{\lambda_3}) | [\phi_{n_{\rho_b} l_{\rho_b} m_{i_{\rho_b}}}(\mathbf{r}_{\rho_3}) \phi_{n_{\lambda_b} l_{\lambda_b} m_{i_{\lambda_b}}}(\mathbf{r}_{\lambda_3})]_{Lm_L} \rangle \\
& = N_{n_{\rho_a} l_{\rho_a}} N_{n_{\lambda_a} l_{\lambda_a}} N_{n_{\rho_b} l_{\rho_b}} N_{n_{\lambda_b} l_{\lambda_b}} \frac{1}{(\nu_{n_{\rho_a}})^{l_{\rho_a}} (\nu_{n_{\lambda_a}})^{l_{\lambda_a}} (\nu_{n_{\rho_b}})^{l_{\rho_b}} (\nu_{n_{\lambda_b}})^{l_{\lambda_b}}} \\
& \times \sum_{m_{i_{\rho_a}} m_{i_{\lambda_a}}} (l_{\rho_a} m_{i_{\rho_a}} l_{\lambda_a} m_{i_{\lambda_a}} | Lm_L) \sum_{m_{i_{\rho_b}} m_{i_{\lambda_b}}} (l_{\rho_b} m_{i_{\rho_b}} l_{\lambda_b} m_{i_{\lambda_b}} | Lm_L) \\
& \times 4\pi \left(\frac{\pi}{A_{r_3}} \right)^{\frac{3}{2}} \sum_{k_a K_a k_b K_b} C_{l_{\rho_a} m_{i_{\rho_a}} k_a} C_{l_{\lambda_a} m_{i_{\lambda_a}} K_a} C_{l_{\rho_b} m_{i_{\rho_b}} k_b} C_{l_{\lambda_b} m_{i_{\lambda_b}} K_b} \\
& \times \frac{1}{(2m+1)!} \int_0^\infty V(r_{\lambda_3}) \text{Exp}(-B_{r_3} r_{\lambda_3}^2) r_{\lambda_3}^{2m+2} dr_{\lambda_3} \frac{\tilde{g}_{24}^{l_{\lambda_a}} \hat{g}_{13}^{l_{\rho_a}}}{l_{\rho_a}!} (\mathbf{D}_1 \cdot \mathbf{D}_3)^{l_{\rho_a}} (\mathbf{D}_2 \cdot \mathbf{D}_4)^{l_{\lambda_a}}
\end{aligned} \tag{95}$$

$$\tilde{g}_{24} = 2c_2 c_4, \quad \hat{g}_{13} = \frac{1}{2A_{r_3}} d_1 d_3 \tag{96}$$

$$c_2 = 2\nu_{n_{\lambda_a}}, \quad c_4 = 2\nu_{n_{\lambda_b}}, \quad d_1 = 2\nu_{n_{\rho_a}}, \quad d_3 = 2\nu_{n_{\rho_b}}, \tag{97}$$

A.5 Relations used in matrix elements of the tensor term

$$(\mathbf{S} \cdot \hat{\mathbf{r}}_\rho)_1 = \begin{pmatrix} 0 & \frac{1}{2}\sin\theta\cos\phi \\ \frac{1}{2}\sin\theta\cos\phi & 0 \end{pmatrix} \quad (98)$$

$$(\mathbf{S} \cdot \hat{\mathbf{r}}_\rho)_2 = \begin{pmatrix} 0 & -\frac{i}{2}\sin\theta\sin\phi \\ \frac{1}{2}\sin\theta\sin\phi & 0 \end{pmatrix} \quad (99)$$

$$(\mathbf{S} \cdot \hat{\mathbf{r}}_\rho)_3 = \begin{pmatrix} \frac{1}{2}\cos\theta & 0 \\ 0 & \frac{1}{2}\cos\theta \end{pmatrix} \quad (100)$$

$$\mathbf{S}_1 \cdot \hat{\mathbf{r}}_\rho \mathbf{S}_2 \cdot \hat{\mathbf{r}}_\rho = \sum_{i=1}^3 \sum_{j=1}^3 (\mathbf{S} \cdot \hat{\mathbf{r}}_\rho)_i \otimes (\mathbf{S} \cdot \hat{\mathbf{r}}_\rho)_j \otimes I \quad (101)$$

$$\begin{aligned} \chi_{s41} &= \chi_{\frac{1}{2}} \otimes \chi_{\frac{1}{2}} \otimes \chi_{\frac{1}{2}} \\ \chi_{s42} &= \frac{1}{\sqrt{3}}(\chi_{-\frac{1}{2}} \otimes \chi_{\frac{1}{2}} \otimes \chi_{\frac{1}{2}} + \chi_{\frac{1}{2}} \otimes \chi_{-\frac{1}{2}} \otimes \chi_{\frac{1}{2}} + \chi_{\frac{1}{2}} \otimes \chi_{\frac{1}{2}} \otimes \chi_{-\frac{1}{2}}) \\ \chi_{s43} &= \frac{1}{\sqrt{3}}(\chi_{-\frac{1}{2}} \otimes \chi_{-\frac{1}{2}} \otimes \chi_{\frac{1}{2}} + \chi_{-\frac{1}{2}} \otimes \chi_{\frac{1}{2}} \otimes \chi_{-\frac{1}{2}} + \chi_{\frac{1}{2}} \otimes \chi_{-\frac{1}{2}} \otimes \chi_{-\frac{1}{2}}) \\ \chi_{s44} &= \chi_{-\frac{1}{2}} \otimes \chi_{-\frac{1}{2}} \otimes \chi_{-\frac{1}{2}} \\ \chi_{s21} &= \frac{1}{\sqrt{6}}(\chi_{\frac{1}{2}} \otimes \chi_{-\frac{1}{2}} \otimes \chi_{\frac{1}{2}} + \chi_{-\frac{1}{2}} \otimes \chi_{\frac{1}{2}} \otimes \chi_{\frac{1}{2}} - 2\chi_{\frac{1}{2}} \otimes \chi_{\frac{1}{2}} \otimes \chi_{-\frac{1}{2}}) \\ \chi_{s22} &= -\frac{1}{\sqrt{6}}(\chi_{\frac{1}{2}} \otimes \chi_{-\frac{1}{2}} \otimes \chi_{-\frac{1}{2}} + \chi_{-\frac{1}{2}} \otimes \chi_{\frac{1}{2}} \otimes \chi_{-\frac{1}{2}} - 2\chi_{-\frac{1}{2}} \otimes \chi_{-\frac{1}{2}} \otimes \chi_{\frac{1}{2}}) \\ \chi_{As21} &= \frac{1}{\sqrt{2}}(\chi_{\frac{1}{2}} \otimes \chi_{-\frac{1}{2}} \otimes \chi_{\frac{1}{2}} - \chi_{-\frac{1}{2}} \otimes \chi_{\frac{1}{2}} \otimes \chi_{\frac{1}{2}}) \\ \chi_{As22} &= \frac{1}{\sqrt{2}}(\chi_{\frac{1}{2}} \otimes \chi_{-\frac{1}{2}} \otimes \chi_{-\frac{1}{2}} - \chi_{-\frac{1}{2}} \otimes \chi_{\frac{1}{2}} \otimes \chi_{-\frac{1}{2}}) \end{aligned} \quad (102)$$

